

# Newsletter

Year **18** n°3

Autumn 2021

## What lies in the future for simulation?

The Red Planet may have an influence...



Ku-band filter design for high power space applications using Ansys simulators



Quick and easy estimation of the usage of a battery-powered electrical vehicle to explore cooling system performance



Pipistrel: flying straight from simulation to production

Knowledge for tomorrow's automotive engineering.

## Stay informed and advance your knowledge

with over 130 seminars, events and up-to-date technical knowledge in:

- » Passive Safety
- » Active Safety
- » Autonomous Driving
- » Electric Mobility
- » Dummy & Crash-Test
- » Engineering & Simulation



Order your free copy!

[www.carhs.de/companion](http://www.carhs.de/companion)

**Now available:** Special edition celebrating C-NCAP's 15th anniversary with 12 additional pages on the current and future C-NCAP test program: pedestrian protection, motorized two-wheeler (scooter) protection, child presence detection, and Roadmap 2025.

[www.carhs.de](http://www.carhs.de)

**carhs**  
Empowering Engineers

## Euro NCAP UpDate

Get ready for Euro NCAP's latest rating revision! ★★★★★

**December 14 – 15, 2021**

Hanau, Germany

[www.carhs.de/euroncap](http://www.carhs.de/euroncap)

**carhs**  
Empowering Engineers

ON SITE & ONLINE



## SAFETYUPDATE +active

Knowledge for the vehicle development of tomorrow

**February 07 – 08, 2022**

Graz, Austria

[www.carhs.de/gsu](http://www.carhs.de/gsu)

**carhs**  
Empowering Engineers

# Flash

This year, the International CAE Conference and Exhibition, taking place in Vicenza from 17-19 November, is a hybrid event – offering participants, exhibitors and speakers, the option of participating either virtually, or in person, according to their preferences and possibility. Once again, the program offers a breadth and depth of content that the event's numerous regular attendees have come to expect, from the inspirational to the incredibly technical.

Speakers at this year's event include Paolo Bellutta, a Mars exploration rover driver who will share with delegates the role that simulation has played in this truly astonishing adventure, as well as Professor Ichiro Hagiwara from Meiji University in Japan who will discuss the evolution of Origami Engineering, an approach inspired and nurtured by the ancient Japanese folding culture. In addition, in honor of the host-country, there is also a panel discussion with prominent personalities from the political and business worlds about *Italian Pathways to the Digital Future: an overview of the country's economic recovery and the paths to creating an innovative Italy*.

Of course, participants can also attend the regular technical tracks which will offer a deep dive into case studies, best practices, and expert approaches to different aspects of simulation in the four macro sectors of energy, manufacturing, automotive and transportation. Other event features, which have now become traditional, are the Research Agorà, which offers an opportunity to interact with industrial and academic research consortia and explore the new frontiers of simulation, and the Poster Award which rewards the innovative application of CAE technologies by students from around the world and highlights the bright new talents due to graduate imminently.

A further feature of this year's event is the platform on which the hybrid event has been created, which offers all the participants, speakers, and exhibitors the opportunity to engage with the entire

event community – colleagues, clients, suppliers, researchers, and academics – in a business social media-like manner. Once registered, the system will send out a link where each attendee can create a personal profile to facilitate meetings, interactions, and idea exchange with the others in the CAE Conference and Exhibition event community. Registration to the event is, as always, free of charge, but mandatory. Visit [www.caeconference.com](http://www.caeconference.com) for more details. This issue of the *Newsletter* offers a foretaste of some of the content you can explore in greater depth at the event. I particularly draw your attention to the mini CAE Conference preview on pages 38 to 52.

One area that challenges engineers in various fields is bridging the gap between prototype testing and simulation – an essential criterion to ensure that our simulation models reliably match experimental results. This is explored on page 50 in an article by EikoSim which offers a pathway towards using optical measurement techniques to achieve this.

In addition to product updates and overviews from Ansys, Esteco, and Tech Soft 3D, among others, there are, as usual, a number of case studies in this issue. One of these looks at how high-fidelity Multiphysics CAE is being used in the DEMO Tokamak to assist in the UE's ambitious quest to generate power from nuclear fission. Another looks at how the use of simulation has allowed Pipistrel in Slovenia to skip the prototyping phase for a hybrid-electric aircraft propeller. A further case study looks at how simulation was able to quickly and easily estimate the cooling system performance of a battery-powered electrical vehicle.

There are also several technical contributions about how simulation is being applied in leading edge research such as a detailed article about the FE analysis being done to further develop an experimental flexible electronic board built using innovative materials in a project being funded by the EU and the Piedmont region that you can find on page 22.

As always, you will find much food for thought in the *Newsletter*! I wish you an interesting read and look forward to seeing you – either virtually or in person – at the 2021 CAE Conference and Exhibition in Vicenza.

**Stefano Odorizzi**  
Editor in Chief

# Contents

## Case Studies



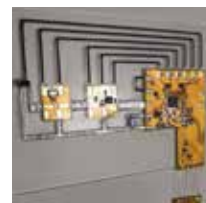
**6** Ku-band filter design for high power space applications using Ansys simulators  
*by RF Microtech*



**20** Pipistrel: flying straight from simulation to production  
*by ESTECO*



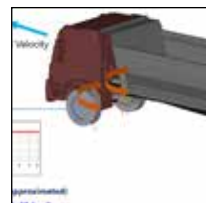
**12** New solution for cost-effective electromagnetic analysis  
*by EnginSoft*



**22** Static and thermal FE analysis of a Flexible Electronic Board (FEBO) prototype and the characterization of its innovative materials  
*by ITACAE*



**14** Quick and easy estimation of the usage of a battery-powered electrical vehicle to explore cooling system performance  
*by Stellantis*



**28** Co-simulation of multibody dynamics and particle analysis with Ansys Motion and Ansys Rocky  
*by TSNE*

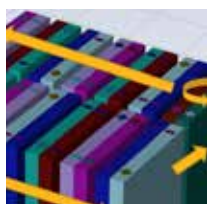


**17** Application of Particleworks to the design and performance evaluation of waterproofing for automotive air conditioning systems  
*by akf and Prometech Software*



**31** pyCONSOLE: a Python-based data intelligence environment integrated into an MDO engineering framework  
*by ESTECO*

## Software Updates



**34** Ansys 2021 R2: CFD release highlights  
*by EnginSoft*

**PAST ISSUES at**  
[www.enginsoft.com/magazine](http://www.enginsoft.com/magazine)

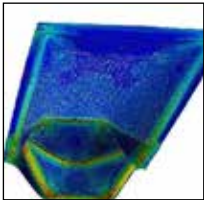
A grid of 16 magazine covers arranged in two rows of eight. Each cover features a different image related to engineering or technology. The covers are labeled with their respective issue numbers and dates: Winter 2018, Year 15 n. 3 Autumn 2018, Year 15 n. 2 Summer 2018, Year 15 n. 1 Spring 2018, Winter 2017, Year 14 n. 3 Autumn 2017, Year 14 n. 2 Summer 2017, and Year 14 n. 1 Spring 2017.

\*Cover picture - Credit NASA/JPL-Caltech/Cornell University

## 37<sup>th</sup> International CAE Conference SPECIAL SUPPLEMENT

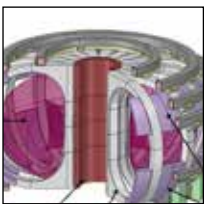


- 38** What lies in the future for simulation? The Red Planet may have an influence...



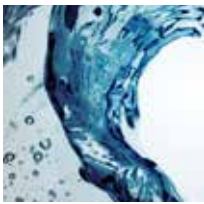
- 40** Analyzing the process of filling a flexible pouch by coupling multi-flexible-body dynamics and particle-based CFD simulation

*by University of Trento*



- 44** Reshaping the DEMO Tokamak's TF Coil with high fidelity Multiphysics CAE and advanced mesh morphing

*by University of Rome Tor Vergata*

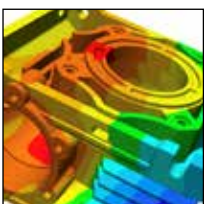


- 49** Announcing LeaPS, a water Leak Prediction System



- 50** Bridge the gap between testing and simulation

*by EikoSim*



- 52** Component-based development for CAE with Tech Soft 3D's toolkits

*by Tech Soft 3D*



- 54** The Revolution in Simulation Initiative continues to expand as EnginSoft joins a growing alliance of sponsors

### EnginSoft Newsletter Year 18 n°3 - Autumn 2021

To receive a free copy of the next EnginSoft Newsletters, please contact our Marketing office at: [info@enginsoft.it](mailto:info@enginsoft.it)

*All pictures are protected by copyright. Any reproduction of these pictures in any media and by any means is forbidden unless written authorization by EnginSoft has been obtained beforehand. ©Copyright EnginSoft Newsletter.*

#### EnginSoft S.p.A.

24126 BERGAMO c/o Parco Scientifico Tecnologico  
Kilometro Rosso - Edificio A1, Via Stezzano 87  
Tel. +39 035 368711 • Fax +39 0461 979215  
50127 FIRENZE Via Panciatichi, 40  
Tel. +39 055 4376113 • Fax +39 0461 979216  
35129 PADOVA Via Giambellino, 7  
Tel. +39 049 7705311 • Fax +39 0461 979217  
72023 MESAGNE (BRINDISI) Via A. Murri, 2 - Z.I.  
Tel. +39 0831 730194 • Fax +39 0461 979224  
38123 TRENTO fraz. Mattarello - Via della Stazione, 27  
Tel. +39 0461 915391 • Fax +39 0461 979201  
10133 TORINO Corso Marconi, 10  
Tel. +39 011 6525211 • Fax +39 0461 979218

[www.enginsoft.com](http://www.enginsoft.com)  
e-mail: [info@enginsoft.com](mailto:info@enginsoft.com)

*The EnginSoft Newsletter is a quarterly magazine published by EnginSoft SpA*

#### COMPANY INTERESTS

EnginSoft GmbH - Germany  
EnginSoft UK - United Kingdom  
EnginSoft France - France  
EnginSoft Turkey - Turkey  
VSA-TTC3 - Germany  
[www.enginsoft.com](http://www.enginsoft.com)

CONSORZIO TCN [www.consorziotcn.it](http://www.consorziotcn.it) • [www.improve.it](http://www.improve.it)  
M3E Mathematical Methods and Models for Engineering [www.m3eweb.it](http://www.m3eweb.it)  
AnteMotion

#### ASSOCIATION INTERESTS

NAFEMS International [www.nafems.it](http://www.nafems.it) • [www.nafems.org](http://www.nafems.org)  
TechNet Alliance [www.technet-alliance.com](http://www.technet-alliance.com)

#### ADVERTISING

For advertising opportunities, please contact our Marketing office at: [info@enginsoft.com](mailto:info@enginsoft.com)

#### RESPONSIBLE DIRECTOR

Stefano Odorizzi

#### PRINTING

Grafiche Dalpiaz - Trento

Autorizzazione del Tribunale di Trento  
n° 1353 RS di data 2/4/2008

The EnginSoft Newsletter editions contain references to the following products which are trademarks or registered trademarks of their respective owners:

Anslys, Ansys Workbench, AUTODYN, CFX, Fluent, FORTE, SpaceClaim and any and all Ansys, Inc. brand, product, service and feature names, logos and slogans are registered trademarks or trademarks of Ansys, Inc. or its subsidiaries in the United States or other countries. [ICEM CFD is a trademark used by Ansys, Inc. under license]. ([www.ansys.com](http://www.ansys.com)) - modeFRONTIER is a trademark of ESTECO Spa ([www.esteco.com](http://www.esteco.com)) - Flownex is a registered trademark of M-Tech Industrial - South Africa ([www.flownex.com](http://www.flownex.com)) - MAGMASOFT is a trademark of MAGMA GmbH ([www.magmasoft.de](http://www.magmasoft.de)) - FORGE, COLDFORM and FORGE Nxt are trademarks of Transvalor S.A. ([www.transvalor.com](http://www.transvalor.com)) - LS-DYNA is a trademark of LSTC ([www.lstc.com](http://www.lstc.com)) - Cetol 6σ is a trademark of Sigmatrix L.L.C. ([www.sigmatrix.com](http://www.sigmatrix.com)) - RecurDyn™ and MBD for Ansys is a registered trademark of FunctionBay, Inc. ([www.functionbay.org](http://www.functionbay.org)) Maplesoft are trademarks of Maplesoft™, a subsidiary of Cybernet Systems Co. Ltd. in Japan ([www.maplesoft.com](http://www.maplesoft.com)) - Particleworks is a trademark of Prometech Software, Inc. ([www.prometechsoftware.com](http://www.prometechsoftware.com)) Multiscale.Sim is an add-in tool developed by CYBERNET SYSTEMS CO.,LTD., Japan for the Ansys Workbench environment



by Paolo Vallerotonda<sup>1,2</sup>, Fabrizio Cacciamani<sup>1</sup>, Luca Pelliccia<sup>1</sup>,  
 Francesco Aquino<sup>1</sup>, Cristiano Tomassoni<sup>2</sup>, Vittorio Tornielli di Crestvolant<sup>3</sup>  
 1. RF Microtech - 2. University of Perugia - 3. ESA ESTEC

## Ku-band filter design for high power space applications using Ansys simulators

*This paper presents the design and first experimental results of a very compact Ku-band bandpass filter for high power satellite applications. The filter was designed and simulated using the Ansys HFSS and Mechanical simulators. Proposed as part of an ESA ARTES Advanced Technology project, the filter is based on dielectric loaded combline resonators. Several dielectric materials were considered and two models of the same filter are presented in this paper. The geometries and materials were chosen to improve the performance in terms of power-handling and multipactor up to 150 W continuous wave of input RF power. Barrel-shaped metal cavities and high-permittivity ceramic materials were mixed to minimize volume occupancy while maintaining high unloaded Q-factor values (>4500).*

This paper proposes the design of a Ku-band filter based on dielectric loaded combline resonators for high power space applications. The requirements of the ESA ARTES AT project, named DOMUK (Dielectric-loaded high-power Output de-MUltiplexer at Ku/Ka-band, ESA Contract Number: 4000125645/19/NL/NR) were considered as a benchmark. In this scenario, output De-Multiplexers (ODEMUXs) are used in current multi-beam Ku/Ka systems to separate the signals intended for each beam. A large number of identical ODEMUXs are required in multi-beam systems due to the nature of the frequency re-use scheme. This implies very stringent requirements for the ODEMUX in terms of mass and footprint. There are numerous solutions in the literature to achieve more compact and lightweight filter structures without compromise the radio frequency (RF) performance. A general description of the techniques and technologies related to filter development is presented in [1]-[3]. Dielectric resonators

(DRs) are the preferred solution to minimize volume occupancy by high-permittivity ( $\epsilon_r$ ) materials. This solution is widely used for Input Multiplexer (IMUX) channels in all bands, and for high power Output Multiplexer (OMUX) channels in C-band. However, this approach is limited to moderate power levels per channel when considering K-band OMUXs with narrow bandwidth. The design of a high-power Ku-band filter is described in this paper where the architectures and materials have been carefully chosen to improve the performance of the filter with respect to power handling and multipactor up to 150 W of input RF power.

Several promising solutions could be adopted for our purpose;  $TM_{010}$  or  $TE_{01\delta}$  dielectric resonator mode-based filters are an example.  $TE_{01\delta}$  modes could represent the best compromise to obtain compact filters where low losses and high discharge handling capability are required. On the other hand, the main drawback of this solution concerns the thermal management [4] since the DR is not directly joined to the metal cavity of the filter, but is supported by a material with low dielectric permittivity generally characterized by a very poor thermal conductivity. With respect to the  $TM_{010}$  mode solution, the main limitation concerns the mechanical stability of the dielectric-metal contact [5]. In fact, the different Coefficients of Thermal Expansion (CTE) of the metal cavity and the ceramic element can produce detachment at the interfaces of the two materials when the operating temperature changes. Any small airgaps are sufficient to worsen the filter response as the boundary conditions change. In this scenario, dielectric combline resonators [6] would likely be a good compromise to minimize the critical aspects that could be encountered using the  $TM_{010}$  or  $TE_{01\delta}$  approaches.

The design of a high-power sixth-order pseudo-elliptic filter based on dielectric combline resonators is proposed in this paper. Preliminary results are also described in [7] and [8], however this paper shows updates in which two similar filter models are proposed using different permittivity values of the dielectric elements. The 3D filter models were designed using the Ansys software suite, in particular HFSS was used for electromagnetic design while Ansys Mechanical was chosen to simulate the mechanical/thermal performance. Details of the software configuration and the results achieved are also presented in the paper, along with the preliminary test results.

## Filter Design

The basic 3D model of the dielectric loaded combline resonators designed using Ansys HFSS software is shown in Fig. 1. The metal cavity is loaded by the dielectric cylinder with high permittivity values in order to increase the volume and mass saving (more than 50%) compared to standard TE113 resonators. The dielectric element is only joined to one side of the cavity, as shown in Fig. 1b.

Two sixth-order filter models were designed considering the different permittivity values of commercially available dielectric elements. The proposed resonator model for the filters is presented in Fig. 2; the high permittivity dielectric element is mixed with “barrel-shaped” metal cavity. Fig. 2a shows the combline resonator, which is based

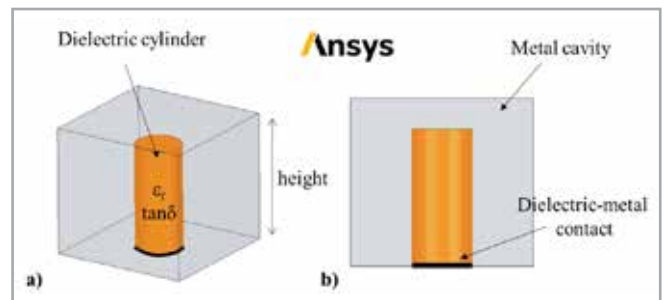


Fig. 1 - Dielectric loaded combline resonator designed in Ansys HFSS: a) 3D view, b) side view.

on ceramic material characterized by a permittivity of 12.6 and low loss-tangent ( $8e-5$ ). This solution allows for a very compact structure while maintaining high unloaded Q-factor values ( $>4500$ ) when considering a standard square cavity.

According to [7] and [8], along with the cavity height, the shape of the cavity can also be optimized to improve the Q-factor. It is well-known that a spherical shaped cavity is the best solution to maximize the Q-factor, however this approach could become critical to achieve the required coupling values for our filter since it increases the distance between two adjacent resonators.

Based on preliminary eigenmode analyses [7] performed in HFSS, the best cavity shape to further improve the Q-factor is the “Barrel” which allows the simulated unloaded Q-factor of the resonator in Fig. 2a to be increased up to 6000. In [7], [8] multiple parametric analyses were performed in HFSS with respect to the variation of the main parameters such as the radius of dielectric cylinder, cavity height, and curvature of the barrel cavity. As a result, (see Fig. 2a), the required aspect ratio of the ceramic cylinder to maximize the unloaded Q-factor is very high but a potentially vibration-sensitive structure is obtained. Therefore, support mechanisms (Teflon cups) were used to lock the ceramic cylinder in place on the top of the cavity. Along with the properties of the dielectric elements, the non-ideal characteristics of metallic material are also considered. The finite conductivity background conditions used in the models shown in Fig. 2a and Fig. 2b are set in order to consider the loss contribution due to the metal casing, as shown in Fig. 2c. Aluminum’s similar bulk conductivity ( $\sigma=3e7$  S/m) was also considered despite a silvering process having been performed on the cavity surfaces, which allows for a margin over than the desired true Q-factor.

In Fig. 2, the first prototype resonator (Fig. 2a) is compared with a smaller barrel-shaped resonator (Fig. 2b) in which a ceramic material with higher permittivity is used. Due to  $\epsilon_r=24$ , additional shrinkage of the structure is achieved while maintaining a sufficiently high unloaded Q-factor value (about 4000-5000). The barrel shape of the cavity is less pronounced in the second resonator solution. To increase the “barrel-shape” to be similar to the first prototype, the diameter of the ceramic cylinder must be decreased. However, in this case, a minimum diameter of 2 mm was chosen to avoid possible criticality due to the robustness of the ceramic parts; for this reason a less pronounced barrel was obtained.

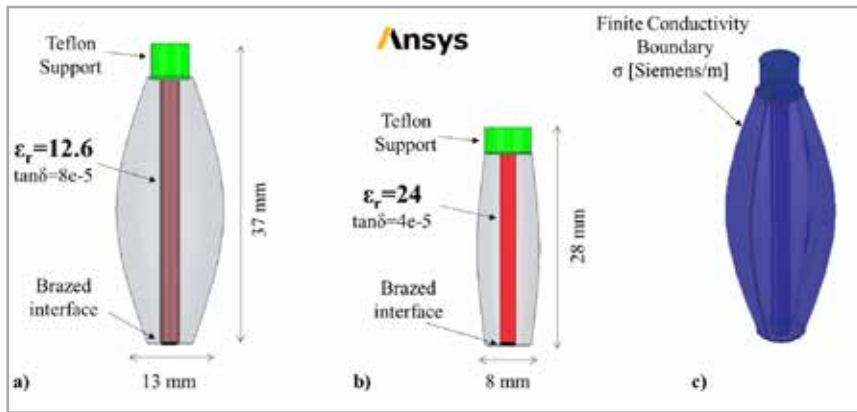


Fig. 2 - Proposed dielectric loaded combline resonator designed in Ansys HFSS: a) side view of resonator with  $\epsilon_r=12.6$ , b) side view of resonator with  $\epsilon_r=24$ , c) 3D view of resonator with background conditions of metallic cavity.

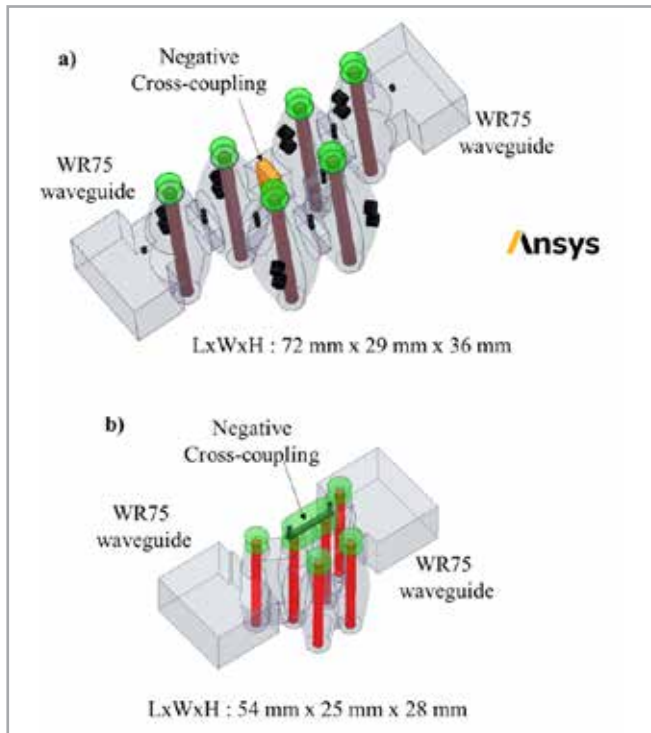


Fig. 3 - 3D view of sixth-order Ku-band filters: a) Model 1 ( $\epsilon_r=12.6$ ), b) Model 2 ( $\epsilon_r=24$ ).

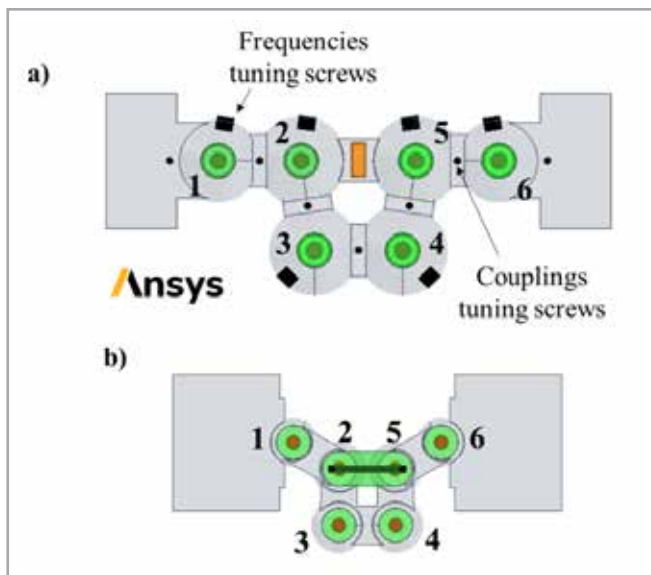


Fig. 4 - Top views of sixth-order Ku-band filters: a) Model 1 ( $\epsilon_r=12.6$ ), b) Model 2 ( $\epsilon_r=24$ ).

Two sixth-order elliptical filter models were designed using the dielectric loaded combline resonators in Fig. 2. The 3D models of proposed Ku-band filters are compared in Fig. 3 where the difference in size is highlighted.

Both filters are based on the same folded configuration in which all positive couplings between adjacent resonators are used while a negative cross-coupling has been designed between the non-adjacent resonators 2-5 to achieve two transmission zeros (TZs) in the lower and upper stop bands. The difference in footprint is shown in Fig. 4 where top views of the filters are presented.

The intra-couplings were designed by simulating odd and even resonant modes (eigenmode analysis) between each resonator duplet; whereas the Group Delay (GD) method was used to design the input couplings [9] where the WR75 waveguide interface was used. In this scenario, the GD of the reflection characteristic was simulated by performing a Driven Modal analysis of the S-parameters in HFSS. The models used to design the input and intra-couplings are shown in Figs. 5a and 5b, respectively, while Figs. 5c and 5d are the models used to design the negative cross-couplings.

In the first filter model in Fig. 3a, the negative cross-coupling was achieved by using a capacitive iris loaded with high-permittivity ( $\epsilon_r=24$ ) material [7]. This cross-coupling solution is impractical

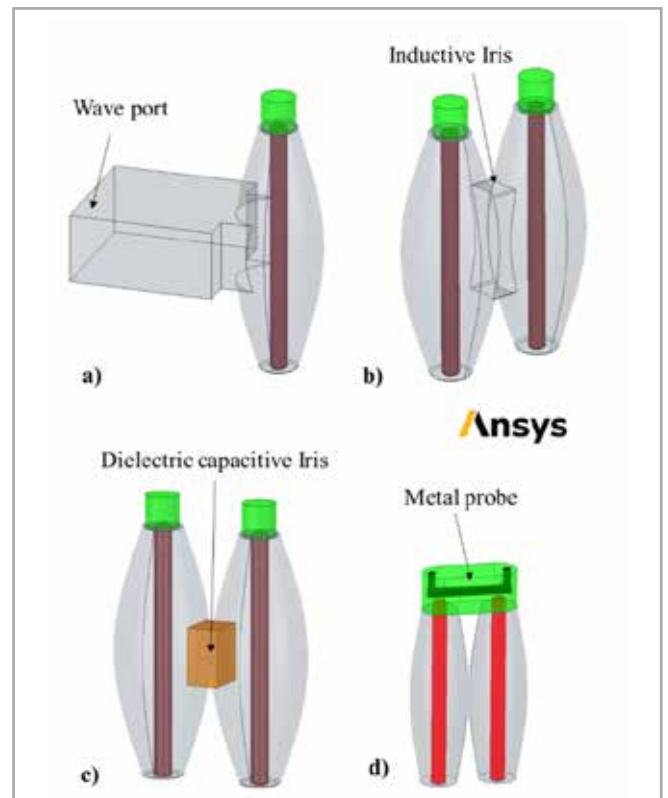


Fig. 5 - Ku-band filter duplet for coupling design: a) Input coupling design model, b) Intra-positive coupling design model, c) Negative cross-coupling design Model 1, d) Negative cross-coupling design Model 2.

in the second filter model because the smaller size of the structure does not allow the desired negative coupling value to be achieved. However, in this case the cross-coupling was achieved by designing a shaped metal probe supported by a Teflon interface (Fig. 5d).

In the first filter model (Fig. 3a), tuning screws were added to the cavity and coupling irises to compensate for the variation in filter response due to manufacturing tolerances. Similar tuning mechanisms can be used in the second filter model, however the structure shown in Fig. 3b is only a preliminary model, and the tuning screws are not present.

**Simulated Results**

Driven Modal simulations were performed in HFSS to simulate and optimize the S-parameters of both sixth-order Ku-band filters. In each case, the wave-ports were defined as signal excitations of the 3D model while the adaptive meshing solutions were used for the simulation setup. The central frequency of the filter (11 GHz) was chosen as the single solution frequency. Concerning the mesh, curvilinear elements were applied since the models show numerous curved surfaces. The full-wave response of the first sixth-order filter model (Fig. 3a) is shown in Fig. 6, while the simulated S-parameters of the second prototype (Fig. 3b) are depicted in Fig. 7. Both simulations converged with a maximum Delta-S magnitude of less than 0.01.

All in-band and out-of-band requirements (Fig. 6) are satisfied in the case of the first filter model. Return loss (RL) greater than 19 dB and insertion loss (IL) less than 0.8 dB are over the entire passband (240 MHz), while all near-band rejection requirements are met due

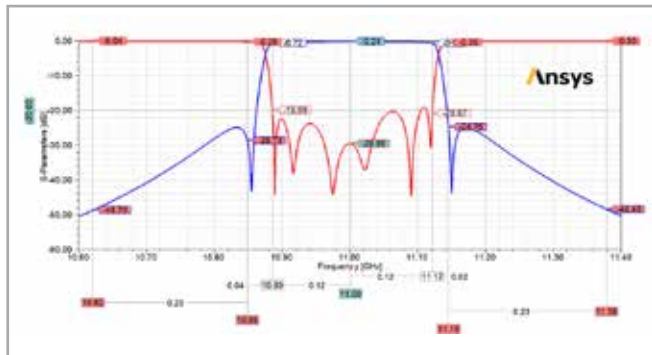


Fig. 6 - Simulated response of Ku-band filter Model 1 (blue line is transmission characteristic, red line is reflection characteristic).

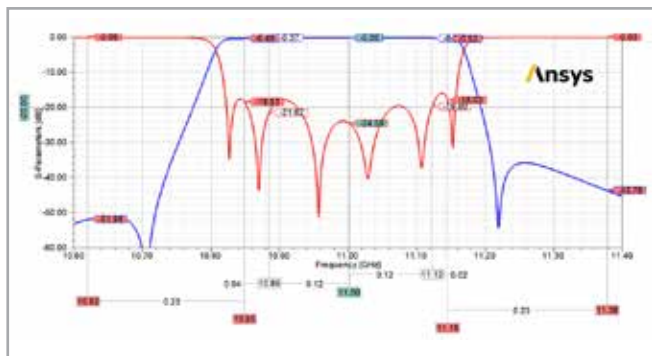


Fig. 7 - Simulated response of Ku-band filter Model 2 (blue line is transmission characteristic, red line is reflection characteristic).

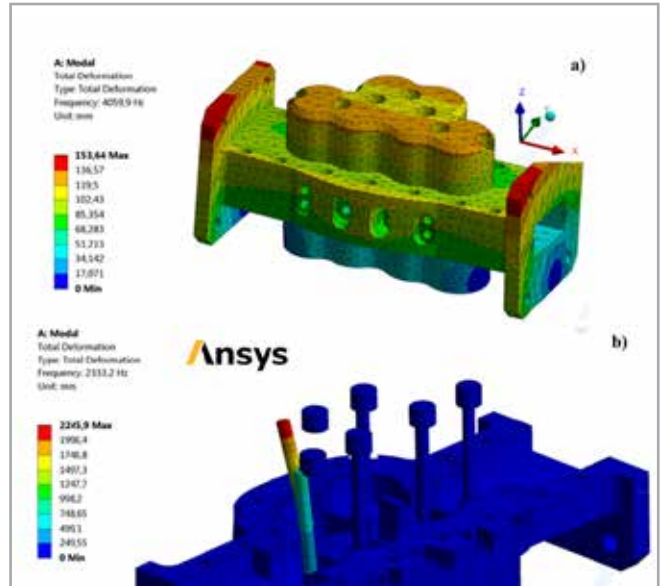


Fig. 8 - Ansys vibration analysis of the sixth-order filter Model 1.

to the TZs. Regarding the second filter model, similar results were obtained but a wider bandwidth was achieved despite using the higher permittivity values of the ceramic elements have been used. This shows that “strong” coupling values can be achieved with the proposed design even though the E-field is more confined within the dielectric elements.

The first model was chosen for manufacturing because it is less critical in terms of manufacturing tolerances, and therefore additional analyses were performed during the design procedure. Vibration analyses were performed in Ansys Mechanical to identify the first

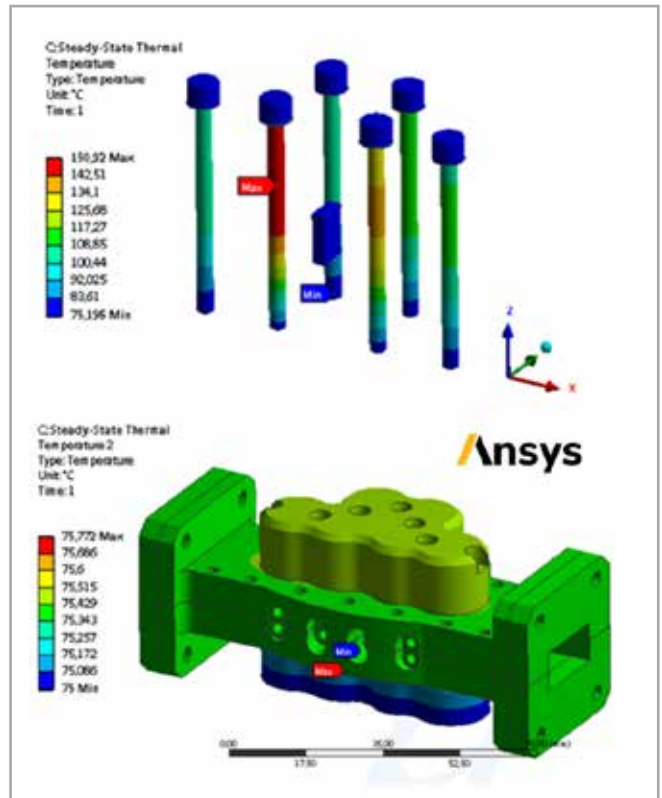


Fig. 9 - Ansys and HFSS high-power thermal simulations of the sixth-order filter Model 1 at the central frequency.

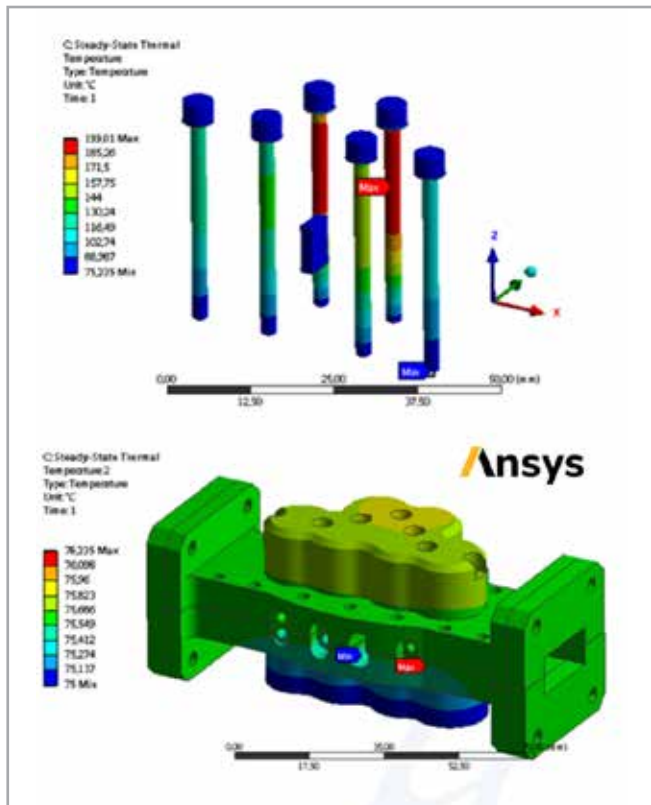


Fig. 10 - Ansys and HFSS high-power thermal simulation of the sixth-order Model 1 filter at the edge of the passband.

mechanical resonance mode of the sixth-order filter in Fig. 3a. As shown in Figs. 8a and 8b, the first modes are at 4059.9 Hz for the aluminum casing and at 2245.9 Hz for the ceramic cylinders, respectively; these are above the range of the specification for the vibration level (2000 Hz). Simulated results of the high-power thermal analyses performed at the central frequency are shown in Fig. 9.

A combination of HFSS and Mechanical simulations in Ansys Workbench was used to calculate the thermal drift with 150 W input power and to calculate the thermal drift of the S-parameter response. The simulations were performed including all physical properties of the metallic and dielectric parts. The estimated change in relative permittivity over the predicted temperature for the dielectric parts was also considered. A similar high-power thermal analysis was also performed at the passband edge frequency. The maximum temperature is reached on the ceramic elements, in particular the maximum temperature is 130 °C for the central frequency and 200 °C for the passband edge.

Concerning the thermal drift of the frequency, the maximum shift estimated by simulation is in the range 8 ÷ 16 MHz corresponding to 5 ÷ 8 ppm/°C (higher for the edge frequency, and lower for the central frequency). Fig. 10 shows the high-power thermal results of the analysis at the passband edge frequency.

High-power thermal simulations were also performed on the second filter model. However, the estimated temperature rise is greater due to the smaller volume and the smaller heat transfer surfaces. The maximum temperature reached on the ceramics is over 200°C.

**Test Results**

The first sixth-order Ku-band filter model was manufactured by achieving a volume reduction of about 50% compared to a standard filter based on the TE113 resonators, while keeping the Q-factor values compliant with the requirements. Fig. 11 shows the prototype of the manufactured filter and its 3D mechanical model, the structure is made of silver-plated aluminum. The final size (LxWxH) is 92mm x 45mm x 41mm with a mass of less than 200g in accordance with expectations. The comparison between the measured (solid lines) and simulated (dashed lines) responses is shown in Fig. 12. According to [7], the measured response has shifted upward in frequency by about 100 MHz compared to the simulated response in Fig. 6. This is attributed to the actual value of the dielectric constant of the ceramic resonators that have a tolerance that is difficult to compensate for using only tuning screws. The actual value of the permittivity of the dielectric elements ( $\epsilon_r = 12.4$ ) was used in the simulation for a proper comparison with the measurement as shown in Fig. 12.

The measured unloaded Q-factor is above 4500 as expected, and the out-of-band attenuation is very good taking into account the frequency shift. In addition, the insertion loss of less than 1 dB (objective) over the entire passband is compliant.

According to [8], the final environmental and high-power tests were also performed in this filter model and promising results were

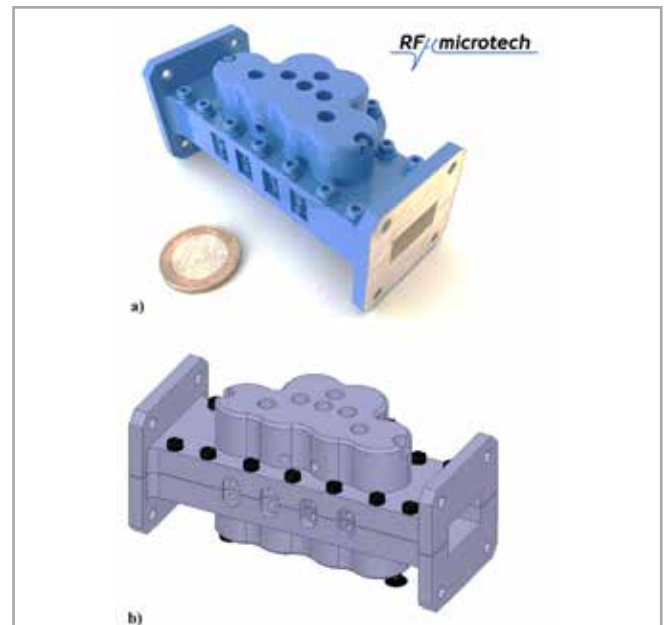


Fig. 11 - Manufactured (a) and mechanical (b) architectures of Ku-band filter Model 1.

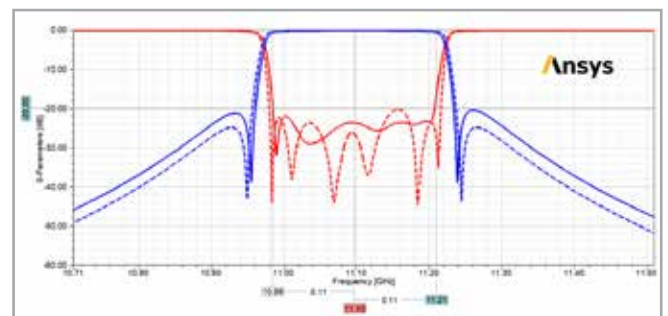


Fig. 12 - Comparison between measurement (solid lines) and simulation (dashed lines) of the designed Ku-band filter Model 1.

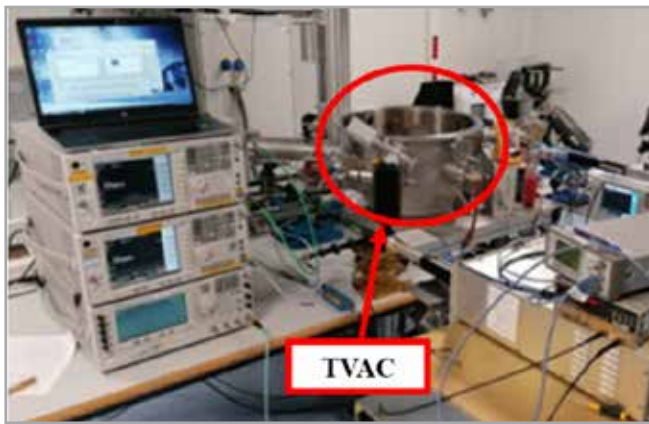


Fig. 13 - RF breakdown test setup.

obtained. Fig. 13 shows the RF breakdown test setup in which the filter is placed inside the Thermal Vacuum Chamber (TVAC).

## Conclusions

Two compact sixth-order Ku-band elliptic filters for high-power satellite applications were designed as part of an ESA ARTES AT project in which compactness and power-handling in space environment are key requirements. In this paper, filters based on TM dielectric-loaded combline resonators combined with barrel-shaped cavities were presented in this paper and first experimental results are shown. Filter design and simulation were performed using Ansys software from both electronic and thermo-

mechanical perspectives. In both filter cases, the geometries and materials were carefully chosen in order to improve the high-power performance in terms of power-handling and multipactor. A first model was designed considering dielectric resonators with permittivity of 12.6 achieving volume and mass savings of about 50% compared to standard TE113 resonators. A second smaller prototype was proposed using ceramic elements with higher permittivity ( $\epsilon_r=24$ ), however only a detailed analysis of the first model was performed and it was chosen for preliminary manufacturing and testing processes since it is less critical in term of manufacturing tolerances. In this scenario, the measured filter response of the first model shows promising results with an unloaded extrapolated Q-factor of about 4900.

According to preliminary test [8], multipactor discharges up to 1400 W at the central frequency were not obtained, while 130 W at continuous wave (CW) concerns the maximum power achieved from the power-handling point of view, which is slightly lower than the expected value (150 W). During the power-handling test, there was a non-negligible temperature rise in line with that predicted by thermo-mechanical simulations.

## Acknowledgment

*The filters described in this paper are the outcome of the ESA ARTES AT project named DOMUK (ESA Contract Number: 4000125645/19/NL/NR). We would like to thank the staff of ESA ESTEC (in Noordwijk, The Netherlands), ESA-VSC Lab (in Valencia, Spain) and the University of Perugia (in Perugia, Italy) for their contributions and support.*

*This work is dedicated to the memory of Prof. Roberto Sorrentino, whose work, honesty, and integrity will forever inspire his past students and colleagues towards excellence.*

For more information:

Andrea Serra - EnginSoft

[a.serra@enginsoft.com](mailto:a.serra@enginsoft.com)

## References

- [1] R. V. Snyder, G. Macchiarella, S. Bastioli and C. Tomassoni, "Emerging Trends in Techniques and Technology as Applied to Filter Design", IEEE Journal of Microwaves, vol. 1, no. 1, pp. 317-344, winter 2021.
- [2] R. V. Snyder, A. Mortazawi, I. Hunter, S. Bastioli, G. Macchiarella and K. Wu, "Present and Future Trends in Filters and Multiplexers", Microwave Theory and Techniques, IEEE Transactions, vol. 63, n. 10, 2015.
- [3] X. Chi Wang and Kawthar A. Zaki, "Dielectric Resonators and Filters", IEEE Microwave Magazine, pp. 115-127, October 2007.
- [4] M. Yu, "Power-handling capability for RF filters", IEEE Microwave Magazine, vol. 8, n. 5, pp. 1527-3342, 2007.
- [5] L. Pelliccia, F. Cacciamani, A. Cazzorla, D. Tiradossi, P. Vallerotonda, R. Sorrentino, W. Steffè, F. Vitulli, E. Picchione, J. Galdeano, P. Martin-Iglesi, "Compact On-board L-band Dielectric-loaded Diplexer for High-power Applications", 49th European Microwave Conference, EuMC, Paris, 2019
- [6] S. Chi Wang, K. A. Zaki, A. E. Atia and T. G. Dolan, "Dielectric combline resonators and filters," in IEEE Transactions on Microwave Theory and Techniques, vol. 46, no. 12, pp. 2501-2506, Dec. 1998, doi: 10.1109/22.739240.
- [7] P. Vallerotonda, F. Cacciamani, L. Pelliccia et al., "Dielectric-loaded Ku-Band Filter for High-power Space Applications based on Barrel-shaped cavities". Accepted for European Microwave Week Conference (EuMW), London, February 2022.
- [8] P. Vallerotonda, F. Cacciamani, L. Pelliccia et al., "Ceramic-loaded Barrel-shaped Ku-band filter for High-power Satellite Applications". Accepted for International Microwave Filter Workshop (IMFW), Perugia, Italy, November 2021.
- [9] Richard J. Cameron, Chandra M. Kudsia and Raafat R. Mansour, "Microwave Filters for Communication Systems," 2007.

## About RF MICROTECH

RF Microtech is a service company that develops customized products and smart solutions for industries and system integrators operating in the field of telecommunications, SatCom, aerospace, localization and the manufacturing sector.

The company is based in Perugia (Italy). It offers innovative solutions in the fields of antennas, phased arrays, beam forming networks, microwave filters and multiplexers, tunable and reconfigurable devices, for satellite and terrestrial communications, radar, sensing, localization and tracking systems for industrial applications.

RF Microtech supports its customers at every stage of the production cycle, from feasibility studies, custom design, prototyping, manufacturing, and testing. It also pursues R&D in emerging technologies for advanced microwave applications.

RF Microtech is ISO 9001 certified for Design Development, Prototyping and Production of customized application.

Visit [rfmicrotech.com/](http://rfmicrotech.com/) and follow the company on LinkedIn.



# New solution for cost-effective electromagnetic analysis

EnginSoft's contribution recognized in the F4E Technology Transfer Program

by Giovanni Falcitelli  
EnginSoft

On the 25<sup>th</sup> of March 2021, EnginSoft participated as an exhibitor in an important webinar hosted by Fusion for Energy (F4E), called: "Fusion technology applications in advanced simulation and modelling". This event was part of a wider F4E initiative - The Technology Transfer Program - which aims to promote the transfer of fusion technologies to European industry.

In the webinar EnginSoft was able to talk about its long-standing collaboration with F4E in the broad area of Electromagnetic FEM Analyses for the ITER components. EnginSoft's presentation covered many of the technical details of its acknowledged "Solution for cost effective electromagnetic analysis".

The main problem with a large Tokamak design is how to properly evaluate the Lorentz forces that form as a result of the coupling between the high intensity magnetic field and the currents that develop inside each metal component after a plasma disruption and/or the failure of the Coil System.

A disruption is a violent event that terminates the magnetic confinement of plasma. One of the magnetic effects of a disruption is the generation of large magnetic forces in the metallic structures surrounding the plasma. This phenomenon is associated with the sudden loss and displacement of the net plasma current, which induces an eddy current in the metallic structures.

EnginSoft's cost-effective solution was successfully created in collaboration with F4E's expert teams after numerous years spent developing and testing tools, algorithms and customized interfaces in each phase of the Electromagnetic FEM analysis workflow.

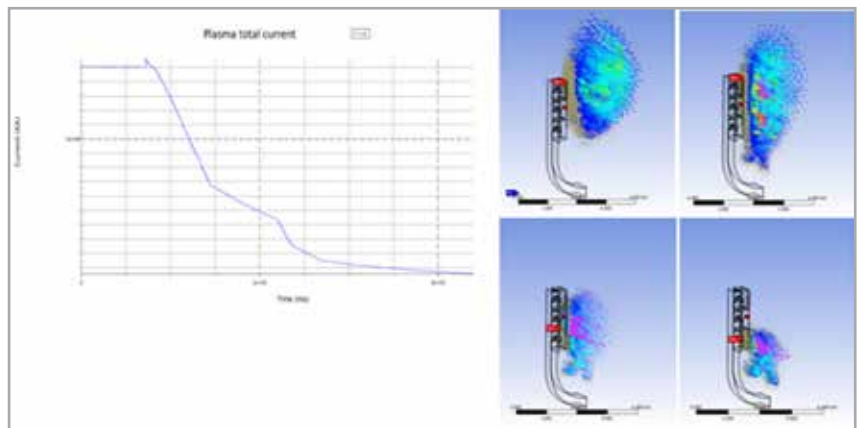


Fig. 1 – A typical plasma disruption VDE III Down event in ITER: (left) the graph of the total plasma current evolution vs time; (right) four images of the plasma current density at different times

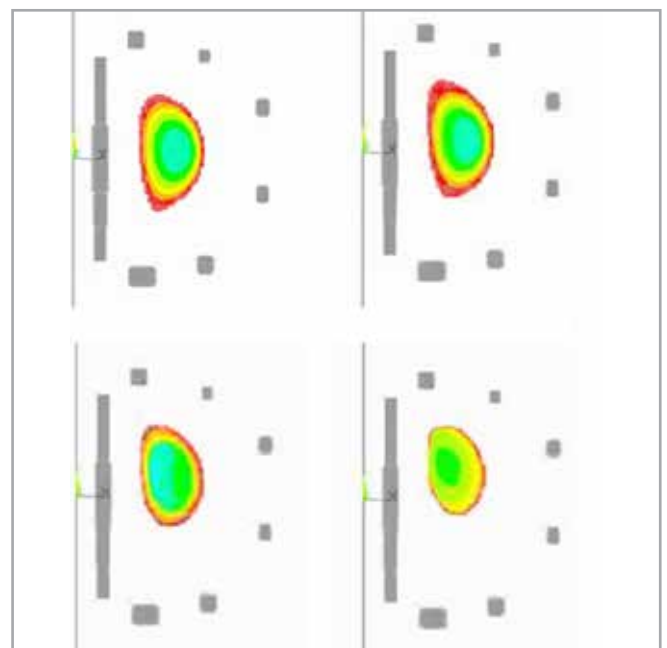


Fig. 2 – Sequence of plasma current density at 4 different time instants during a VDE II UP rapid plasma disruption event. The mapping algorithms from the "Current Filaments" from the DINA files to any mesh domain is one of the most important outputs for the quality of each result.

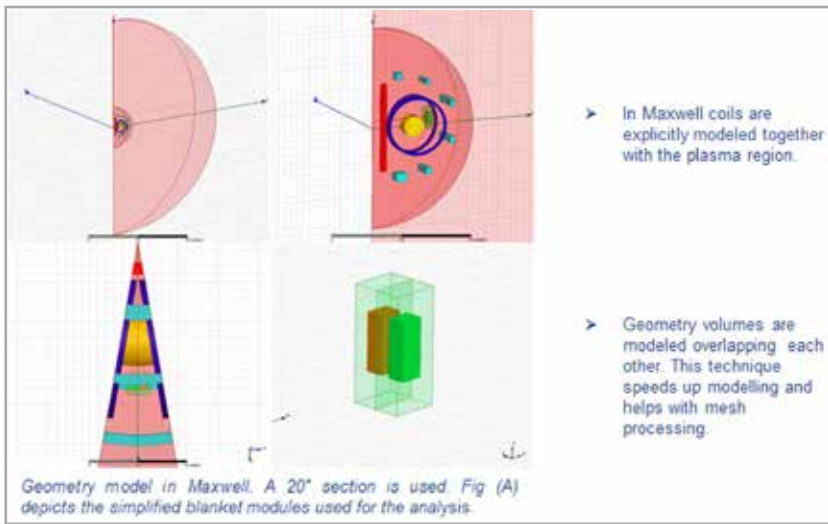


Fig. 3 – Custom and intuitive parametric user interface for Ansys Electronic Desktop for quick configuration of the geometry and loads

These include:

1. Robust, tested algorithms for extracting plasma current values from DINA files and mapping the corresponding plasma current densities to a generic mesh with no data loss.
2. The intuitive custom parametric user interface for Ansys Electronic Desktop for quick configuration of the geometry and loads
3. Auto-adaptive mesh algorithms for Ansys Maxwell to cross-check FEM accuracy
4. Powerful Ansys APDL macros to quickly and accurately extract results from millions of electromagnetic DOF FEM models.

Over the past two decades, EnginSoft has achieved a high level of specialization in the analysis and design of a range of electromagnetic and electromechanical devices:

- Electromagnets & Permanent Magnets

- Electromechanic Actuators & Sensors
- Electric Motors
- Electric Generators
- Electric Transformers
- Power Electronic Components and Devices

In all these applications, the tools developed with F4E as part of the “Solution for cost effective electromagnetic analysis” are particularly useful for:

- increasing the capability to perform Multiphysics Analysis
- improving ease of use of the basic tools
- reducing overall simulation process times

### Conclusion

There are many uses for the technologies and the FEM techniques that have been developed within

this context in the broader universe of SBES for Electronics and so EnginSoft is proud to have been selected by F4E as one of its partners for the “Technology Transfer Program”.

For more information:

Giovanni Falcitelli - EnginSoft  
[g.falcitelli@enginsoft.com](mailto:g.falcitelli@enginsoft.com)

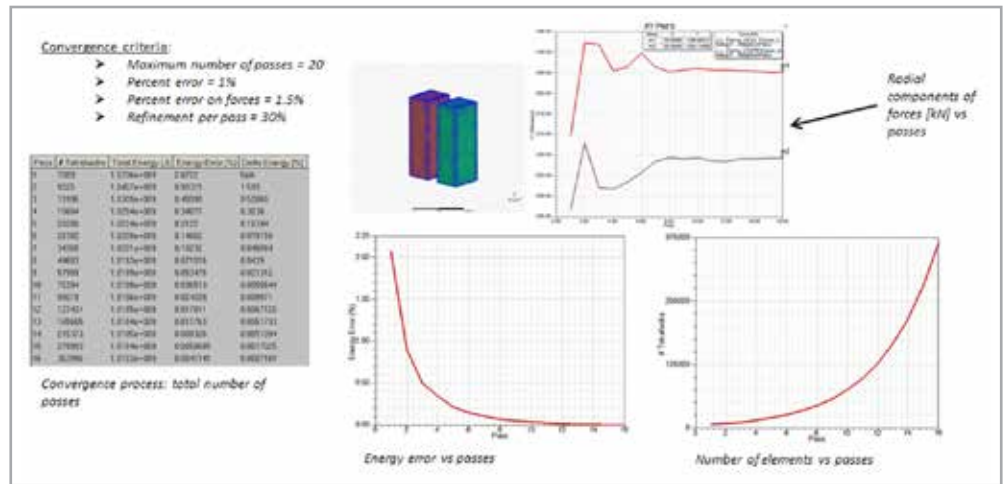


Fig. 4 - Auto-adaptive meshing algorithms for Ansys Maxwell to cross check FEM accuracy

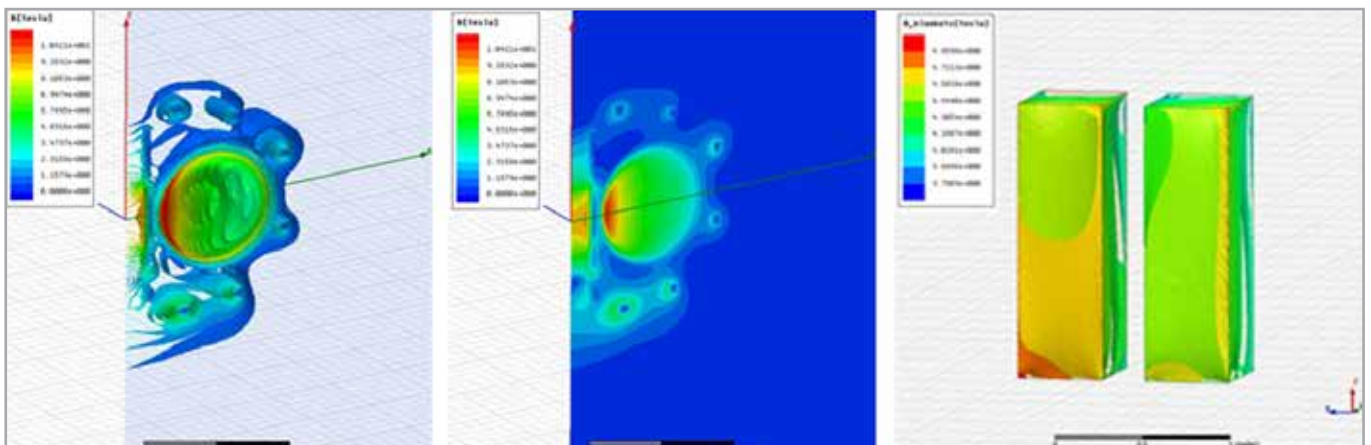


Fig. 5 – High quality post-processing tools in Ansys Maxwell



Fig. 1 – The Little St. Bernard pass

# Quick and easy estimation of the usage of a battery-powered electrical vehicle to explore cooling system performance

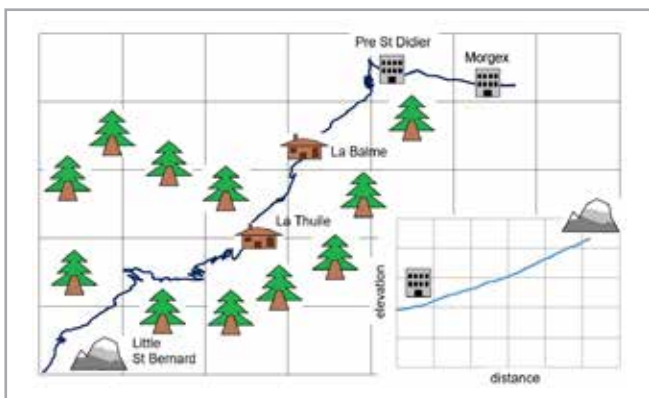
A case study of a real-world mountain road

*Both effective and proposed European Union regulations to mitigate global warming represent a game changer for the automotive industry. The main pillars of this strategy are a ban on fossil fuel-powered passenger vehicles and the replacement of in-facility fuel economy tests with Real Drive Emissions roadside checks. The design of the cooling system of a battery-powered electric vehicle (BEV) now requires an understanding of customer car usage which must be predicted by often-busy performance experts. This process is more effective if thermal engineers run their own simplified, rapid-response vehicle performance software to feed their priming models during early development of the vehicle.*

Effective automotive systems and their controls are major enablers for extending the range of battery-powered electric vehicles (BEVs) and attracting more customers. This result comes at a price; many driving patterns have to be explored by vehicle performance experts in a tight, advanced engineering schedule, and this process can be slow and expensive.

One possible solution is distributed simulation, taken by the SETI project from 1999 to 2020 creating a crowdsourced computer network to analyze radio signals from space. A similar approach relying on basic engineering skills and simplified software to predict BEV power lap times was shown to be effective in a previous study. This case study goes further by investigating the thermal response of a BEV's cooling system when driving on a mountain road.

Two pieces of software are used for this purpose. Vehicle performance is estimated using a freeware based on concentrated mass and tire grip. It does not consider longitudinal or lateral mass transfer, and the tire rolling resistance is basic, but it does feature a detailed road design suite. The BEV cooling system is modelled in Flowmaster© 1d computational fluid dynamics (CFD) software and configured for transient thermal simulations, thus enabling the efficiency of the pumps, valves, and fan controls to be investigated. [1]



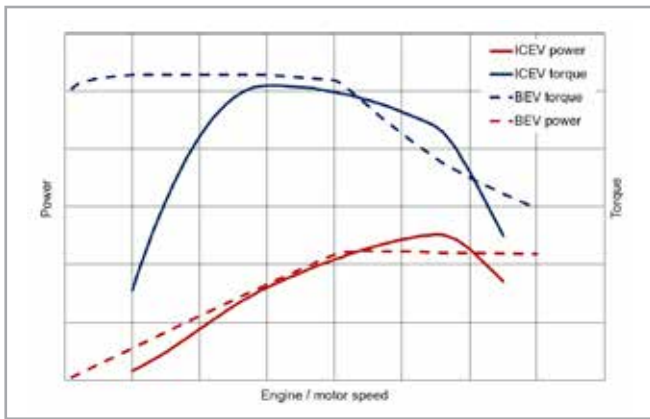


Fig. 2 – Virtually created BEV motor performance

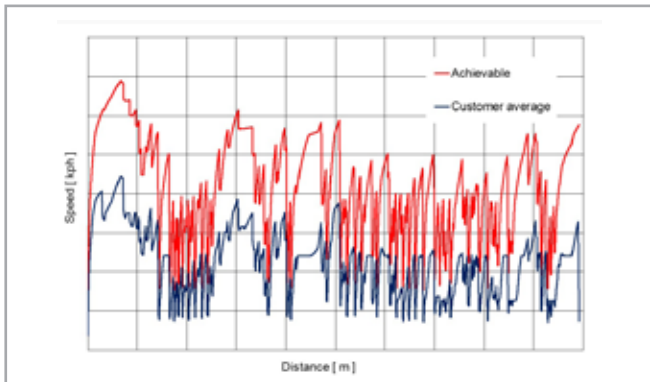


Fig. 3 – Calculated reference ICEV average customer and maximum achievable driving patterns

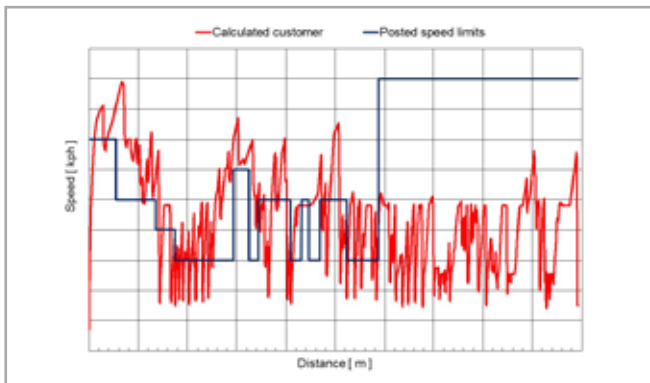


Fig. 4 – Calculated ICEV average customer driving pattern vs sign-posted speed limits

The study begins by selecting a mountain route, well suited to modelling the driving style of an average customer. The Little St. Bernard Pass (Italian road SS26) is chosen. This is a 25 km long summer vacation route with a moderate gradient of 5% and a summit elevation of 2,188 m and includes switchbacks, straights, tunnels, urban zones, and sign-posted speed limits. The road has been projected using both digital maps and GPS records, the reliability of which is noteworthy as far as positioning is concerned but poor as regards elevation, unless the barometric altimeter is calibrated and activated. This combination permits a trip length error of 3% and an elevation error of 5%. [2]

This is followed by the vehicle model setup and reliability evaluation using the same GPS records for an internal combustion engine vehicle (ICEV). The calculated top speed and acceleration

results are compared to the official specifications and found to be in fair agreement. The ICEV is then virtually transformed into a BEV by replacing the parts of the fuel-driven powertrain with an equivalent electrical motor and a battery pack providing same range. The BEV and ICEV share the same aerodynamic drag, rolling resistance, and grip coefficients, but the BEV's curb mass is increased by 400 kg.

The next step is to simulate driving the Little St. Bernard Pass. The reference maximum achievable performance for the ICEV is calculated first by setting full engine capacity, redline revs per minute (RPM) gear shifts, maximum tire grip, and driver-only payload. Then the average ICEV customer's driving pattern is explored, assuming a three-passenger payload, peak torque gear shifts, limited tire grip, and reduced engine power due to the elevation.

The calculated results of the average ICEV customer driving pattern show half the average speed and three times less energy demand, compared to the results of the maximum achievable driving pattern.

The overall average speed difference for the route is 16% but falls to 3 km/h, below the software-reported error level, when operating in the upper, open road portion beyond last settlement. This road section is not regulated by any sign-posted speed limit and achievable speed is provided by vehicle specifications, engine performances, tire grip and driver's skill.

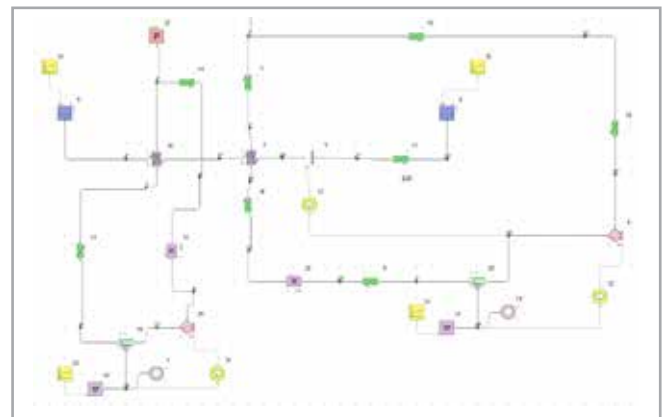


Fig. 5 – Model of the BEV engine cooling system

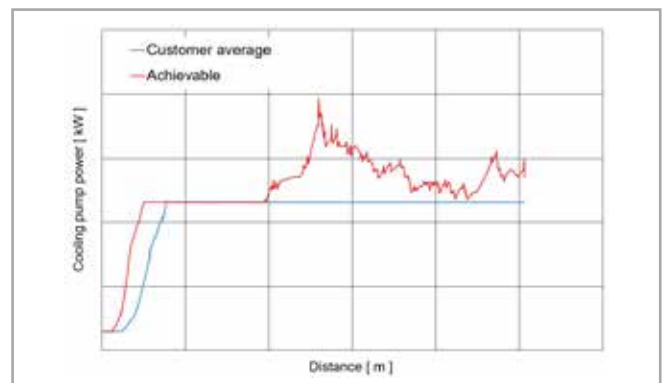


Fig. 6 – Activation of the cooling system on the Little St. Bernard Pass

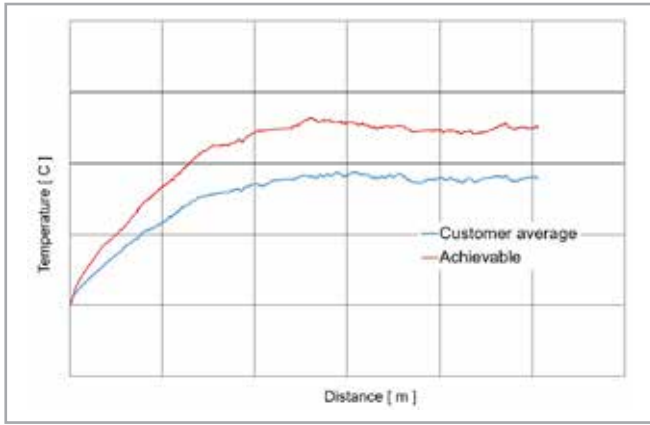


Fig. 7 – eMotor (battery) temperatures on the Little St. Bernard Pass

The model of the driving pattern of the average BEV customer also includes a three-person payload and the same tire grip, but no decrease in engine power due to elevation and the motor RPM is limited to the steady torque region only. Again, the average speed of the customer driving pattern is halved compared to the maximum possible figure, but the difference in energy demand is not as great as that detected for the ICEV model. More interestingly, both the average BEV and ICEV customer driving patterns achieve similar speeds, and their energy demands are close: the BEV's higher energy demand due to its increased mass is offset by better powertrain efficiency. [3]

The final operation is to perform the BEV cooling simulation. The BEV thermal model describes two separate cooling circuits, one serving the e-motor, the other serving the traction battery, and their heat exchangers are stacked one on top of the other to allow the use of a single fan to supplement the cooling airflow. The

**References**

- [1] B. Xu, M. Leffert, M. and B. Belanger, "Fuel Economy Impact of Grille Opening and Engine Cooling Fan Power on a Mid-Size Sedan," SAE Technical Paper 2013-01-0857, ISSN 0148-7191
- [2] A. Kulkarni, R. Sapre, and C. Sonchal, "GPS Based Methodology for Drive Cycle Determination", SAE Technical Paper 2005-01-1060, 2005, ISSN 0148-7191
- [3] G. Gotta, Stellantis, "BEV performance by freeware: faster, cheaper. And better too?" International CAE Conference: on the digital transformation of industry, November 30-December 4, 2020, Vicenza, Italy.

entire system and its controls are designed to reduce the use of pumps, valves, and fans, and to save energy.

Subsequently, the summer environment of the Little St. Bernard road is set and both the average BEV customer driving pattern and the full-performance driving pattern are introduced.

The cooling system requires 30% more energy to handle the aggressive mountain driving, but the temperature is successfully controlled without engaging the most effective thermal stage.

This study confirms that a distributed and simplified simulation process can support the early development of BEV automotive cooling systems. Further investigations are planned to explore the relationship between BEV performance and range, and then to analyze the response of the cooling system to the selected solution.

For more information:  
 Giancarlo Gotta – Stellantis  
[giancarlo.gotta@stellantis.com](mailto:giancarlo.gotta@stellantis.com)





by Kosuke Masuzawa<sup>1</sup>, Shun Fujimoto<sup>2</sup> and Akiko Kondoh<sup>2</sup>  
 1. akf, Inc - 2. Prometech Software, Inc.

# Application of Particleworks to the design and performance evaluation of waterproofing for automotive air conditioning systems

When it comes to cars, people tend to focus on driving performance and safety. However, one should not forget about the air conditioning system, which plays a crucial role in enabling a comfortable ride over long periods, even in extremely hot or cold weather conditions or in heavy rain. There was a time when air conditioning in cars, which we now take for granted, was a luxury only found in expensive cars. After years of development and innovation, all vehicles today are equipped with air conditioning systems. However, the design of such systems is not simple since they operate at full capacity in all weather conditions. As with the vehicle body and various other automotive parts, it is necessary to evaluate the system's performance through experiments that assume driving under real weather conditions and through simulations using CAE. This article introduces a case study on

the waterproofing of an automotive air conditioning system for rainy conditions using Particleworks, a particle method CFD software.

Air conditioning in cars inevitably requires ventilation inlets to introduce external air. A waterproof design is necessary since rainwater is likely to enter with the exterior air. To evaluate the impermeability of an air conditioning system, a simulation tool that considers water droplets and free surfaces is required. Using these tools usually requires a high degree of skill. However, Particleworks, which uses the particle method, is a simple tool that non-professionals can use to study waterproofing.

In many modern cars, the air conditioning system, commonly referred to as an HVAC, provides integrated air conditioning control with heaters (heating), ventilation, and air conditioning (air conditioning and cooling).

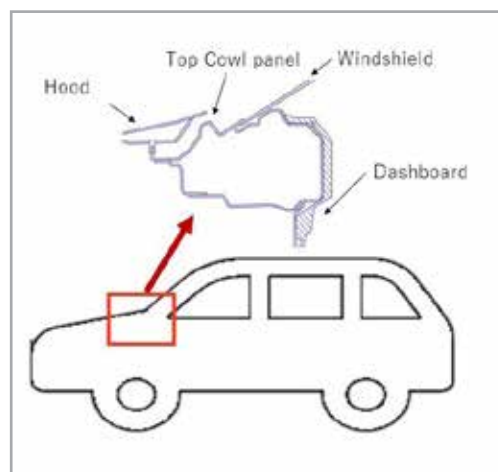


Fig. 1 - Cross-section of top cowl panel

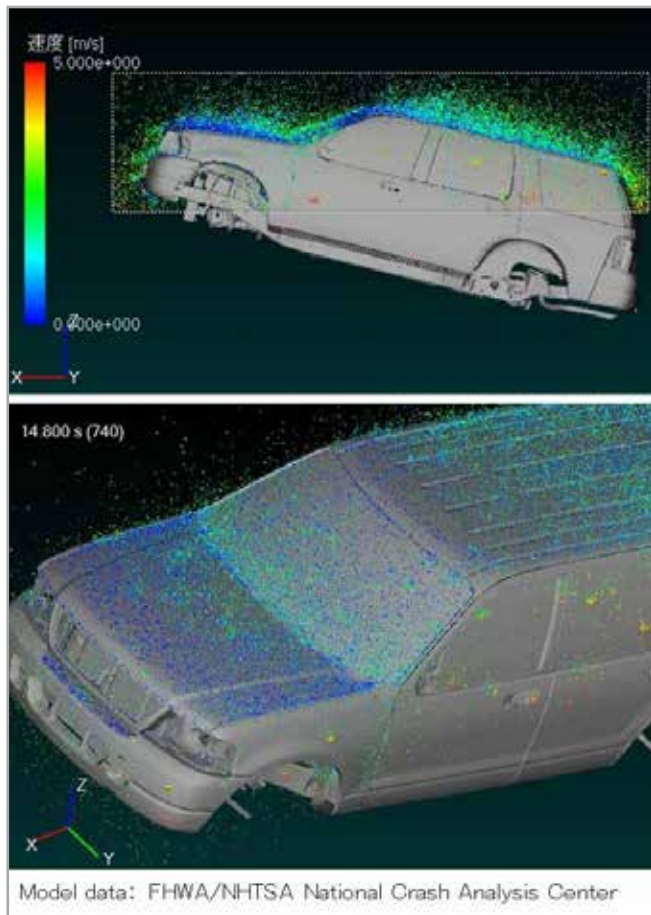


Fig.2 - Rainfall simulation of the whole vehicle body inclined uphill at a 15-degree angle

The heater heats the interior air of the vehicle with a radiator using hot coolant from the engine, while the ventilation function controls between recirculating internal air and introducing external air. In addition, air conditioning sends cool air into the car through a refrigeration cycle that uses a compressor and a condenser. This simulation using Particleworks, focused on the ventilation portion of the system.

Internal air recirculation, which is one of the ventilation functions, only enables the recirculation of air inside the car without any incoming air from outside. It is used to improve the cooling capacity in scorching weather. It operates when the user deliberately blocks polluted external air from entering, such as when driving behind a large vehicle. However, there are some disadvantages, including the tendency for windows to fog up due to increased humidity in the cabin. There is also the possibility that the driver's concentration may fall due to the lack of oxygen because of decreased air freshness.

On the other hand, external air induction is a function that delivers fresh air from outside the car into the cabin. By drawing external air from the front of the vehicle and expelling it from vents in the rear of the vehicle, the air inside the car cabin

is refreshed. Most modern cars are equipped with automatic air conditioners. In setting up their control, it is common to essentially set the air conditioner to introduce external air, except in scorching weather.

So, what do we need to pay attention to when introducing external air? Since the HVAC system is located in the front of the vehicle, external air is introduced from the front of the vehicle. However, the front of the vehicle is also home to the engine compartment that generates heat due to the combustion from the engine itself, and is also the site of the heat dissipation from heat exchangers such as the air conditioning condenser and radiator. This means that it is essential to introduce fresh air that avoids these high temperatures. Therefore, as shown in Fig. 1, it is common to introduce external air from the upper cowl vents between the windshield and the hood. However, the problem arises that water enters through these vents during rain. It is therefore necessary to design a waterproofing system that separates the air from the liquid, allowing only the air to enter the HVAC system and preventing water from entering the passenger compartment.

In the Particleworks simulation, we first analyzed the rain patterns for the full vehicle when parked to reproduce the overall rain situation. Here, assuming that the car was parked on a flat surface, we were able to confirm that the rainwater falling on the vehicle body flowed to the top of the cowl across the windshield. Next, to evaluate the results in more severe conditions, a rainfall analysis was performed with the vehicle body inclined uphill at a 15-degree angle. This confirmed that a large amount of rainwater flowed back to the car cabin from the hood area, and mainly from the windshield when stopping the car (Fig. 2). In other words, it was apparent that it was necessary to design the top section of the cowl to allow fresh air to flow in and to enable waterproofing of the cabin.

To evaluate the water flow into the top of the cowl in greater detail, a simplified model as shown in Fig. 3 was used. The area enclosed by the black dotted frame and surrounded by the windshield, hood, and fenders, and including the exterior air inlet, is the subject of this analysis. This model is well separated from the engine compartment when viewed from the side and has holes on both ends for drainage. The red frame seen on the inside of the model is the air intake for the HVAC unit and we will study its design to prevent rainwater from entering here.

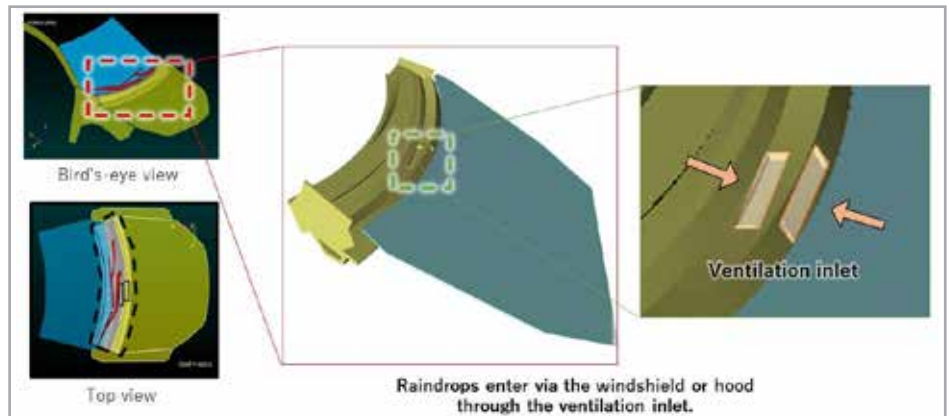


Fig. 3 - Simplified simulation model

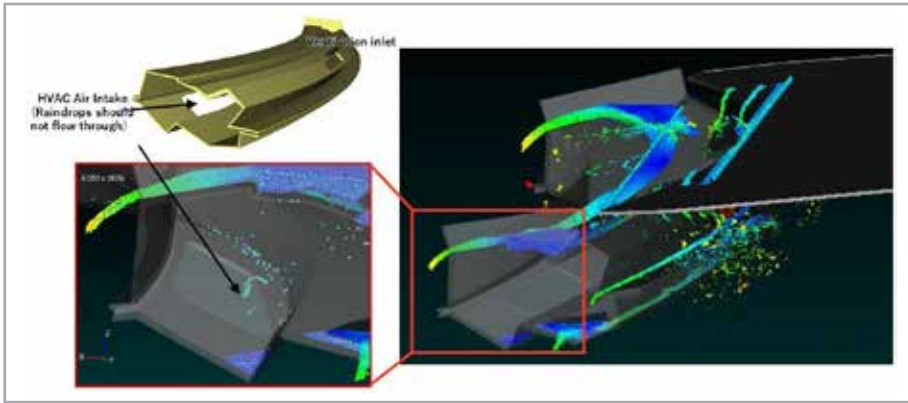


Fig. 4 - Water flow simulation of top section of cowl at a 15-degree uphill incline

Fig. 4 shows the results of the water flow analysis at the top of the cowl top with a 15-degree inclination. In this case, based on the results of the whole car rain analysis, the mass flow rate conditions were set to reproduce the flow from the windshield and hood areas, and the other conditions were analyzed using the Particleworks default settings. We were checking to see if water was entering the exterior air inlet. At this 15-degree inclination, it was confirmed that the water flow from the hood was the inflow path to the top of the cowl. We also found that the water that had accumulated due to the slope was overflowing into the vicinity of the external air inlet.

Having confirmed the above, it was found that there are two possible routes for water to enter the external air inlet: one being the path where raindrops that have entered and dripped down enter as droplets, the other being the water that has accumulated near the opening overflows and enters when the car inclines. Various countermeasures can be considered here, and the design plan will be discussed while factoring in the cost.

In this study, we considered two countermeasures for the original cowl top and conducted simulations. Countermeasure 1 adds a simple wall to the bottom edge. Although it is basically necessary to prevent all splashes, and a simple wall would not be sufficient, we decided to only add a wall in countermeasure 1 to see what improvement could be achieved at the lowest cost. In countermeasure 2, we examined the shape of a cover to simultaneously prevent splashing and water overflow. We modeled a part that inverted a typical range hood or duct cover (see Fig. 5).

Fig. 6 shows a comparison of the initial shapes, countermeasure 1 and 2 and the simulation results, and Fig. 7 shows a graphical

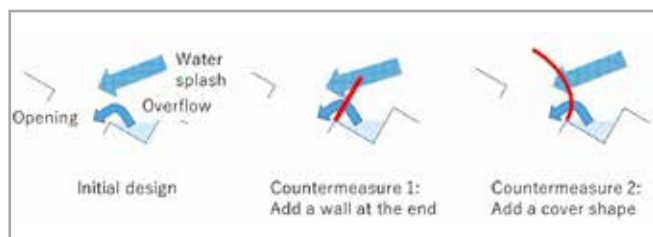


Fig.5 - Considerations of countermeasure design ideas

comparison of the number of particles (the amount of water) entering into the air inlet with the initial shape, with countermeasure 1, and with countermeasure 2. We found that countermeasure 1 prevented the water from overflowing, but was not sufficient to prevent droplets. In contrast, countermeasure 2, a design proposal that adds a duct cover, reduced water infiltration by about 90% compared to the initial shape.

Using Particleworks to study the waterproofing design of the external air intake of a car air conditioning system, it is possible to visualize the event itself by simulation, to clarify the problems and causes generated by the initial shape, and study the countermeasures and their effectiveness. As you can see from the simulation results, we were successfully able to use Particleworks to improve the waterproofing performance by preventing drops from entering the cabin.

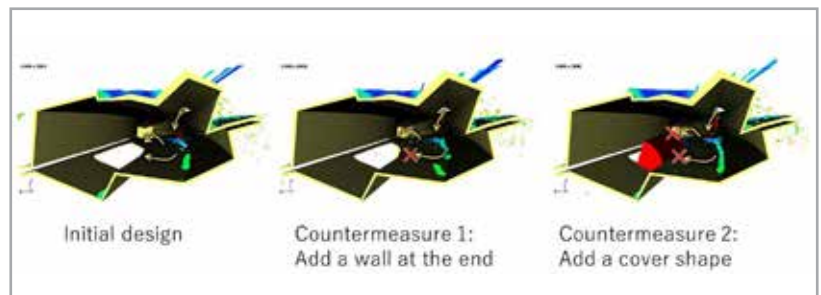


Fig.6 - Comparison of simulation results for each countermeasure design proposal

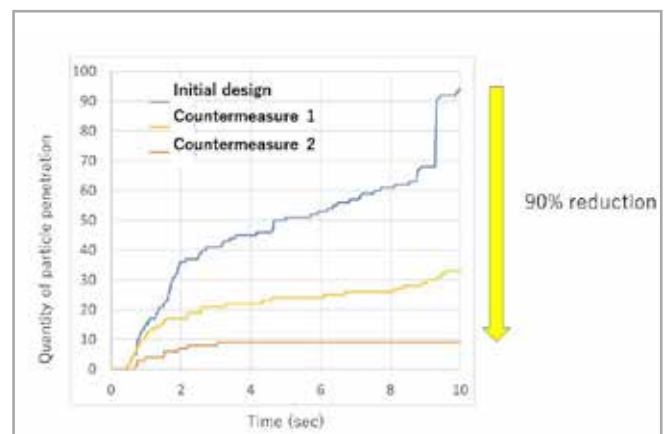


Fig.7 - Comparison of water inflow for each countermeasure design idea

The advantage of using Particleworks in this project was that it was easy to model and simulate without any meshes. In particular, we were able to quickly compare multiple design proposals, reflecting simple countermeasure shapes.

Particleworks is expected to be used more widely in the future as a tool that can quickly and stably simulate such various fluid behaviors.

For more information:  
 Akiko Kondoh - Prometech Software  
[kondoh@prometech.co.jp](mailto:kondoh@prometech.co.jp)



# Pipistrel: flying straight from simulation to production



ESTECO optimization technology as a way to skip the prototyping phase for a hybrid-electric aircraft propeller

*Pipistrel, an aviation and aerospace company based in Slovenia, chose ESTECO technologies to design the propeller for a highly efficient, hybrid-electric aircraft. The work was part of the EU-funded project MAHEPA (Modular Approach to Hybrid Electric Propulsion Architecture), which aimed to advance two variants of a low-emission, serial, hybrid-electric propulsion architecture to Technology Readiness Level (TRL) 6. modeFRONTIER process automation and optimization software enabled the simulation process to be automated so that innovative and optimized designs could be identified in a limited amount of time.*

## Challenge

Pipistrel's engineers faced the challenge of designing a propeller driven by a hybrid-electric propulsion system while taking into account the different conditions an aircraft encounters during the four phases of flight: takeoff, climb, cruise, and descent. Considering that the requirements for speed, power, and thrust change during flight, the objective was to maximize takeoff thrust and power recovery during descent and minimize power use during the climb and cruise phases. The optimization involved three stages: the preliminary optimization of the propeller, optimization of the airfoil, and the final optimization of the propeller.



*“We trust the results we get with modeFRONTIER so much that we do not expect to require a prototype. We will go straight into production”*

**David Eržen**  
Aerodynamics Engineer at Pipistrel

**Solution**

For this multi-phase optimization project, Rok Lapuh and David Eržen, aerodynamics engineers at Pipistrel, used modeFRONTIER coupled with CHARM (Comprehensive Hierarchical Aeromechanics Rotorcraft Model) and XFOIL, an interactive program for designing and analyzing subsonic isolated airfoils. By taking advantage of ESTECO's process automation technology, Pipistrel could automate the simulation workflows, evaluate thousands of designs simultaneously and identify innovative optimized results. This process was conducted completely autonomously leaving Pipistrel's engineers only with the task of selecting the most appropriate design.

In the first propeller optimization, Pipistrel optimized the chord and torque distribution to achieve maximum thrust and minimum power for a given set of airfoils. These results were then used as the requirements for the airfoil optimization. The design team used modeFRONTIER to design the airfoil based on specific geometric constraints (thickness, curvature, or leading-edge radius), while increasing lift and reducing drag. They initiated a Design-of-Experiments phase and then used the HYBRID genetic algorithm to successfully perform the airfoil optimization and obtain the Pareto front with the optimal designs. Lastly, they used the optimal airfoil for the final propeller optimization. With the ESTECO optimization algorithms, Pipistrel's engineers were able to evaluate nearly five thousand designs in a limited time and increase thrust by 30% during takeoff.

**Benefits**

Before using modeFRONTIER, Pipistrel used a manual process to simulate multiple designs and choose the preferred one. After introducing the ESTECO technology, Pipistrel's engineers were not only able to automate this process but could also evaluate options that would otherwise not have been considered. "modeFRONTIER optimization technology gave me the opportunity to think outside

**About Pipistrel**

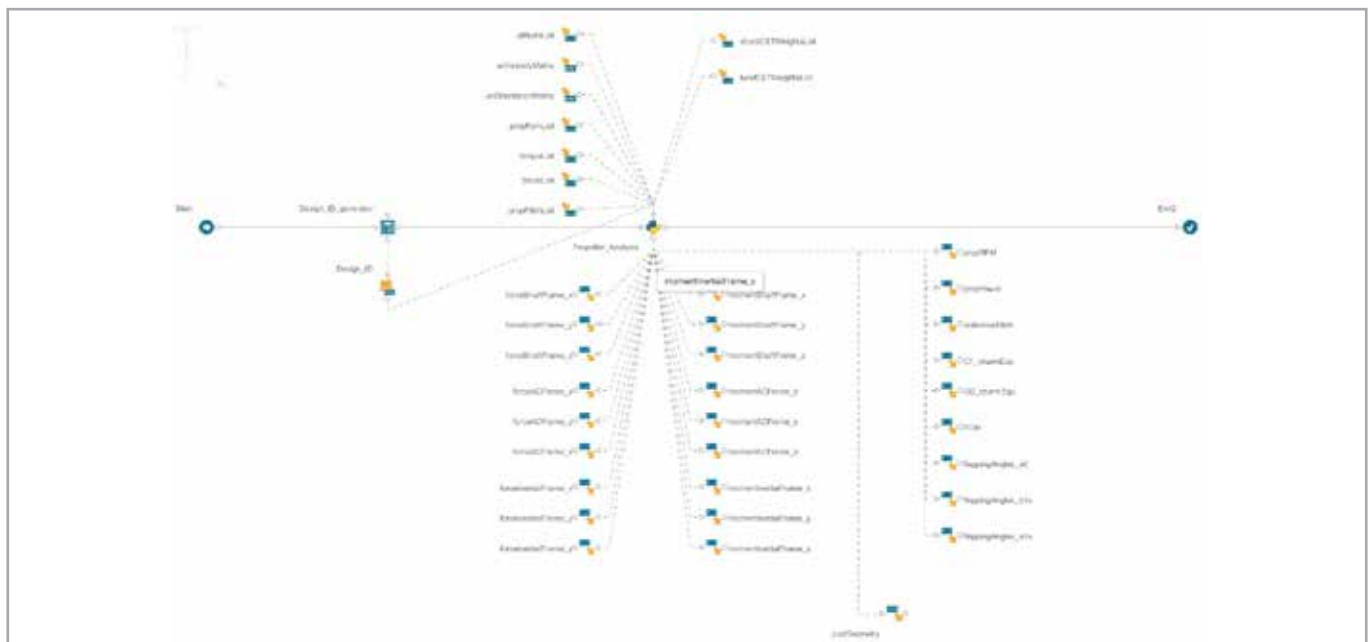
Pipistrel is an aviation and aerospace company based in Slovenia. It has more than 30 years of experience in the ultralight and general aviation industry. Starting as a small business it has become a leading producer of efficient aircraft with electric and hybrid propulsion systems.

**About Esteco**

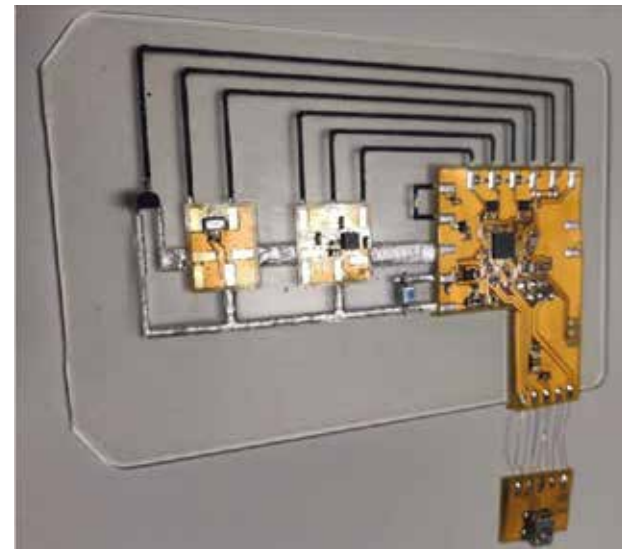
ESTECO is an independent software company, highly specialized in numerical optimization and simulation process and data management. With a 20-year experience, ESTECO supports over 300 international organizations in excelling in their digital engineering experience, accelerating the decision making process and reducing development time. Ford Motor Company, Honda, Lockheed Martin, Toyota and Whirlpool are just a few of the major companies relying on ESTECO technology. ESTECO is the owner of VOLTA, the collaborative web platform for Simulation Process and Data Management and design optimization, and modeFRONTIER, the comprehensive solution for process automation and optimization in the engineering design process. [esteco.com](http://esteco.com)

the box," said Rok Lapuh, Aerodynamics Engineer at Pipistrel, "We could find a design that is completely different to what we are used to, but that may work even better." The company has also dramatically reduced its time to market as it has moved from the simulation directly to production. "We trust the results we get with modeFRONTIER so much that we do not expect to require a prototype," stated David Eržen, Aerodynamics Engineer at Pipistrel, "We will go straight into production."

For more information:  
[info@esteco.com](mailto:info@esteco.com)



# Static and thermal FE analysis of a Flexible Electronic Board (FEBO) prototype and the characterization of its innovative materials



by Guido Servetti<sup>1</sup>, Federico Valente<sup>1</sup>, Marta Zaccone<sup>2</sup>, Valentina Bertana<sup>3</sup>, Gianluca Melis<sup>3</sup>  
1. ITACAe - 2. Proplast - 3. Politecnico di Torino

*An FE model of an experimental flexible electronic board was built to determine its performance in terms of mechanical and thermal distortions, heat and transient thermal flow, thereby detecting critical issues and identifying opportunities for improvement. Commercial sensors were connected to the flexible board (100x40x2mm), which was based on a commercial thermoplastic polyurethane (TPU), with a PEDOT-based conductive resin trapped in a PEGDA network, a biocompatible polymer. Three thermal loads ( $\Delta T=175^{\circ}\text{C}$ ,  $\Delta T=100^{\circ}\text{C}$ ,  $\Delta T=50^{\circ}\text{C}$ ) were applied which revealed critical stresses for high  $\Delta T$ s but at  $\Delta T=50^{\circ}\text{C}$  only the connectors had a critical  $\sigma_{\text{vm}}$  while for  $\Delta T=50^{\circ}\text{C} + 1\text{mm}$  displacement a critical strain value occurred in one area of the substrate. Heat transient analysis and overheating simulations were performed to determine the heat flow behavior for the photodiode and accelerometer. FE analyses allow more studies to be undertaken to improve material properties and suggest redesign activities for similar concept demonstrators. The funds of the European Union and the Piedmont Region, and agreements with the most important players in SBE (Simulation Based Engineering) software sales and services, allowed the authors (ITACAe srl, Proplast, and Politecnico di Torino) to conduct industrial research and experimental development together with manufacturers and users of innovative technologies to identify, study and optimize the design parameters of the board while simultaneously contributing to its technological development.*

A demonstrator of a flexible electronic board concept using novel materials was created with the intention of contributing to forward innovation by building a prototype to be used for different applications. The demonstrator's flexibility is a definite advantage for its applicability since it could be used in various types of

structures. The goal of the study was to demonstrate the functionality of a flexible electronic board made from innovative materials and to assess its operating conditions. The novel materials used were also examined in this study, first by characterizing their material properties and then by using finite element analysis (FEA) to understand their capabilities and importance in the demonstrator's design. The proposed analysis aimed to evaluate the mechanical and thermal characteristics of the prototype and to describe its applicability in different mechanical and thermal conditions.

FE software, in particular MSC Apex for the mechanical analysis and Ansys Mechanical for the thermal analysis, was used. This study was conducted as part of a regionally funded "SMART3D" project. Among the partners, contributions to the study presented come from ITACAe, which performed the FE analysis of the demonstrator; Microla, which provided the design characteristics and geometries of the demonstrator; Proplast, which developed and characterized the commercial thermoplastic polyurethane (TPU); and the Politecnico di Torino, which worked on the characterization of the PEGDA/PEDOT used to deposit the conductive traces.

## Description of the flexible board

The board consists of several electronic components assembled on a flexible commercial TPU substrate manufactured by Covestro [1]. The initial design had two different configurations, one with a flexible substrate and the other with a non-flexible substrate.

The analyses presented in this article concern the design with the flexible substrate, consisting of a temperature sensor, a pressure sensor, one LED, a photodiode, an accelerometer, and a microcontroller board. The sensors used came from a list of commercial models supplied by one of the SMART3D project partners (Argotec) and, in the end, the following items were

selected: temperature sensor “TMP36GT9Z”, pressure sensor “MS5611-01BA03”, LED 1206 SMD, photodiode “BPW34”, a MEMS-based 3-axis linear accelerometer “LIS344ALH”. The microcontroller was made from typical materials for electronic boards, namely copper wired to a rigid polyamide plate. The flexible rectangular substrate was obtained by an injection molding process of the TPU granules. The connections between the sensors were made with the innovative PEGDA/PEDOT material [2].

### Layout of the electronic board

The layout of the electronic board is presented in Fig. 1 below, while the sensors’ operating conditions are summarized in Table 1.

Temperature sensor	-55°C <Temp<150°C
Pressure sensor	-40°C<Temp<85°C
Photodiode	-40°C<Temp<100°C
Accelerometer	-45°C<Temp<85°C
LED	-40°C<Temp<85°C

Table 1: Operating conditions of the sensors.

The accelerometer and pressure sensor were mounted on a conventional electronic board while the temperature sensor, photodiode and LED were mounted directly on the flexible substrate. The conventional electronic board increases the stiffness of the flexible board causing relevant stress gradients that will be discussed later. Such change of stiffness is produced by all three boards but the microcontroller area has the greatest effect because it occupies the largest area, as seen in the layout.

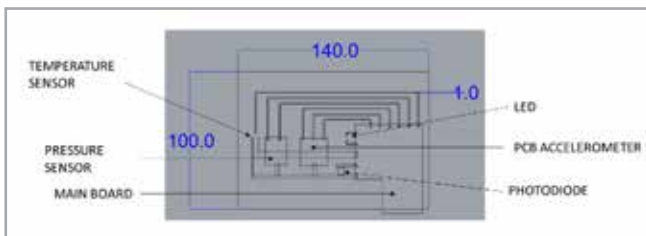


Fig.1 – Schematic layout of the electronic components on the Flexible Electronic Board (FEBO)

### Aim and objectives

The aim of the study is to understand which areas with critical deformations are important and how to modify them in the design of the board. In addition, actually producing the demonstrator will allow the feasibility of manufacturing and assembling it to be determined. Furthermore, the FE modelling presents a practical analytical approach to use while some its methodological limitations can be explored to improve its accuracy.

Last but not least, novel materials were used to fabricate the board. While integrating them into large-scale production could present difficulties, they could pave the way for a whole new manufacturing concept for highly customized electronic devices.

## Characterization of the materials

### TPU Desmopan 9370AU DPS 070

#### Polymer matrix

As previously mentioned, the polymer matrix selected was a commercial-grade ether-based thermoplastic polyurethane (TPU) (the Desmopan 9370 AU DPS 070), manufactured by Covestro. This material is specifically formulated for the injection-molding process and, in fact, this technology was processed to obtain a flexible rectangular-shaped board measuring 100x140x2mm.

This polymer was selected to prepare the flexible substrate based on a preliminary feasibility study completed by the SMART3D project in which experiments were done with different thermoplastic polymers, such as polyethylene terephthalate glycol (PETG) and ester-based TPU, processed with different fabrication techniques, namely film cast extrusion and injection molding.

The Desmopan 9370 AU DPS 070 was found to offer the best compromise among processability, flexibility, transparency, and cost and was therefore chosen to prepare the Flexible Electronic Board (FEBO) prototype.

#### TPU characterization

The TPU matrix was thermally characterized using thermogravimetric analysis (TGA) in an inert atmosphere (N<sub>2</sub>) with a temperature range of 50°C to 800°C. This specific test was performed to verify the polymer’s thermal behavior and resistance both at the typical temperature used for the manufacturing process and at the working temperatures of the applied sensors. The test detected a thermal resistance and stability of up to about 300°C.

The flexible polymer was also characterized in terms of its thermal conductivity. This test provided indications regarding the thermal capacity and thermal conductivity of the selected material. As expected for a polymer matrix, TPU was found to be thermally insulating, presenting a thermal conductivity of about 0.2 W/mK, as shown in Table 2.

Material	E (GPa)	Poisson	Density (g/cm <sup>3</sup> )	Thermal expansion	Thermal conductivity (W/(m·K))	Specific Heat (J/Kg·K)
Copper	122	0.33	8.96	1.7e-5	3.93	386
Silicon	47	0.28	2.332	8e-5	148	700
Polyamide	3.7	0.3	1.34	4.3e-5	0.22	1040
PEGDA/PEDOT	0.021	0.4	0.4	16e-5	0.23	1046
TPU Desmopan	0.011	0.4	1.06	1.24e-4	0.186	2300

Table 2: Material properties

#### PEGDA/PEDOT

##### Resin composition

As mentioned earlier, the board consists of a flexible substrate, electronic elements, and conductive polymer wiring. The latter was obtained by selective deposition of a new blend, PEGDA/PEDOT resin. As the name implies, it is prepared using two main ingredients: Poly (ethylene glycol) diacrylate or PEGDA and Poly

## ■ CASE STUDIES

(3,4-ethylenedioxythiophene) or PEDOT. PEGDA is a biocompatible hydrogel and forms the “structural” ingredient in the blend. PEDOT is an electrically conductive polymer well-known in the field of printable electronics.

The PEGDA and PEDOT were blended in a ratio of 55:45 of the final resin weight. 1%wt (relative to the PEGDA weight) of the radical photo initiator, IRGACURE 819, was also added. In fact, this resin was intended for use both in the custom fabrication process discussed here, and in commercial stereolithography 3D printers.

Therefore, this liquid mixture can be deposited in layers and then, when irradiated with an appropriate wavelength (in this case 405nm) will polymerize and harden.

### **Electrically conductive properties of PEGDA/PEDOT**

Previous work has demonstrated the varying electrical conductivity of mixtures containing different PEGDA/PEDOT ratios. For the work reported here, the 55:45 ratio was chosen for two main reasons. Firstly, the quantity of PEDOT, which is more viscous than PEGDA, provides a fair compromise between low spreadability (on the substrate) and good flowability (through the syringe and tube used for its deposition).

Secondly, this quantity of PEDOT ensures a conductivity of 0.05 S/cm for the polymer. Additional testing, which is beyond the scope of this article, has shown that this conductivity level will guarantee that the flexible electronic board operates correctly.

### **FE Analysis**

The FE study consisted of several analyses that have been summarized below:

- CAD model of the demonstrator geometry using MSC/APEX, PTC/CREO Parametric.
- FE model construction (MSC/APEX)
- FE analysis (MSC/Apex, MSC/NASTRAN [3], Ansys Mechanical 2020 R2 [4])
- Modal analysis
- Mechanical load analysis
- Thermal load analysis
- Heat flow and transient thermal analysis

The purpose of the analyses is to determine the critical stresses and strain gradients resulting from the movement of the flexible board, and then to make design recommendations.

In addition, the thermal loads were considered to understand how they affect the demonstrator’s criticality, and then a heat flux study was conducted to discover the board’s transient and critical temperatures.

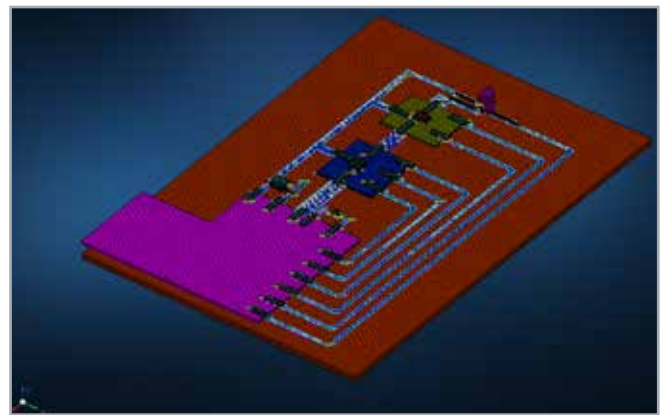


Fig. 2 – FE Model of the demonstrator

### **Model description**

The demonstrator was modelled using Hexahedral for the 3D elements (8 nodes) and Quad Element for the 2D element (4 nodes). The average element size is approximately 1mm. The properties of the materials used are summarized in the Table 2.

A “mesh independent tie” was used in the FEM to model the interactions between the electronic components and the substrate. This allowed the connections between the 2D and 3D elements, as well as between all the 3D elements to be modeled. As already mentioned, the FE model was created using both 2D and 3D elements. Initially two different configurations were evaluated to understand the influence of the “mesh independent tie”, after which the second configuration, consisting predominantly of 3D elements, was chosen because it was more accurate and did not require excessive computing time.

### **Results and comments**

#### **FE results: mechanical**

The mechanical analysis was performed by imposing a fixed displacement on the board to determine in which areas the high gradient occurred when the substrate moved.

#### **Modal analysis**

The first analysis was a modal analysis to understand the frequency of the modes. This was a “free-free” dynamic analysis, i.e. without any constraints. A first comparison showed the difference between the case of the substrate only and the case of the entire electronic

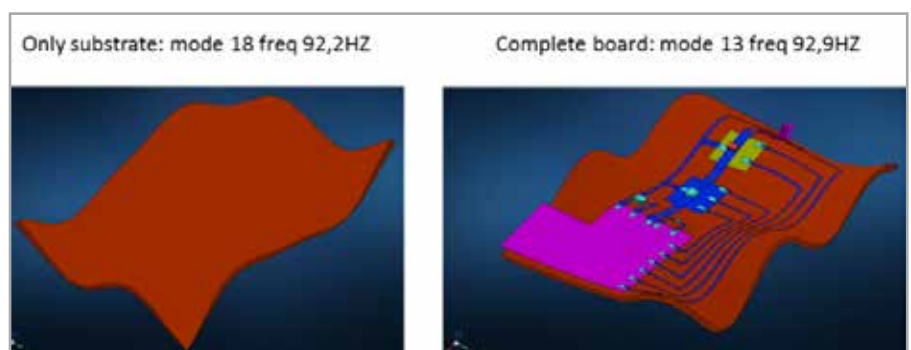


Fig. 3 – Comparison of similar frequency modes

board. Comparable frequencies showed a comparable oscillation, however the rigid board of the accelerometer, of the pressure sensor, and of the microcontroller all determine the shape of the oscillations.

**Imposed fixed displacement**

To understand the behavior of the board and its components, two cases of imposed fixed displacement were analyzed; one in which

temperature sensor. The values shown in both these cases are below the critical values for the respective materials.

**Mechanical load**

This case involved applying an external load of 1MPa (20Kg) to one short edge of the board while the opposite edge was fixed in all degrees of freedom in a similar manner to that used in the case of the imposed fixed displacement. The Von Mises stresses show higher values at the copper connectors of the temperature sensor and photodiode with values of 466MPa and 541MPa, respectively. The rigid sensor boards also have some critical stress values with a maximum  $\sigma_{vm} = 42.1\text{MPa}$  at the short edge of the microcontroller's rigid board near the edge of the substrate and connections. The PEGDA/PEDOT connections showed elevated values of  $\sigma_{vm} = 5.19\text{MPa}$  at the larger connection between the micro-controller and the accelerometer board. The substrate also showed critical values of  $\sigma_{vm} = 3.93\text{MPa}$  in the same area and, similarly, the longitudinal strains were in the substrate showing a maximum value of  $\epsilon_{xx} = 0.294$  near the side of the accelerometer board facing the microcontroller.

**Thermal load**

An analysis was performed by applying a thermal load to assess the deformation produced by a thermal step. The thermal load was applied to the entire model with boundary conditions at the four sides of the substrate. In particular, there were three cases of thermal load:  $\Delta T = 50^\circ\text{C}$ ,  $\Delta T = 100^\circ\text{C}$ ,  $\Delta T = 150^\circ\text{C}$ . Table 3 shows that for  $\Delta T = 100^\circ\text{C}$  and  $\Delta T = 150^\circ\text{C}$ , all components showed criticalities while for  $\Delta T = 50^\circ\text{C}$  only the connectors at the temperature and chip sensors had high Von Mises stress values, i.e.:  $\sigma_{vm} = 516\text{MPa}$  at the temperature sensor connectors and  $\sigma_{vm} = 73.4\text{MPa}$  at the

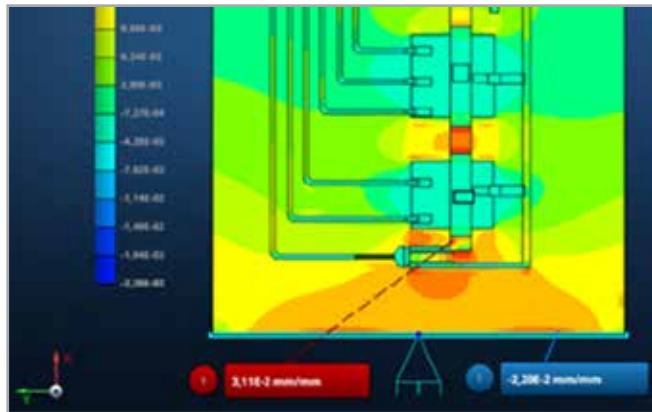


Fig. 4 –  $\epsilon_{xx} = 0.0311$  at the downward imposed displacement

the displacement was imposed downward by 98.9 mm, and the second case in which the displacement was imposed upward. In both analyses, one short edge (the side near the temperature sensor) was constrained in all degrees of freedom while the opposite side had the imposed displacement. The results show that the stress gradients are most relevant in the areas close to the temperature sensor (see Fig. 4), and the Von Mises stress values are similar:  $\sigma_{vm}$  of 71.5MPa and 73.5MPa for the displacement imposed downward and upward, respectively.

A greater difference is seen in the longitudinal strain maps where the higher value of  $\epsilon_{xx} = 0.0311$  is found in the area of the temperature sensor at the PEGDA/PEDOT connections for the displacement imposed downward. The case with the upward displacement shows a maximum longitudinal strain  $\epsilon_{xx} = 0.0222$  in the lower part of the substrate below the

Component with Max $\sigma_{vm}$	Max $\sigma_{vm}$ (MPa) ( $\Delta T = 175^\circ\text{C}$ )	Max $\sigma_{vm}$ (MPa) ( $\Delta T = 100^\circ\text{C}$ )	Max $\sigma_{vm}$ (MPa) ( $\Delta T = 50^\circ\text{C}$ )	Material	$\sigma_y$ (MPa)	$\sigma_{ut}$ (MPa)
Copper connectors	1800	1030	516 (a)	Copper	100	200
Sensors	257	147	73.4 (b)	Silicon	N/A	62
Connector plate	229	131	65.4 (c)	Copper	100	200
Sensor board	38.8	22.2	11.1 (d)	Polyamide	50	80
Connectors	2.31	1.32	0.661 (e)	PEGDA/PEDOT	1.75	2
Substrate	1.40	0.8	0.4 (f)	TPU Desmopan	12	25.7

Table 3: Von Mises stresses from the thermal expansion analysis, and the mechanical properties.

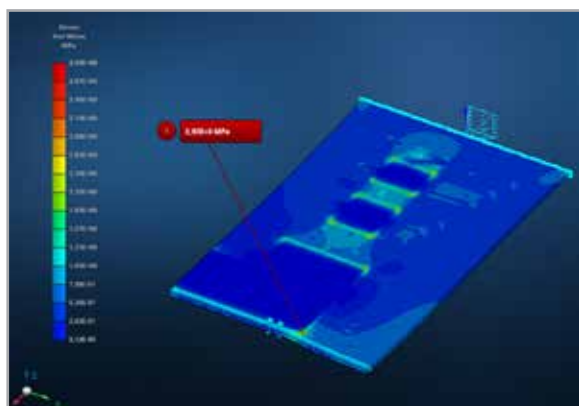


Fig. 5 – Imposed load: Von Mises stresses at the substrate,  $\sigma_{vm} = 3.93$

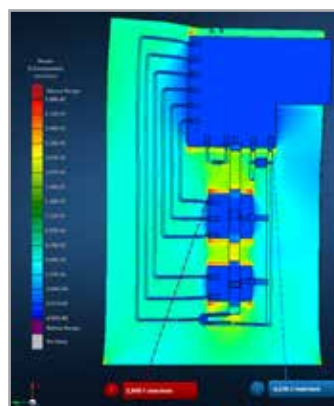


Fig. 6 – Imposed load: longitudinal strain  $\epsilon_{xx} = 0.294$

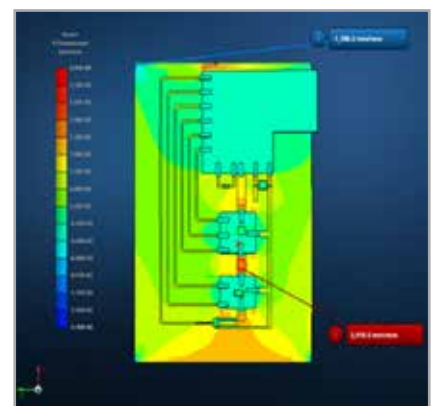


Fig. 7 – Longitudinal deformation  $\epsilon_{xx} = 0.0215$

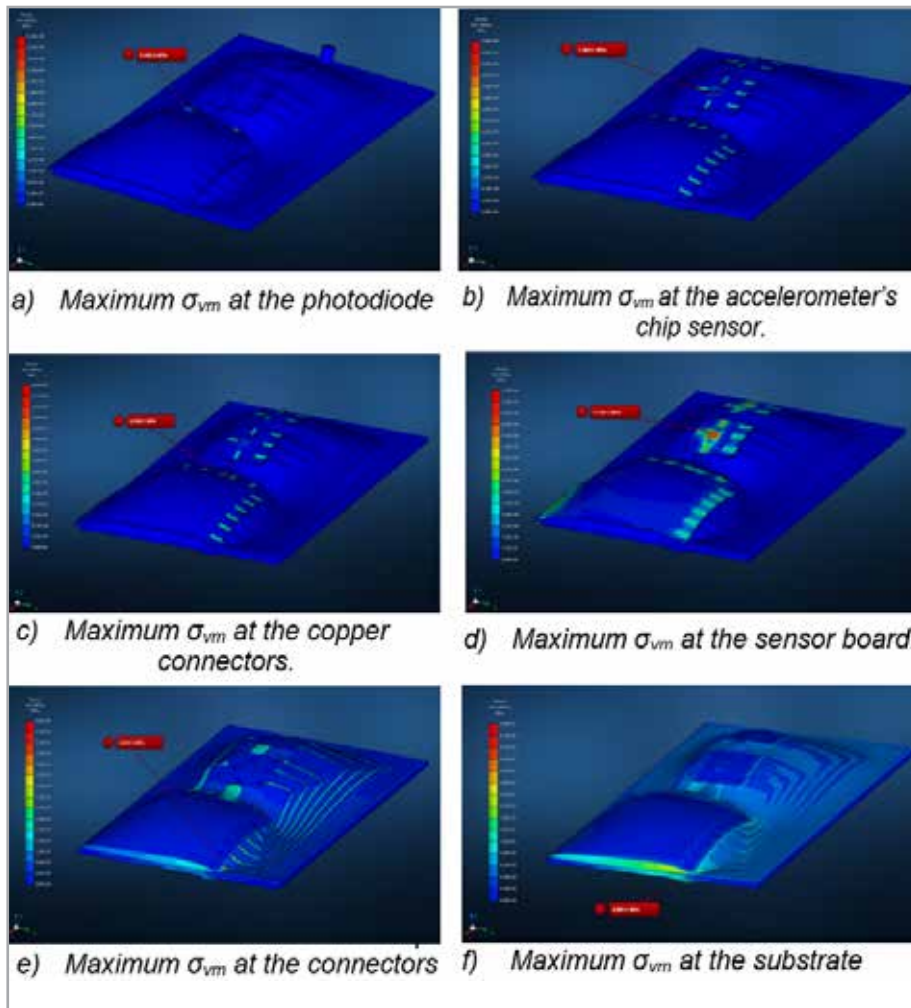


Fig. 8 – Maximum von Mises stresses at the connections with the different components (a – f)

center of the chip sensors. Observing the longitudinal strain, the substrate also showed high values which can be explained by the fact that the different materials (i.e. substrate and rigid board) joined have different thermal properties. The PEGDA/PEDOT connectors showed  $\epsilon_{xx} = 0.0276$  in the area at the connections with the microcontroller board near the substrate edge.

One other area in the longitudinal strain map that shows criticalities is at the corner of the substrate near the microcontroller board, which is effectively the cause of the  $\epsilon_{xx} = 0.017$  strain due to the different material properties of the microcontroller board and the substrate.

Another case was evaluated using  $\Delta T = 50^\circ\text{C}$  along with an imposed downward displacement of 20mm. In this case, the short edge was fixed while the other edge had the imposed displacement. This analysis confirmed the critical areas at the PEGDA/PEDOT connectors and substrate with  $\epsilon_{xx} = 0.0241$  and  $\epsilon_{xx} = 0.0215$ , respectively. However, the stresses at the electrically conductive connectors ( $\sigma_{vm} = 0.18\text{MPa}$ ) and at the substrate ( $\sigma_{vm} = 0.0572\text{MPa}$ ) were not critical.

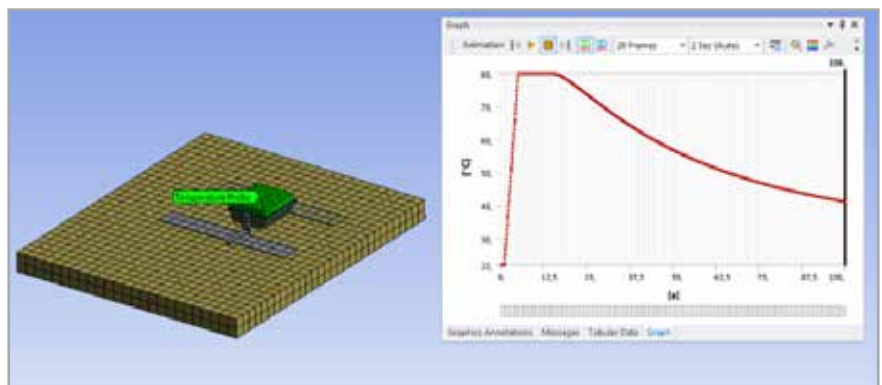


Fig. 9 – Transient temperature of the photodiode

**FE results: thermal**

The thermal analysis was conducted for two single electronic components, namely the photodiode and the accelerometer, to evaluate the difference between a component mounted directly on the substrate and one mounted on a conventional electronic board.

**Heat flux in the photodiode**

An initial analysis was performed by applying a thermal load to the lower part of the substrate. This load started at room temperature and increased to  $200^\circ\text{C}$  two seconds later and was maintained at that level for 100s.

This experiment made it possible to determine a relevant transient time of 42s, which is when the photodiode reaches its critical temperature of  $85^\circ\text{C}$  (its operating limit). The heat flux analysis revealed that the connectors of the photodiode developed the highest heat flow, equal to  $31.895\text{W}/\text{mm}^2$  at 32s.

A second analysis was then performed to simulate the critical conditions for the photodiode. A temperature of  $85^\circ\text{C}$  was applied to the component for 5 seconds after which a heat flow analysis was performed to verify its cooling time.

The analysis time was 100s, as in the previous case. The photodiode's transient temperature is shown in Fig. 9 which illustrates that at the end of the analysis the temperature was still above  $40^\circ\text{C}$ .

**Heat flow in the accelerometer**

Similarly to the previous case, a thermal flow analysis was performed to discover the cooling time of the accelerometer and

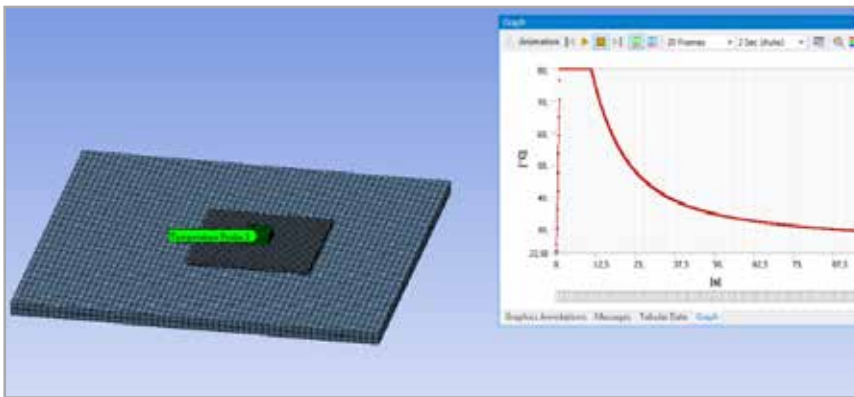


Fig. 10 – Transient temperature of the accelerometer (chip).

to understand the transient temperature from an initial critical temperature of 85°C that persists for about 10 seconds. The total simulation time was 100s. As shown in Fig. 10, the transient flow is much quicker than in the photodiode's with a steep initial gradient while the temperature reaches almost 30°C at the end of the simulation.

### Comments

The mechanical analysis for an imposed displacement showed that high longitudinal strain values ( $\epsilon_{xx}=0.0311$ ) occurred at the PEGDA/PEDOT connectors between the temperature and pressure sensors, and in the substrate ( $\epsilon_{xx}=0.0222$ ) below the temperature sensor. A load imposed in the in-plane direction resulted in critical stress values in the substrate of  $\sigma_{vm}=3.93\text{MPa}$  at the corner of the microcontroller board near the substrate's edge, and a critical longitudinal strain ( $\epsilon_{xx}=0.294$ ) in the substrate near the rigid accelerometer board.

A thermal expansion analysis at different thermal loads showed that for  $\Delta T=100^\circ\text{C}$  and  $\Delta T=150^\circ\text{C}$ , several components had critical values while for a lower thermal load of  $\Delta T=50^\circ\text{C}$  only the connectors showed high Von Mises stress values. The critical areas in this case are at the connectors between the pressure sensor and the accelerometer and the area at the corner of the rigid microcontroller board, close to the substrate board. A possible improvement could be to increase the length of the rigid microcontroller board to avoid the high stresses. The connector area, on the other hand, can be improved by modifying the dimensions of the actual connectors or by varying the thickness of the respective board and its elastic modules since it is this difference that is responsible for the deformation in this zone.

### References

- [1] Desmopan 9730AU, Covestro.
- [2] Stefano Romano, Sviluppo di nuovi materiali polimerici elettricamente conduttivi per stampanti 3D stereolitografiche, Tesi di Laurea magistrale, Politecnico di Torino, Marzo 2018. (Development of new electrically conductive polymer materials for stereolithographic 3D printers, Master's degree thesis, Politecnico di Torino, March 2018)
- [3] MSC Nastran 2018 documentation.
- [4] Ansys Mechanical User Guide 2020 R2.

A further comparison between the board-mounted sensors and the sensor mounted directly on the substrate showed a faster transient cooling time for the board-mounted sensors (accelerometer).

The FE analysis, therefore, showed that design improvements are possible, while the modelling process simultaneously demonstrated its ability to evaluate a re-design; greater accuracy can be realized once a compromise is found with computing time.

### Conclusions

The study presented here demonstrated the feasibility of the flexible electronic board by evaluating its material characteristics and its functionality under thermal and mechanical loading. Heat flow and transient analyses revealed the time taken to reach the critical temperature and evaluated the component's behavior at different temperatures.

The FEA established the critical areas in certain conditions; discovered which components may have critical issues while providing suggestions to improve the design; and demonstrated modeling's ability to determine the demonstrator's behavior for the defined loading conditions.

The design modification suggestions included changing the geometry of the board to avoid the formation of critical stress in the areas identified as well as reviewing the material's properties in those areas that may otherwise cause undesirable deformations.

This study also enabled improvements to the modelling process itself to be determined, specifically how FEA's accuracy and reliability can be improved without increasing the computing time, thereby revealing greater potential for an FE approach. From a materials standpoint, feasibility was demonstrated, so this first prototype can provide a starting point for other similar flexible electronic board concepts.

### Acknowledgments

*This study was funded by the European Union and the Piedmont Region as part of the SMART3D Project: Technology platform for the factory of the future. The partners in the SMART3D consortium that were involved in the FEBO project include: Proplast, CEMAS, IIT (Istituto Italiano di Tecnologia), Politecnico di Torino (DISAT, DET), SAET, ARGOTEC, MICROLA, UPO (Università Piemonte Orientale), ITACAE, TASI (Thales Alenia Space Italia), and Argotec. The authors also wish to thank the other participants of the SMART3D project that contributed to the development of the FEBO demonstrator, namely: Paolo Sirianni, Massimiliano Messere, and Matteo Manachino.*

For more information:

Guido Servetti – ITACAE srl

g.servetti@itacae.com

# Co-simulation of multibody dynamics and particle analysis with Ansys Motion and Ansys Rocky



Enables structural and particle behaviors based on structure-particle interactions to be analyzed

by Hyungkuk Kim  
TSNE

*Structures commonly experience deformation as a result of the effects of the contact forces of the particles with which they interact. Analyzing the mechanisms and situations in which structural and particle movements occur in combination was not previously possible. Now however it can be done by using co-simulation of Ansys Rocky and Ansys Motion, allowing each individual software package to compensate for the limitations of the other.*

The aim of this article is to show the purpose and process of conducting co-simulation between Ansys Motion and Ansys Rocky. It is common for structures to be deformed by the contact forces of particles. For instance, while operating, the reaction forces acting on a tractor vary according to the type of grass and the conditions of the ground. These reaction forces acting on the front and on the wheels of the tractor affect the powertrain and the entire tractor. In analyzing this type of object, the powertrain mechanism that actuates the tractor and the wheel roll must be defined. The simulation model must also consider the properties of the ground and grass.

Ansys Motion and Ansys Rocky can be used to build dynamic analysis models and particle analysis models, respectively. By using

these two software packages together for simulations, engineers can validate the performance and reliability of a range of machines, such as agricultural machinery, excavators, trucks, and cars, operating in a variety of environments. When the excavator is digging soil, the reaction force applied to the excavator varies depending on the mass and velocity of the soil in the bucket. Alternatively, depending on the nature of the soil, the amount of time the truck takes to pour the soil will differ. The vibrations of a car moving off-road will fluctuate due to the different sizes and shapes of rocks encountered.

Previously, dynamics analysis and particle analysis had to be performed separately, so it was not possible to properly analyze the mechanisms in which the structural and particle movements occur in combination. Now, however, this can be achieved using co-simulation of Ansys Rocky and Ansys Motion.

Ansys Rocky can analyze the behavior and destruction of particles. However, because the joint conditions between the structures cannot be defined, the joint reaction forces cannot be calculated. Also, the nonlinear behavior of sticking or slipping between structures cannot be analyzed because the contact between the structures cannot be defined. Ansys Rocky uses motion frames to model the systems in which the structures move. At this time, even if the particles touch the structure and there are reaction forces on the structure, the structure moves in synchrony with the value defined in the motion frame. Therefore, there is no change in the structural behavior as a result of the contact force of the particles.

Ansys Motion, on the other hand, is able to define the connection conditions of complex systems by considering each characteristic. However, analysis of tens of thousands of particles and destructive analysis cannot be performed with Ansys Motion. Co-simulation with both software packages, enables simultaneous analysis of multi-body dynamic systems and particle analysis.



Fig.1 – Co-simulation of Ansys Motion and Ansys Rocky

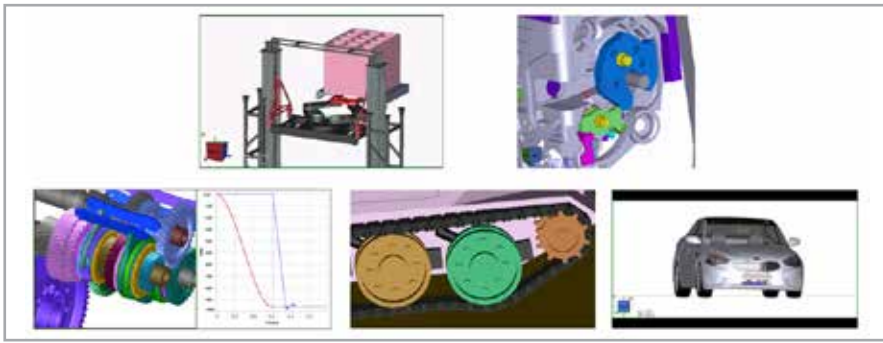


Fig.2 – A dynamics analysis case with Ansys Motion

The conditions required for co-simulation are as follows:

1. Ansys Rocky 4.5.0 or later must be installed.
2. Ansys Motion 2021 R2 or later must be installed.
3. The standalone version of Ansys Motion must be used, not Ansys Workbench.
4. Both the Ansys Motion and Ansys Rocky models must have the same magnitude and direction of gravity.
5. The end time of the Ansys Motion analysis must be greater than the duration of the Ansys Rocky simulation.

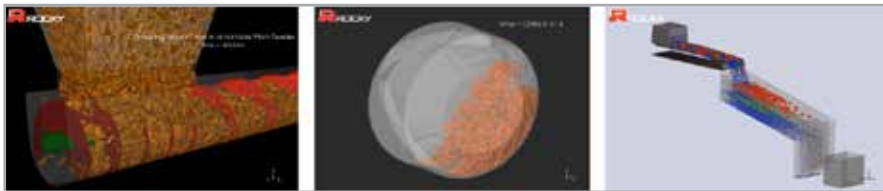


Fig.3 – A particle analysis case with Ansys Rocky

The Ansys Motion FMU file only contains information up to the end time which means it is not possible to co-simulate beyond that time.

### Summary of each software

#### Ansys Motion

- Multi-Body Dynamics Analysis
- Analyzes the reaction force and torque generated by the behavior of the interacting body, and analyzes its effect on the system

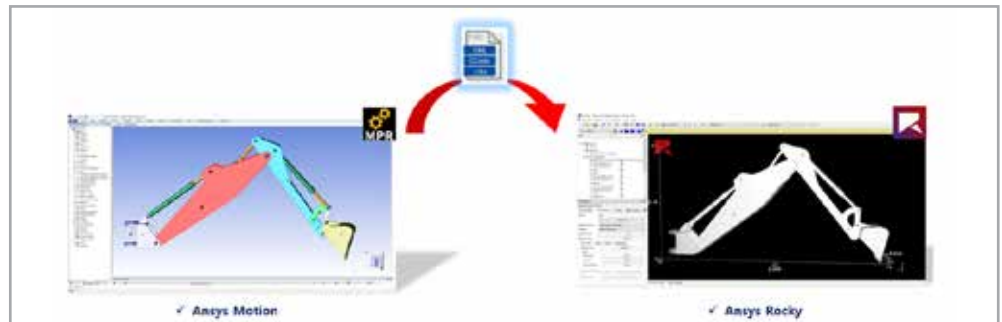


Fig.4 – Ansys Motion and Ansys Rocky co-simulation concept

#### Ansys Rocky

- Discrete Element Modeling
- Numerical analysis to analyze the behavior of individual bulk solids

### What is Ansys Motion and Ansys Rocky co-simulation?

Co-simulation means that separate analysis software packages perform calculations simultaneously. Since both software analysis methods are used for one object, more complex systems can be analyzed by compensating for the functional limitations of each software product.



Fig.5 – The FMU file component

Briefly, the co-simulation process involves building a dynamics analysis model in Ansys Motion and exporting the FMU file. Then, import the FMU file from Ansys Rocky to build the particle model. Finally, run the simulation in Ansys Rocky.

The FMU folder exported from Ansys Motion contains the files below (see Fig.5). The FMU file contains information about the dynamics analysis model and the libraries for interfacing the Ansys Motion solver with Ansys Rocky. The model information relates to object position and velocity, the acceleration of the bodies, and the object and position on which the forces and torques act.



Fig.6 – The conditions required for co-simulation

**Some examples of Ansys Motion and Ansys Rocky co-simulation**

The first example is an excavator. The purpose of this analysis is to calculate the load acting on the bucket and the reaction force at the joint as the excavator digs up the soil. The movement of the hydraulic cylinder is defined as Motion in the joint. Therefore, there is no change in the behavior of the excavator parts even when particles come into contact with them. This is equivalent to defining the Motion Frame as a Boundary in Ansys Rocky. However, the difference is that the forces acting between the boundaries are calculated, and the reaction force is transmitted to the base. The Motion in which the base rotates about its axis is defined as a function of time, as shown in the red graph, and the translational motion of the hydraulic cylinder is defined as a function of time, as shown in the blue graph (see Fig.7).

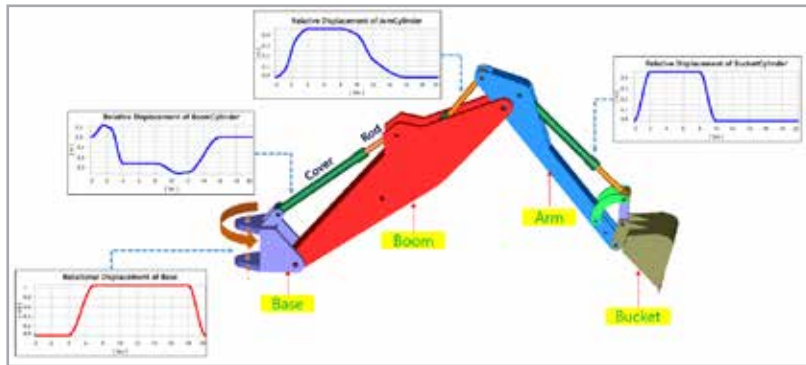


Fig.7 – Example model (excavator)

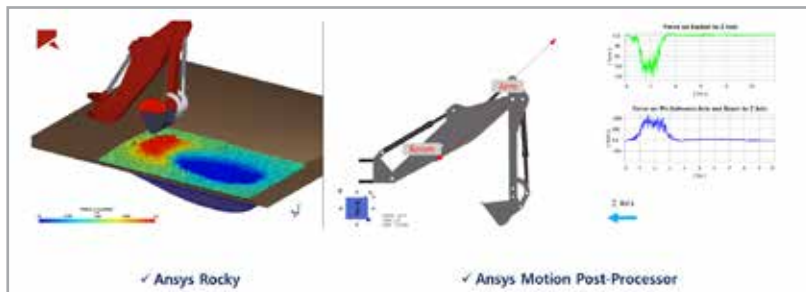


Fig. 8 – The result of the analysis of the excavator

The result of the excavator co-simulation analysis is displayed in Fig. 8. The green graph on the right is the Z-axis load that the particles enact on the bucket. The blue graph below is the reaction force in the Z-axis generated at that time at the rotating joint connecting the boom and arm. To analyze the results, as the bucket is moving in the +Z direction, the particle reaction force occurs in the -Z direction. This is due to the weight and inertia of the particles. The reaction force in the -Z direction is generated at the joint between the boom and the arm, and, due to the lever principle, it is several times larger than the reaction force at the bucket. The red arrow on the gray excavator shows the direction and magnitude of the resultant force at each position.

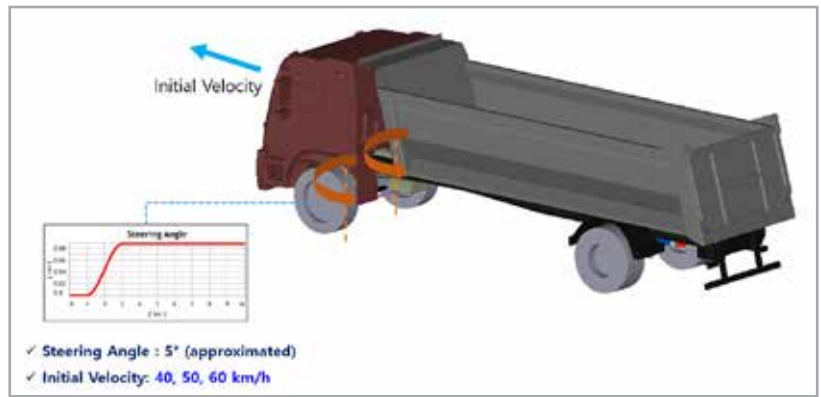


Fig. 9 – Example model (truck)

The second example is of a truck. The purpose of this analysis is to analyze the condition in which the truck overturns during sharp turns. The phenomenon that the truck overturned because it could not withstand the weight of the load of soil it was carrying was analyzed.

As shown in the red graph (see Fig. 9), the front wheels rotate about 5 degrees in three seconds. There are three cases with different initial speeds of 40km/h, 50km/h, and 60km/h.

The truck travels without overturning at 40km/h and 50km/h. But at 60 km/h it overturns. The co-simulation reveals that the weight of the particles is shifted to one side by the inertial force, and this weight modifies the behavior of the truck.

**Summary: Benefits of Ansys Motion and Ansys Rocky co-simulation**

- Ansys Rocky can analyze particle behavior and destruction.
- Ansys Motion can define the connection conditions of complex systems according to each characteristic.
- Co-simulation with both software products enables simultaneous analysis of multi-body dynamic systems and of particles.

For more information:  
Hyungkuk Kim - TSNE  
hkkim@tsne.co.kr

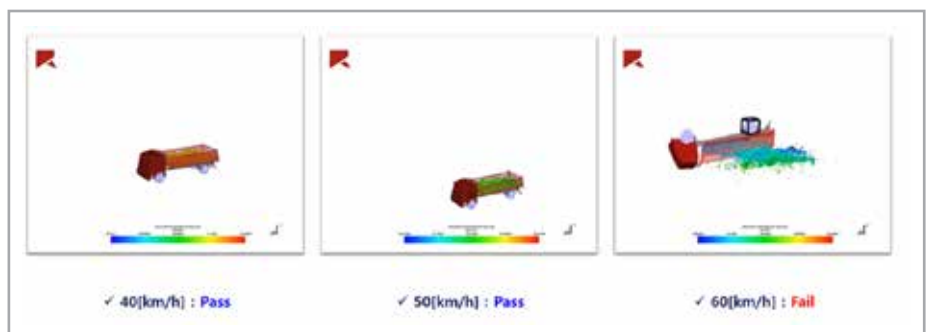
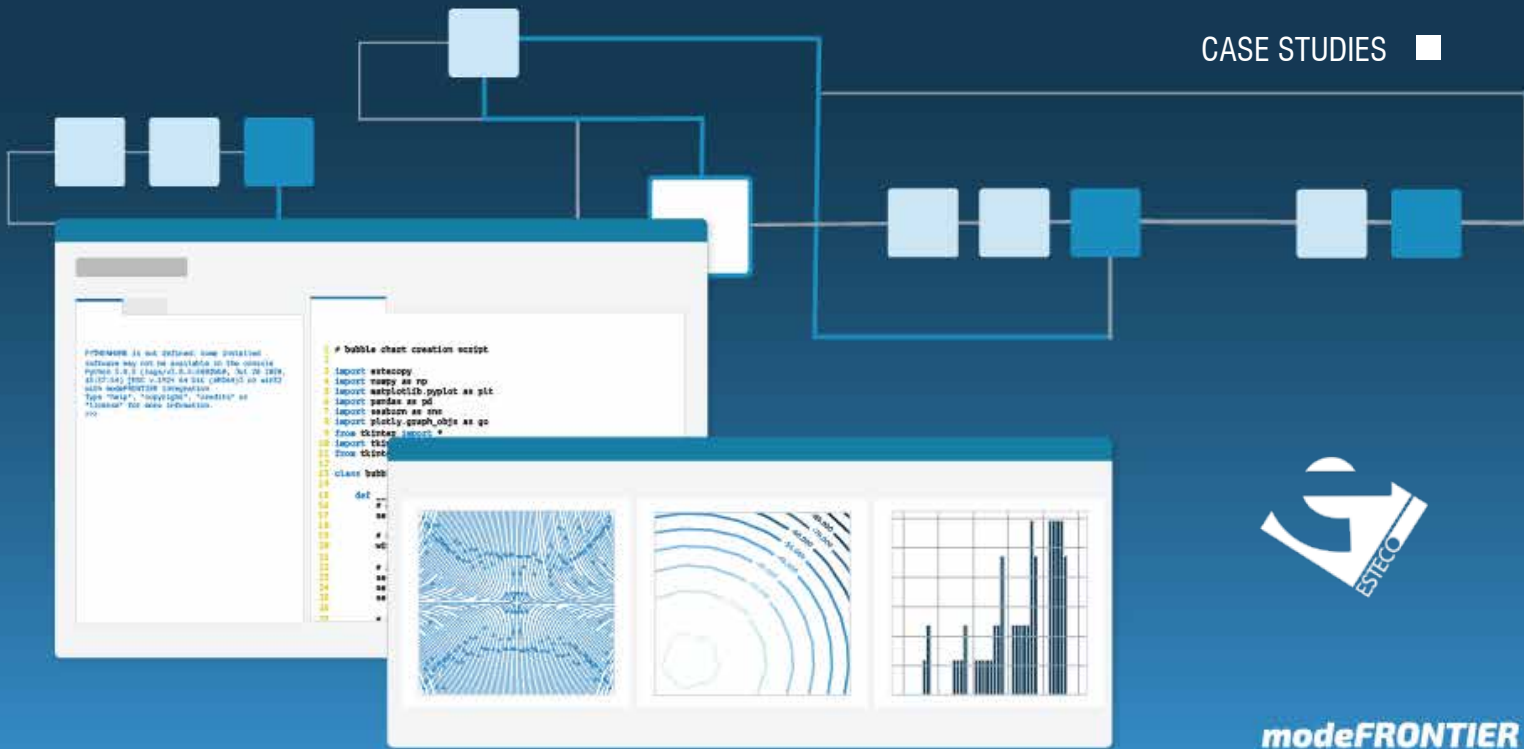


Fig. 10 – The result of the analysis of the truck



# pyCONSOLE: a Python-based data intelligence environment integrated into an MDO engineering framework

The benefits of custom data analysis in an MDO framework

*Any design engineer working on a Multidisciplinary Design Optimization (MDO) project frequently needs to integrate data analysis into the MDO process in a customized way, either in the preliminary phase of the design or in the final decision-making process.*

Engineers optimizing numerical simulation models based on different objectives and requirements may in fact need to analyze and leverage a CAE simulation database for many different reasons:

- To find the most significant variables in the process or redefine the problem with a reduced number of variables.
- To create and re-use metamodels or classification models to save computing time when performing the simulations.
- To modify design charts and tables for a new set of simulations based on the results of the first analysis.

It follows that it is critical for designers to have the freedom to tailor all the available analysis tools to their particular needs, integrating the available process automation modules with the data analysis modules into a single, customized design framework.

The automation and tailoring of data analysis can benefit consistently from the Python language and the support of its vast user community. In fact, its simplicity, diffusion, and flexibility make Python a valuable customized problem-solving tool for any engineer, no matter whether a novice or experienced programmer.

To meet this need, ESTECO has introduced a new Python console environment (pyCONSOLE) for customized data analysis in modeFRONTIER.

## pyCONSOLE for integrated Data Intelligence in modeFRONTIER

Python technology was already available in the modeFRONTIER workflow editor to automate engineering process simulations. With the development of the new Python console, this integration is being extended. The technology offers designers the ability to apply powerful, custom scripts to automate analysis and perform advanced post-processing and decision-making tasks in a single, integrated MDO framework.

To mention just a few of its benefits, with the modeFRONTIER pyCONSOLE users can:

## CASE STUDIES

- Include Python scripts or libraries in a single, fully integrated modeFRONTIER project to interactively analyze data calculated by the modeFRONTIER process automation workflow and directly access analysis results as custom tools in the workflow.
- Leverage the power of Python libraries to perform advanced, automated user-defined analysis on data processed by modeFRONTIER to suit their needs. For instance, they can cross-validate different meta-models or create a classification or reduced order model, which can be used within the same modeFRONTIER process automation workflow to reduce computing costs or gain better results when performing a numerical optimization.
- Re-use the same Python scripts in other modeFRONTIER projects for different applications, without the need to re-create charts each time and configure tools from scratch.
- Improve chart customization by leveraging the high quality of Python's numerical and graphical libraries and applying their preferences to a large number of charts, such as contour or derivative plots, multi-history charts or PDFs, to name a few.

Whatever post-processing tasks they need to perform, engineers can benefit from Python's full integration into modeFRONTIER for a variety of applications and problems. Whether it is to reduce problem complexity and computing time, or to handle large numbers of variables, they can extract data from modeFRONTIER, plot custom charts, or transfer analysis results back into the workflow.

### pyCONSOLE to reduce MDO computing time

In this application example, the designer needs to detect the image of a form of electromagnetic rotor in order to decide whether or not to perform a simulation with JMAG software during an optimization. Computing time can be greatly reduced by avoiding the simulation of geometric configurations that are expected to perform poorly (such as due to a low torque).

By using the KERAS neural network (available as a public library from Python) pyCONSOLE in modeFRONTIER allows this task to be performed in an integrated framework. modeFRONTIER executes a Design-of-Experiments (DOE) sequence of different rotor shapes, whose images are then used by the Python console script to train the neural network model. Thereafter, the neural network model is used in the modeFRONTIER workflow as an intermediate script node between the CAD and JMAG interfaces, so that, depending on the expected torque value, the JMAG simulation is either executed or ignored.

With this methodology, the optimization of the electromagnetic rotor was performed by evaluating less than 40% of the candidate geometries proposed by the optimization, meaning that the overall simulation time was almost halved.

In conclusion, pyCONSOLE enabled:

- Access to a dedicated Python environment directly from modeFRONTIER.
- An advanced deep learning model to be imported directly into the modeFRONTIER workflow to accelerate the entire optimization process.

### pyCONSOLE to handle many design variables

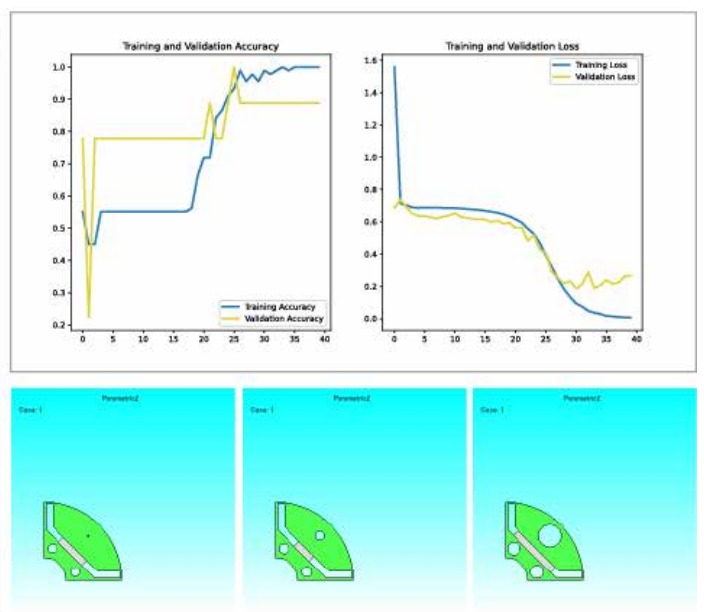
In this application case, pyCONSOLE leverages an external Python library to perform dimensionality reduction in an engine optimization problem. The challenge is to transform the original design space of 30 input variables into an equivalent space of fewer components, in order to simplify the optimization task and achieve the optimal set of solutions by analyzing fewer designs than required by direct optimization.

By using a script in pyCONSOLE based on the Principal Component Analysis (PCA) tool developed by Scikit Learn, it is possible to calculate the principal components of the dataset evaluated by modeFRONTIER and reduce them to the best components only.

```
#!/usr/bin/env python
import matplotlib.pyplot as plt
import os
import tensorflow as tf
from shutil import copyfile
from tensorflow.keras import layers, optimizers
from tensorflow.keras.models import Sequential
from category_encoders import
import numpy as np
import pandas as pd
from PIL import Image, ImageOps
import pathlib
import sys
import time

if __name__ == '__main__':
    # Path to the folder containing the images
    table_name = 'DB_2021-06-22_11:14'
    # Create a logger
    class Logger(object):
        def __init__(self, filename="Default.log"):
            self.terminal = sys.stdout
            self.filename = filename + '.log'
            self.log = open(self.filename, "a")
        def write(self, message):
            self.terminal.write(message)
            self.log.write(message)
        def flush(self):
            pass

    # Get the table from the database
    myTable = db.get_table(table_name).get_rows()
    # Extract table header from first row
    header = myTable[0]
    # Extract features
    data = myTable[1:]
    # Create numpy matrix from data rows. Discard the first 5 columns of the table since they don't contain data
    matrix = np.array([row[5:] for row in data])
    # Build pandas DataFrame
    df = pd.DataFrame(matrix, columns=header[5:])
```



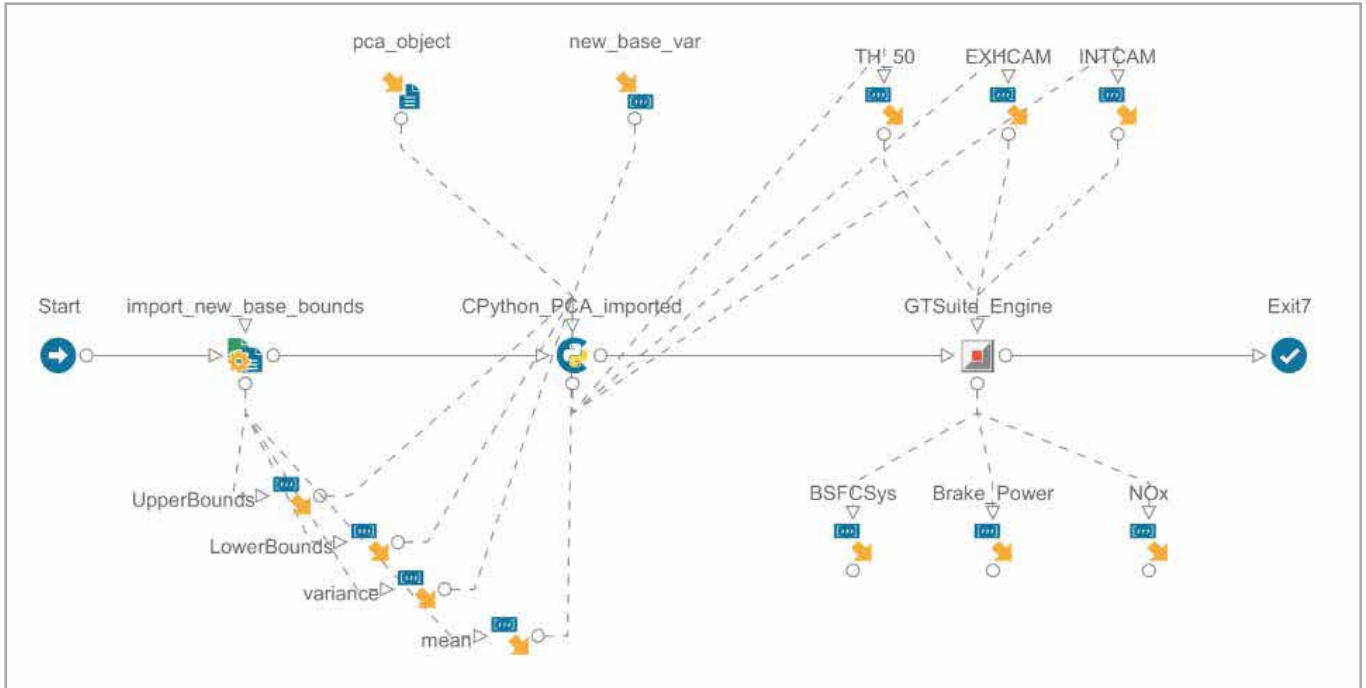
This analysis shows that the first 14 components are responsible for more than 80% of the variance, so the original design space of 30 input variables can be represented by an equivalent space of just 14 of them, without completely discarding the influence of any of the original variables.

The PCA model can then be exported to a CPython script in the modeFRONTIER workflow to revert any design proposed by the optimization algorithm from the new reduced base to the original base for execution of the GT-Power automation node (engine simulation). The integrated workflow is illustrated below:

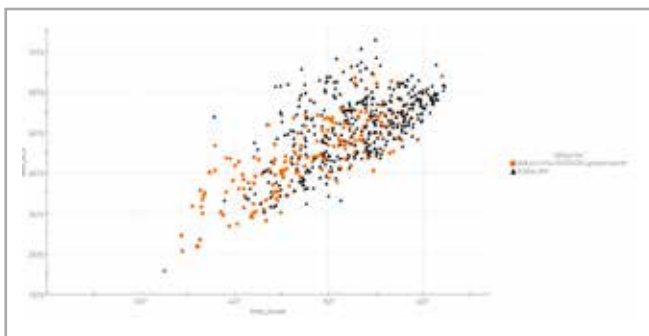
### Full integration of Python with modeFRONTIER

As has been illustrated clearly by these application examples, modeFRONTIER fully supports Python, both within the process integration workflow and in the data analysis environment, improving the customer experience with external customized and advanced post-processing tools. Moreover, the integration of Python allows design engineers to use the optimization technology even more efficiently and fully adapt modeFRONTIER to their specific needs.

ESTECO works constantly to increase the abilities of its software; the integration of the Python scripting language ensures substantial



This approach enabled an optimal set of solutions to be obtained with just 400 designs (orange dots in the chart), whereas a direct MOGA-II optimization (black triangles in the chart) would have required a larger number of designs to achieve the same results.



pyCONSOLE made it possible to efficiently perform the following operations:

- Extract the data from modeFRONTIER, post-process and transform it using dedicated and advanced methods.
- Plot a custom chart created using external Python libraries with data directly available in modeFRONTIER.
- Export the results obtained from the data analysis directly into the workflow.

benefits for all engineers both in terms of process automation and in post-processing analysis. Accessing all of this from a unique integrated framework can make a significant difference to engineers' daily tasks.

For more information:  
[info@esteco.com](mailto:info@esteco.com)

### About Esteco

ESTECO is an independent software company, highly specialized in numerical optimization and simulation process and data management. With a 20-year experience, ESTECO supports over 300 international organizations in excelling in their digital engineering experience, accelerating the decision making process and reducing development time. Ford Motor Company, Honda, Lockheed Martin, Toyota and Whirlpool are just a few of the major companies relying on ESTECO technology. ESTECO is the owner of VOLTA, the collaborative web platform for Simulation Process and Data Management and design optimization, and modeFRONTIER, the comprehensive solution for process automation and optimization in the engineering design process.

[esteco.com](http://esteco.com)



Enables easier workflows and extends depth and breadth of the solver capabilities

# CFD release highlights

By Alessandro Arcidiacono,  
Diana Magnabosco, Fabio Villa  
EnginSoft

*With Ansys 2021 R2, the fluids product line continues to make major advancements in helping to solve some of the toughest challenges in turbomachinery, combustion, fluid-structure interactions, and more. The features and capabilities of this release increase productivity, accuracy, and innovation, as will be described in this article.*

## Ansys Space Claim direct modeler

Space Claim is a powerful tool, particularly for repairing geometries. The Check Geometry function in release 2021 R2 has new options that allow users to better identify and debug problems in imported geometries. The first of these, Hide Others, easily removes any other geometry that may be obscuring the problem. The second option, Create Named Selection, saves a selection set for further investigation. Finally, Delete Face, completely deletes faces from a model for future reconstruction.

**Constraint Based Sketching** includes new icons and two new types of constraints, namely the Symmetric constraint (which makes two objects symmetrical on one axis) and the Equal Length constraint (which sets two curves equal in length, simplifying the workflow within the equal length tool). Engineers can select the Retain Sketch in the tree, which saves the sketch for reuse. Finally, with the Show Constraint Colors option, color highlighting can be turned on/off based on under, fully, or over constrained curves.

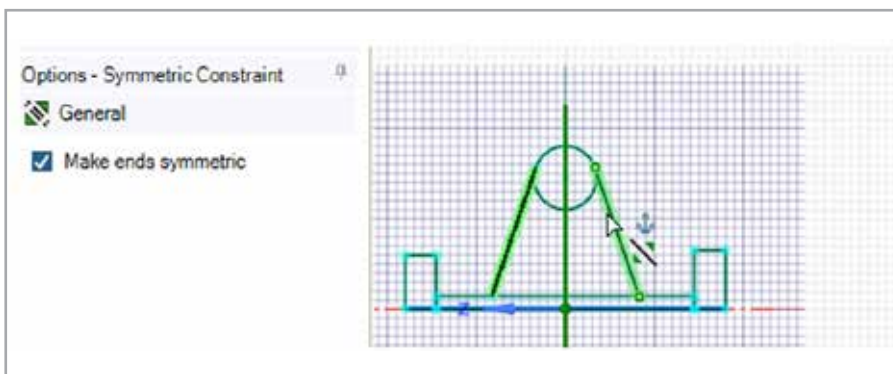


Fig. 1 - Symmetric Constraint allows the creation of constraints on curves and at the end points of curves

For named selections, the Show option has been added to the right-click menu in the Group panel. This allows the visibility of the named selection to be easily changed from hidden to visible without affecting changes to the visibility of the rest of the assembly.

## Ansys Fluent Meshing

Ansys Fluent Meshing guides the user through a simplified workflow to generate high-quality unstructured meshes in a single-window approach. The user interface can now be customized with a **Dockable Workflow Editor** (Fig. 2) allowing the user to separate the workflow task editor from the task list to gain more space to work, especially for complex cases with many regions and/or boundaries.

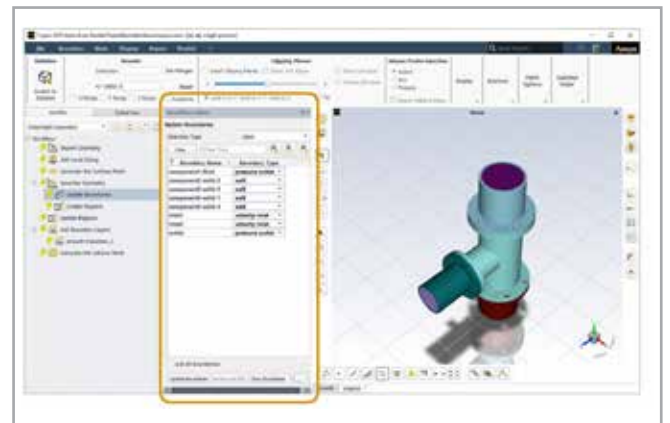


Fig. 2 - Dockable Workflow Editor

In the Watertight Meshing Workflow (WTM) there is a new task called **Extrude Volume Mesh**, which allows extrusion from both planar and non-planar surfaces.

Engineers can also use imported CAD or mesh files to define bodies of influence. Previously it was mandatory to build this into the geometry, but now the user can take advantage of the **Import Body of Influence Geometry** instruction to add it directly during the meshing procedure.

Also in the WTM Workflow, the **Add Linear Mesh Pattern** task now allows for custom patterning (reorientations, two-dimensional patterns, rotation, etc.) and personalized naming conventions to assign a custom name to instantiated cells. This technique is particularly

helpful in battery simulations, where simple linear arrays of cells are often insufficient (Fig. 3).

In the final stages of the WTM Workflow, the user now has additional control over Cell Zones. With the Manage Zone task it is possible to

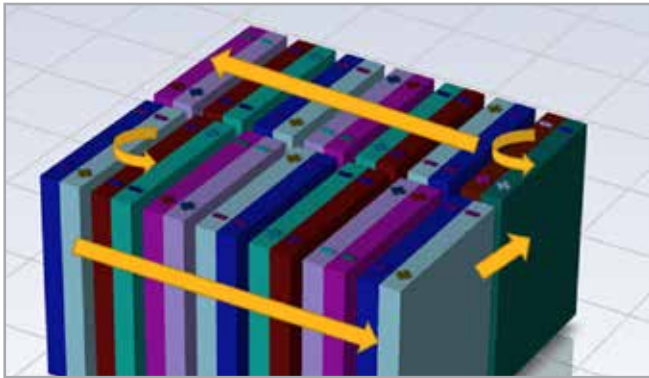


Fig. 3 - Translation and rotation of twin cells is possible

manipulate domains and manage user-defined zone merging using filters, wildcards, and manual selections.

The Fault Tolerant Meshing (FTM) workflow is enhanced in term of speed and robustness with various improvements regarding prism generation, size field management, and the wrapping procedure. This leads to significant savings in size field computing time, reduced mesh count and overall robustness.

Other miscellaneous enhancements in the FTM Workflow include the creation of porous regions via text file import, support for parallel meshing with the polyhedral method, the usability of the **Import CAD and Part Management** task instruction, and other transformation operations.

**Ansys Fluent**

The new capabilities of, and enhancements to, Ansys Fluent are outlined below with regard to User Experience, Post-processing, the Solver, Multiphase Flow, and the Structural Model.

**User Experience and Post processing**

Several improvements are included in the latest version to support Fluent case file setup and post-processing. First, a list of **modified settings** (Fig. 4) allows users to view the setup in a single window, which shows a summary of the case differences from the default settings such as models, cell and boundary conditions, reference values, solution controls, and methods. Users can add the suffix/prefix option for boundary zone names from the Adjacency dialog box. This is a valuable option for cases with a large number of boundary conditions.

The Post-processing tools have been further improved: Report Files and Report Plots are now created by default, and users can save a Display

Setting	Current Value	Default Value
Setup		
Modified Settings	On	Off
Cell Zone Conditions		
Solid		
solid-2 (solid, id=2333)		
energy sources	0_exp_3000 [W m^-2]	0
Specify source terms?	True	False
Boundary Conditions		
Inlet		
inlet1 (velocity-inlet, id=58)		
Velocity Magnitude	2 [m/s]	0 [m/s]
inlet2 (velocity-inlet, id=59)		
Temperature	350 [K]	300 [K]
Velocity Magnitude	...exp_...PVM_Signal * 2 [m/s]	0 [m/s]
Wall		
component1-fluid-component2-solid-2 (wall, id=51)		
Z-Component of Wall Translation	1 [m/s]	0 [m/s]
X-Component of Wall Translation	1 [m/s]	0 [m/s]
Define wall velocity components?	True	False
Wall Motion	Moving Wall	Stationary Wall

Fig. 4 - List of modified settings

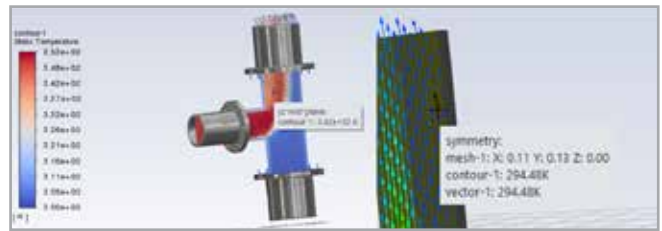


Fig. 5 - Post-processing: Mouse probe tool

States object, which contains view and display attributes stored with graph objects. When using averaging for report definitions, the new Retain Instantaneous Values option offers the ability to change the averaging interval and re-plot the results. Another useful tool is the **mouse probe**, which allows values on post-processing objects such as contour, vectors, and path lines to be probed (Fig. 5).

**Solver and HPC**

An advanced **gap model** to simulate flow blockage in small spaces supports all moving mesh techniques (moving reference frame, moving mesh, dynamic mesh, overset, mesh interfaces). This has significant advantages over dynamic mesh contact detection (Fig. 6).

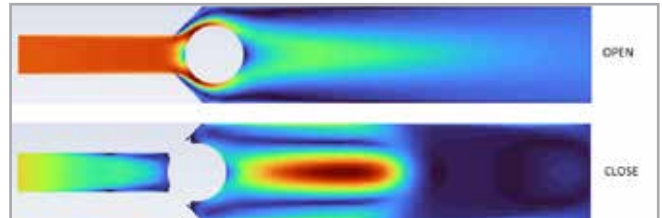


Fig. 6 - Gap Model for simulating flow blockage in small spaces

**Mesh adaptation** can significantly reduce simulation time by using highly refined meshes only where needed. Two new predefined criteria are available, related to combustion and aerodynamics. They are: combustion criteria for finite rate and flame generated manifold (FGM) combustion (Fig. 7), and high-speed aerodynamics (shockwave identification parameter). Mesh Adaptation is now also available for prismatic boundary cells (anisotropic boundary adaptation) to improve the resolution of the boundary layer mesh.

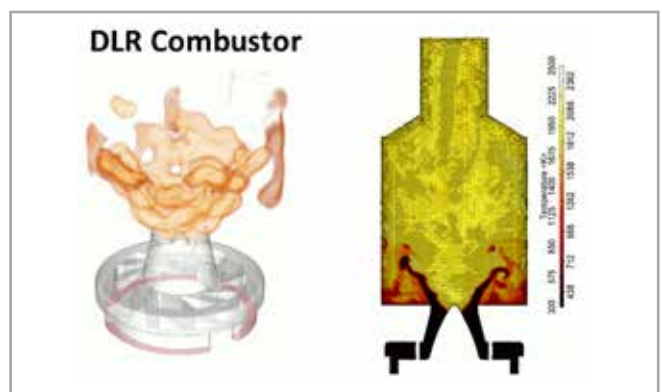


Fig. 7 - Predefined mesh-refinement criteria: combustion

**Multiphase flow**

The fluid volume method is enhanced with a new **Dynamic Anti-diffusion** treatment. This new method minimizes waves/wrinkles at the interface by reducing compression in the tangential direction at the interface (Fig. 8).

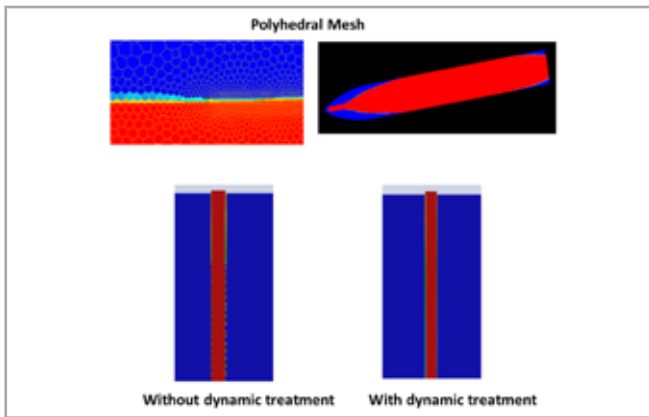


Fig. 8 - Dynamic Anti-Diffusion treatment

**Instability Detector** has been improved with Hybrid NITA (non-iterative time advancement). A new type of CFL (Courant-Friedrichs-Lewy condition) based on interfacial cells has been introduced to synchronize the Instability Detector with the Global Courant Number. In a test case, this allows a 20% reduction in wall clock time for a stirred tank vortex case.

For discrete-phase modeling, **Local coordinate systems** for most injection types are now supported, simplifying the configuration of multi-hole injectors. Particle injections from volumetric regions are also available from this release.

**Structural model**

The functionality of the integrated structural model in Fluent is further extended (intrinsic fluid structure interaction). Rayleigh damping can be used which has very good agreement with the MAPDL Mechanical Solver (Fig. 9). Axisymmetric thermo-elasticity can also be analyzed (e.g. an aluminum pipe with steel rings). The expressions, which are easy to use, can now be used for structural boundary conditions.

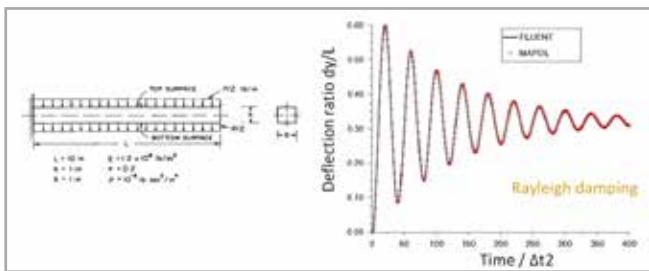


Fig. 9 - Classical Rayleigh damping is viscous damping, which is proportional to a linear combination of mass and stiffness

**Ansys CFX**

Ansys is constantly developing new features to help customers conduct accurate turbomachinery simulations. In 2021 R2, Ansys CFX introduces GPU-accelerated animations and extends support on the Ansys Cloud.

**Ansys BladeModeler** (integrated with Ansys DesignModeler) offers full 3D geometry modeling capabilities and allows the addition of any number of geometric features, such as hub metal, blade fillets, and cut-offs and trims. BladeModeler now supports elastic licensing, allowing users to solve end-to-end blade design workflows on the Ansys Cloud. A new blade optimization parameter for throat areas is available in BladeEditor, which can be combined with tolerance specifications to save time by simulating only designs within a specified tolerance range.

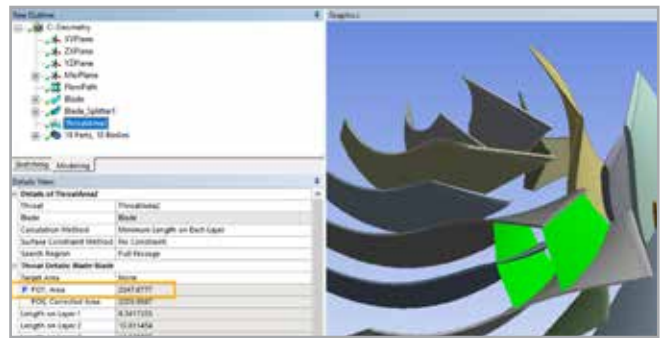


Fig. 10 - Parameters for a throat area

**Ansys TurboGrid** software includes innovative technology that targets full automation combined with an unprecedented level of mesh quality for even the most complex blade shapes. An evolution of Automatic Topology Meshing, called ATM3D, was added in 2021 R2, based on a 3D Elliptic Smoother that offers improved mesh quality along the span direction. ATM3D now supports constant first element height, reducing element proportions on small radius leading/trailing edges. Mesh statistics have also been improved, with histograms showing mesh quality metrics.

**Ansys CFX** is a high-performance computational fluid dynamics (CFD) software tool that delivers reliable and accurate solutions quickly and robustly across a wide range of CFD and Multiphysics applications. Users can now harness the power of the Ansys Cloud via the command line interface to accelerate simulation times 40x compared to a 12-core workstation. GPU-accelerated animations in CFD-Post now support streamlines, enabling users to animate results in real-time. More accurate and robust results for turbomachines can be achieved now that non-reflective boundary conditions have been fine-tuned and validated for turbomachinery applications. Users can specify named selections on shared faces in CFX, splitting faces from Ansys Meshing into Side 1 and Side 2, which simplifies automated workflows because users can keep face names predictable.

For more information:

Diana Magnabosco - EnginSoft  
d.magnabosco@enginsoft.com



Fig. 11- Ansys Cloud portal



# ORCHESTRATING **DIGITAL** TRANSFORMATION THROUGH SIMULATION

VICENZA, ITALY  
17-19 NOVEMBER

# 2021

HYBRID EVENT

# 37<sup>th</sup>

INTERNATIONAL CAE  
CONFERENCE  
AND EXHIBITION

**Simulation's role on Mars, debating the roadmap towards economic recovery and an innovative Italy, origami engineering, digitalization and simulation case studies in four macro industrial sectors, and more!**

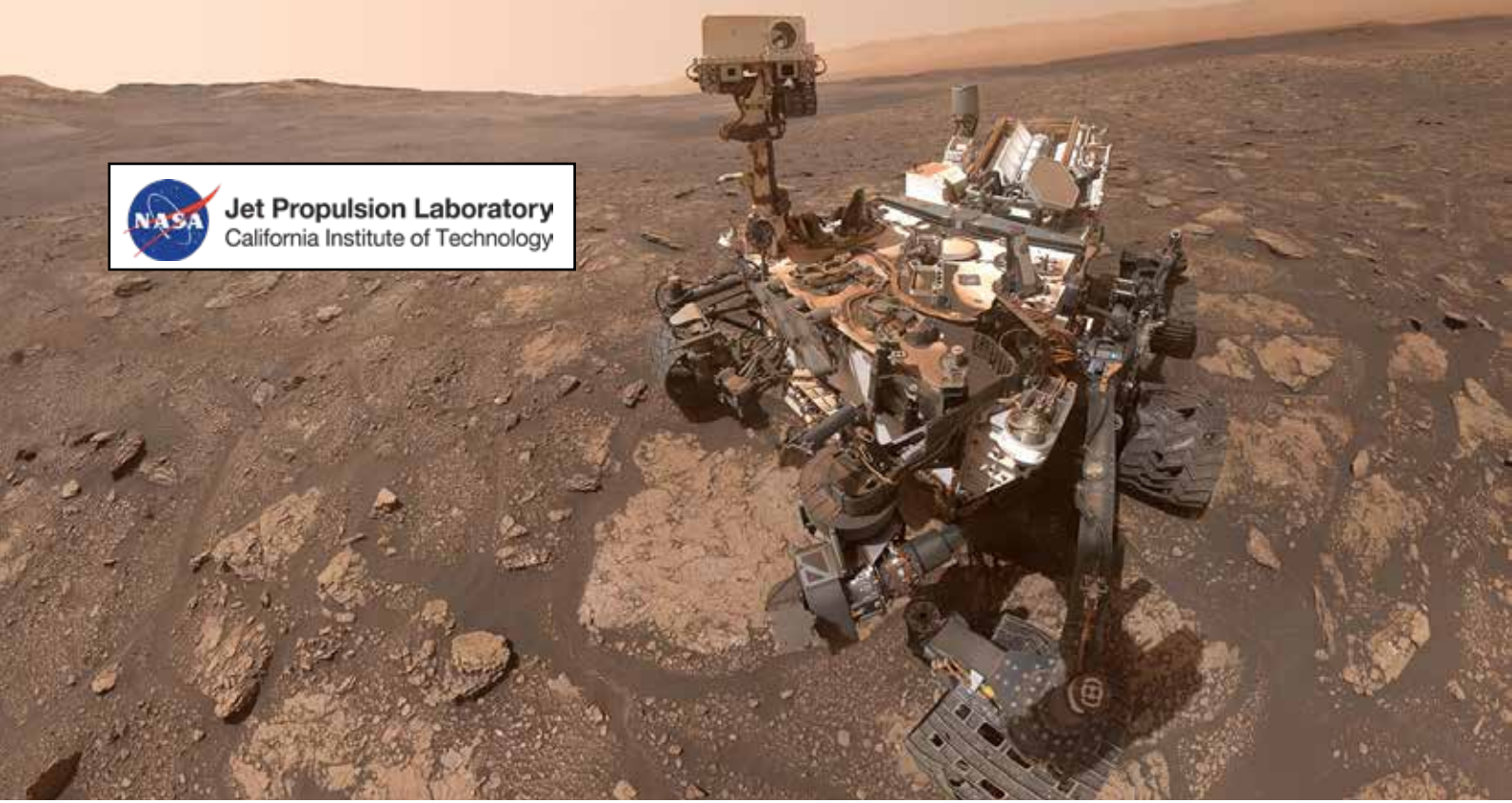
**A foretaste of what you can expect when you attend!**

This year's zero-emissions event, entitled "Orchestrating digital transformation through simulation: Channeling technology, process, and people for sustainable competitive advantage" is being held both online and in person at the Vicenza Convention Centre in northern Italy, from November 17 – 19. In addition to several fascinating keynotes ranging from space exploration to origami engineering, and a panel discussion on the potential paths towards an innovative Italy featuring high level political and business leaders, there will be three technical streams in three industrial sectors: Automotive and Transport; Energy, Oil and Gas; and Manufacturing. All conference sessions will be streamed live, while exhibitors will have either virtual or physical booths – or both. Participants will interact, schedule meetings, and exchange information via the event platform, designed like a social network.

In addition to thought leading content about state-of-the-art developments, and case studies that examine the digitalization and

the application of simulation to real-world challenges, regular annual attendees will also find the traditional features they've come to expect at the event: the Research Agorà, with its focus on results from leading edge research project consortia, and the Poster Award which seeks to connect innovative thinking, problem-solving graduates with the industries with an ever-increasing need for these skills by recognizing the creative use and application of CAE technologies by students around the world.

*In the following pages you will find a selection of articles highlighting various aspects of the content you can expect to find at the 2021 event. If you haven't registered yet, visit [www.caeconference.com](http://www.caeconference.com) to book your place. Some exhibition opportunities are still available, and further information can be found at the conference website. Contact the organizers today to ensure you are part of this eagerly awaited event in the European event calendar.*



# What lies in the future for simulation? The Red Planet may have an influence...

*Paolo Bellutta is a Mars Exploration Rover Driver, officially a "Rover Planner", at the Jet Propulsion Laboratory of NASA's Mars Science Laboratory, in Pasadena, California, which is one of NASA's R&D laboratories in the USA. Bellutta, one of the keynote speakers at this year's International CAE Conference and Exhibition – and his presentation promises to be a highlight of the event – is responsible for moving the Mars rover around the Red Planet, picking the images that the vehicle captures at the end of the day, deciding where it is safe to move the vehicle to approach the various science goals that the geologists and other scientists communicate to him, and so on. The EnginSoft Newsletter interviewed him about what he does and what he would like to see in the future of simulation. If you find this conversation as fascinating as we do, be sure to register to attend the 2021 International CAE Conference and Exhibition at [www.caeconference.com](http://www.caeconference.com) so that you can hear the full inspirational presentation, scheduled for November the 17th, 2021.*

## **Q. What is your view of simulation for innovation and project development.**

A. For those of us that work in an environment that is very difficult to replicate on Earth, simulation is clearly the groundwork for every project that we develop. Obviously, we cannot replicate the conditions that we have on other planets – firstly, it would be too expensive and secondly, it would be too difficult, if not impossible.

Just think, for example, of how one would replicate a different gravity field on Earth; it would be practically impossible. The way that the vehicle interacts with the soil on Mars is different from the way that the vehicle interacts with soil on Earth. Simulation also plays a very important role in the phase of interacting with the atmosphere of the planet. More specifically, since I work on Mars, it is important for us to be able to control the entry, descent, and landing portions of the mission. Being able to simulate the behavior of the atmosphere, depending on the temperature, and the density of the atmosphere is really important. So, innovation to us means being able to have higher and higher fidelity simulations under these conditions. While we have



learnt a little bit of how Mars works, we still need to be able to simulate the entire system before we land. We cannot do real live testing before sending the vehicle to Mars; we can do some testing in real life, but not of the entire system. So for us, the only way of being able to complete our testing is to actually do it through simulation.

**Q. How much do you rely on simulation tools and which benefits could you highlight?**

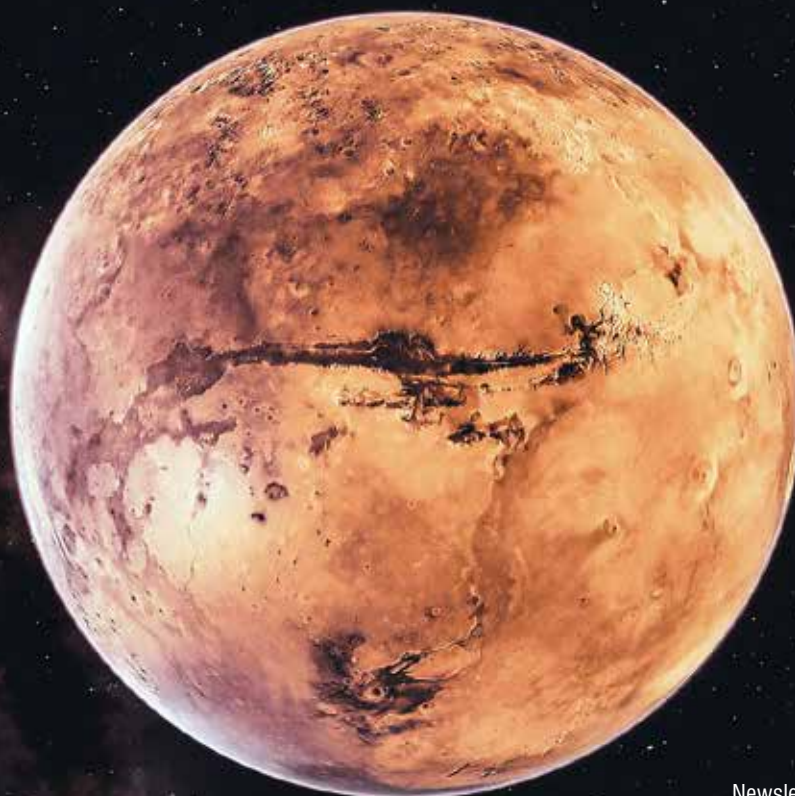
A. This is quite a difficult question. I don't think there is enough communication today about the possibilities of the applications for simulation. So on the one hand, we should have more widespread use of simulation, but on the other side, we sometimes trust simulation too much. By this I mean that the results of a simulation are only as good as the model; so if your model is imperfect, or if your knowledge of the problem is incomplete, your simulation is not perfect – it doesn't provide all the details that you need to have. So in this sense we sometimes trust simulation too much. But, there are many, many fields where simulation could be very important. One example is politics where one could try to simulate what would happen when you make a certain decision for your population and try to figure out what the consequences of your decision would be.

**Q. What are your expectations for the near future in relation to the new challenges you are facing in your job?**

A. The next level of simulation that we would like to have would be the ability to better model how the terrain interacts with the wheels of our vehicle. At the moment we can simulate the interaction of the soil with the vehicle with terramechanics, but these are pretty crude, and



they can only simulate the behavior of the vehicle for a few seconds. And the simulation requires hours of computing time. Being able to simulate what Mars is going to throw at us when we're moving the vehicle, on one hand would enable us to operate our vehicle more safely. On the other hand, when we can compare the expected results from our simulation with what we actually encounter on Mars, it would help us to determine where there are unexpected changes in the terrain. Therefore, from a scientific perspective, it is very important. Whenever there is a different type of terrain that we travel through, it would be interesting to see why there is that change and be able to analyze the terrain immediately. For example, when you're walking on the beach, you can immediately feel with your feet when you are on dry sand versus wet sand. It is the same for the vehicle: it can detect when the terrain changes, but what are the changes relevant to? We need to be able to simulate the behavior of the terrain before we give the commands to the vehicle, and consequently the vehicle itself would then be able to collect scientific samples while driving simply by comparing the data from the simulation to what actually happens.



# Analyzing the process of filling a flexible pouch by coupling multi-flexible-body dynamics and particle-based CFD simulation



Investigating the effects of the parameters to select the optimal machine configuration

by Matteo Berlato<sup>1</sup>,  
 Davide Marini<sup>2</sup>, Michele Merelli<sup>2</sup>  
 1. Department of Industrial Engineering,  
 University of Trento - 2. EnginSoft

*Packaging companies are always striving to stay one step ahead of their competitors in providing the best solutions for product capacity. Furthermore, in most cases, significant effort is devoted to the design of flexible machines: performance is expected to be high and consistent even if the packaged goods, packaging format, or packaging material are changed. Materials, in particular, are heading for a revolution driven by the regulatory restrictions that will take effect over the next few years.*

Coesia partnered with EnginSoft and the University of Trento's Department of Industrial Engineering to simulate a stand-up pouch packaging machine (Doypack®). The stages analyzed were opening, filling with detergent, and closing (Fig. 1). The scope was to develop a digital model to perform the two-way coupling between the flexible package structure and the fluid content.

The problem was addressed using two commercial tools: Particleworks and RecurDyn. The former represents the fluid behavior using particle-based computational fluid dynamics (CFD) while the latter efficiently calculates the deformation and dynamics of the flexible pouch by performing a Multi-Flexible-Body Dynamics simulation. We first demonstrated the feasibility of the analysis and then verified the results using the experience of Coesia's engineers with the Doypack® machine.

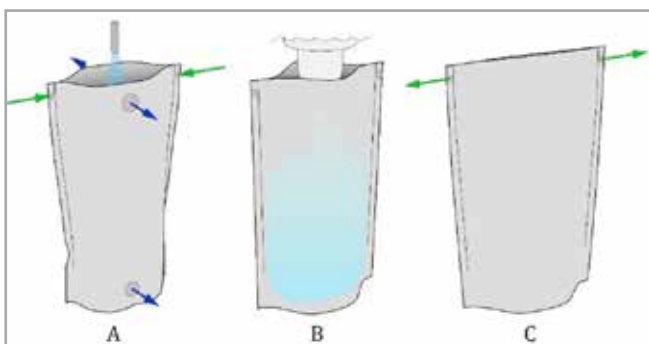


Fig. 1 – Schematic representation of the operations analyzed

Three different simulations were performed to understand the influence of the material properties, pouch thickness, machine velocity, and opening span of the pouch on the process of preparing and filling it.

## Description of the stations

The machine operates cyclically, alternating between pack feeding movements and stationary operations in which each process is executed. The movement is implemented by a set of upper and lower clamps that support the pouch. Each station is equipped with two pairs of upper clamps that restrain the pouch during stationary operations. Forward movement of the pouch to consecutive stations is provided by the lower clamps, which are moved back and forth by a four-bar linkage mechanism. The stations can be widened to accommodate up to three packages per stage (triplex), increasing the capacity of the machine.

The automatic process begins with the unwinding and forming of the film. The film is then trimmed and laterally sealed to obtain each individual flat package.

The focus of the simulation project was to model the subsequent stations (and the lateral movement of the pouch between them). The machine workflow includes:

- A. opening the flat pouch,
- B. filling it with a liquid detergent,
- C. closing the filled pouch.

At the beginning of the opening stage (A), the upper clamps and the lateral suction cups engage (Fig. 2). The suction cups open the pouch by pulling apart and the upper clamps accommodate the opening. Simultaneously, pressurized air is forced into the pouch from above, inflating it to ensure the correct shape. The suction cups are released and the air turns off when the process is complete. The upper clamps release as soon as the lower clamps, responsible for forward movement, pinch the pouch.

As the open pouch nears the filling station (B), the nozzle moves downward, partially entering the package. A second exchange of the support clamps occurs. Once the upper clamps are engaged, the nozzle's shutter is pneumatically moved upward, allowing fluid to flow through the nozzle into the pouch (Fig. 3). Once the pouch is full, the shutter moves downward again.

The lower clamps then move the filled package toward the closing station. Here the clamping switch is repeated. The upper clamps then pull apart, stretching the pouch and restoring the flat configuration at the top, closing the pouch (C).

The remaining machine operations are then performed. The top-sealing stage follows the closing phase. The final operation of the machine is performed at the rejection station (quality check), and the full pouches that conform are distributed through the discharge belt.

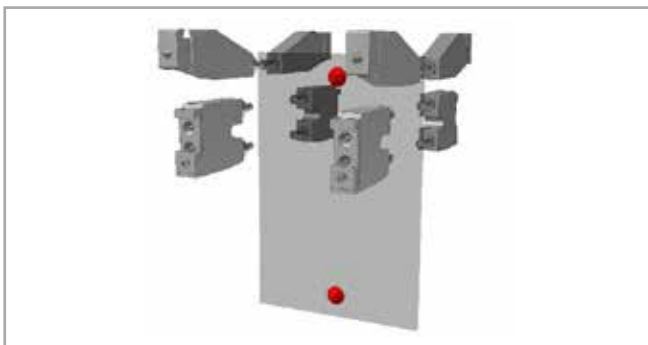


Fig. 2 – Initial configuration at the beginning of the opening process

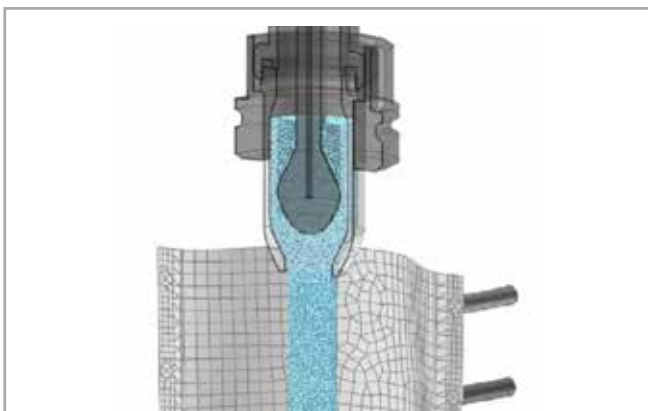


Fig. 3 – Flow of the fluid particles through the nozzle

## Analyses performed

An in-depth knowledge of the processes in a high-capacity automatic machine is essential when the goal is to achieve fast, high-quality production. For this reason, several analyses were prepared to study the operations, focusing on different configurations and parameters.

Three sets of simulations were performed:

- 1) Pouch opening, filling and movement; analysis of the influence of pouch aperture and of the material properties (coupling of Particleworks and RecurDyn)
- 2) DOE of the pouch; analysis of the Young's Modulus and pouch thickness (RedurDyn)
- 3) Sloshing analysis; analysis of the velocity of the machine and pouch aperture (Particleworks)

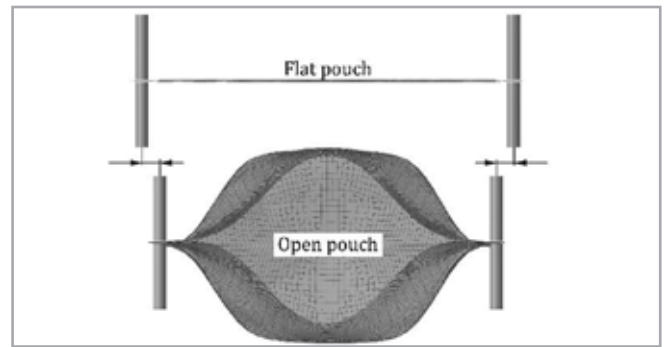


Fig. 4 – Description of the opening configuration (top view)

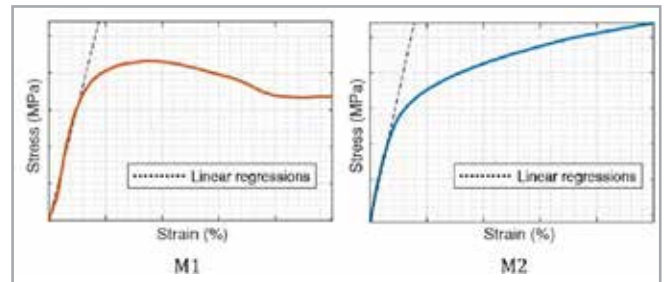


Fig. 5 – Experimental stress-strain results of the analyzed materials

The first analysis was performed on the entire process (opening, filling, and closing) to study the influence of two parameters:

- the span of aperture during opening (Fig. 4), defining two configurations in which the pouch is less (A1) or more (A2) open,
- the physical properties of the pouch material (Fig. 5), by selecting two different types of film (M1 and M2).

The second analysis focused on the sensitivity to variations in the physical properties of the packaging film (thickness and Young's modulus), compared to a reference configuration.

The stability and shape of the package were studied, evaluating the influence of percentual variations to the pouch properties (-10%, -5%, +5%, +10%).

The final study was conducted focusing on the phenomenon of sloshing, which occurs when the pouch moves from the filling to the closing station. This was analyzed by considering two configurations of opening and varying the speed of the machine. The fluid level cannot exceed a predefined limit to ensure that the sealing area remains clean. Higher machine speeds tend to increase the internal sloshing and an upper limit for the velocity can be identified based on the minimum distance required from the top of the pouch.

## Modeling of the problem

The multi-body and structural parts of the model were developed in RecurDyn. The rigid components (i.e. upper and lower clamps, suction cups, nozzle, and shutter) were inserted into the RecurDyn model using their CAD designs and assigning them their specific laws of motion.

The structure of the pouch was modeled using the Full Flex approach: a series of flat geometries was created (Fig.6a), meshed with 4-node 6-DOFs shell elements (Fig.6b), and merged to obtain a single Finite Element (FE) flat structure. The shell elements are well suited

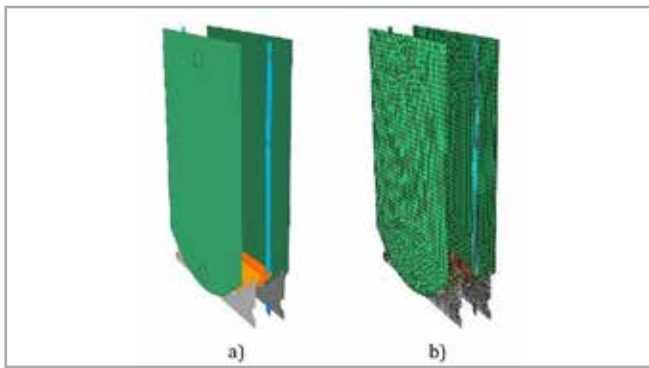


Fig. 6 – Development of the Full Flex structure of the pouch

to representing thin films. RecurDyn’s Full Flex method also enables efficient and effective simulation of nonlinearities related to large displacements and contacts.

To accelerate and automate the calibration of the pouch model, a script was developed (using the integrated PNet environment) to easily repeat the steps of structure definition and meshing. By varying a few parameters in the code, an iterative procedure was accomplished to correctly define the properties of the FE structure.

Once each component was correctly defined, the interaction of the package with the tips of the clamps and the suction cups was configured.

Particleworks is a mesh-less CFD software based on the Moving Particle Simulation (MPS) Method. The underlying Lagrangian approach is ideal for analyzing free-surface flows, such as the injection of the fluid into the pouch (jet flow and splashing phenomena). An annular surface was defined and positioned above the shutter. From this surface, fluid particles are generated with a constant flow rate. Among the physical properties of fluids, the most influential is the rheological law.

Detergents and foods injected into pouches frequently exhibit non-Newtonian behavior, with viscosity that varies according to the local shear rate. In this analysis, the liquid detergent displays a shear-thinning behavior (with viscosity decreasing at higher shear rates). The experimental data was fitted and applied to the fluid settings. The particle size and numerical settings were selected by evaluating the desired sensitivity of the simulation results, while also considering the computational cost.

The co-simulation configuration is assisted by a communication strategy already implemented between the two tools, RecurDyn and Particleworks. A two-way Fluid-Structure Interaction (FSI) can therefore be used to simulate these tightly coupled physical domains.

## Results

The results of the complete analysis at different frames are depicted in Figs. 7-9. During the first process (Fig.7), the progressive unfolding and opening of the pouch can be observed. The structure is represented displaying the von-Mises stress. Fig. 8 shows a cross-sectional view of the gradual filling of the package. The velocity and pressure distribution of the particles can be seen, allowing a detailed analysis of

the detergent flow into the pouch and its interaction with the lateral film and the bottom gusset. Fig. 9 illustrates the closing process.

One of the most interesting results with respect to the analyzed configurations concerns the lateral deformation of the filled pouch as it exits the filling station. The deformation is defined by the difference between the nominal and the actual mean position of the bottom gusset (Fig.10). The deformation of the pouch is more strongly influenced by a less (A1) or more (A2) open package, rather than by a less (M1) or more (M2) rigid material.

A summary of the results of the variational analysis is shown in Fig 11. The stability of the bottom gusset during the opening operation is the aspect that is most sensitive to changes in the physical properties of the film. A collapse of this part tends to refold the entire package, blocking the execution of the subsequent operations. The results show that a stiffer film increases the possibility of the gusset collapsing. The variations analyzed in the properties help define the boundaries for a successful filling process.

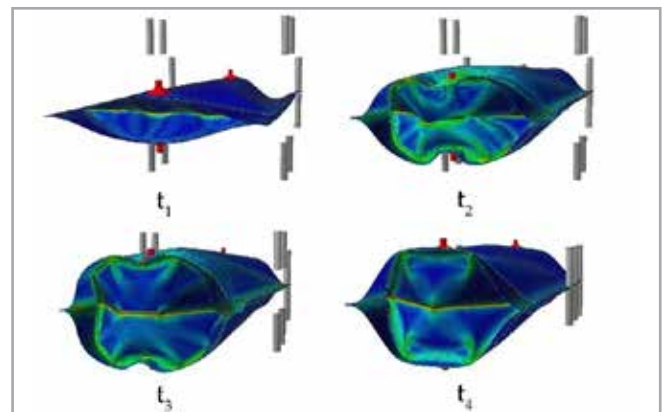


Fig. 7 – Progression of the opening process showing the von-Mises stress (bottom view)

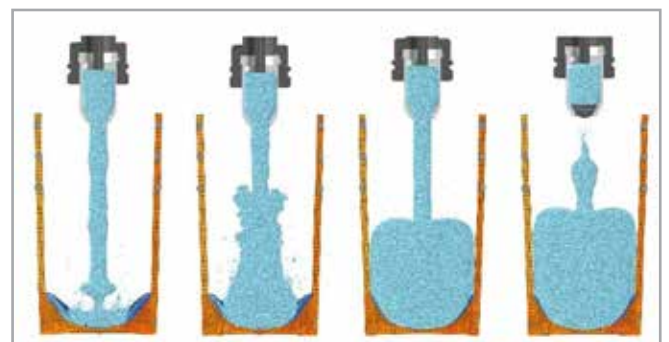


Fig. 8 – Progressive filling of the pouch with the liquid detergent

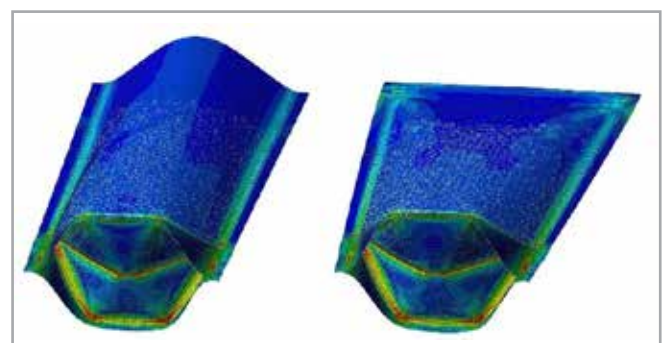


Fig. 9 – Von-Mises stress of the filled pouch before (left) and after (right) the closing process

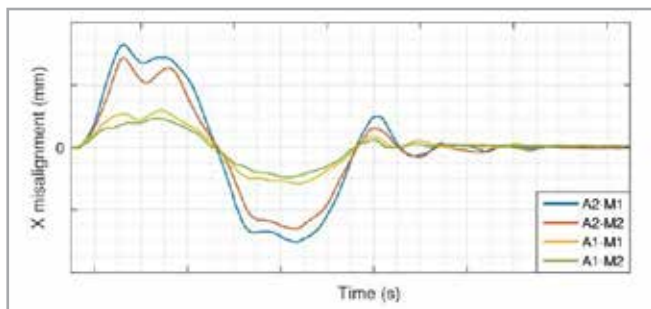


Fig. 10 – Pouch deformation for four different combinations of the pouch aperture (A1 less open than A2) and the pouch stiffness (M1 more flexible than M2).

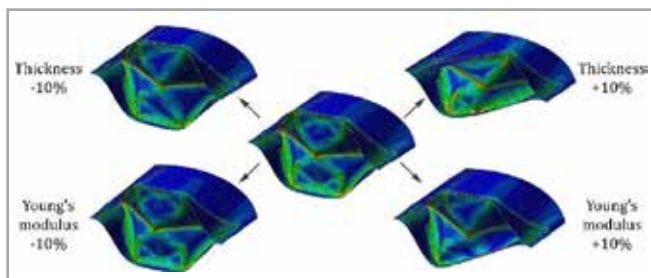


Fig. 11 – Results of the parametric analysis of the effects on the structure of the bottom gusset

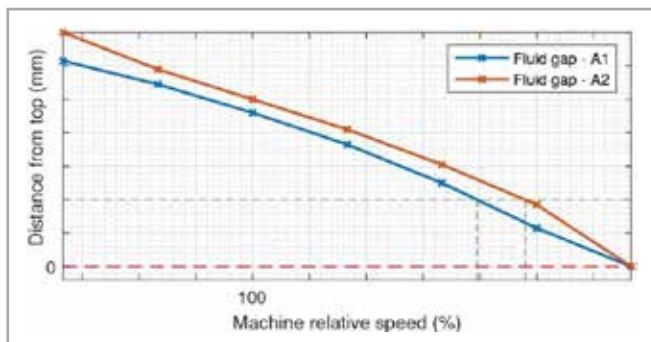


Fig. 12 – Gap between the fluid and the top of the pouch at different machine speeds, for a less (A1) or more (A2) open pouch.

Fig. 12 presents the results of the sloshing analysis. The gap between the maximum fluid level and the upper bond of the pouch is shown for different machine speeds and two apertures of the pouch. The waves in the fluid, caused by the acceleration and deceleration of the package, reach a greater height (smaller gap) when a faster machine speed is selected. At the same machine speed, the more closed pouch has a higher fluid level. If limiting the maximum fluid height is the primary design requirement, then A2 allows higher machine speeds than the A1 version.

## Conclusions

This study demonstrated the powerful capabilities of the tools that were used to address a complex two-way FSI simulation. The results are promising: they can be used to select the best combination of parameters and to predict performance as the machine configuration or package characteristics change. Both structural and fluid behavior can be analyzed in detail, providing key information that cannot be retrieved experimentally.

All simulations were performed using a standard workstation with an entry-level graphics processing unit (GPU) card. Despite this, the entire simulation was performed in 10 hours allowing it to be run overnight

## About Coesia

Coesia is a group of companies specialised in highly innovative industrial and packaging solutions, headquartered in Bologna, Italy. Isabella Seràgnoli is the sole shareholder.

Coesia companies are leaders in the sectors of:

- Advanced automated machinery and packaging materials
- Industrial process solutions
- Precision gears

Coesia's customers are leaders in a wide range of market sectors, including Aerospace, Ceramics, Consumer goods, Electronics, Healthcare, Luxury Goods, Pharmaceuticals, Racing & Automotive and Tobacco. [coesia.com](http://coesia.com)

without the need for a high performance computing (HPC) facility. Furthermore, the use of mid-range or high-end GPU cards can easily reduce this time.

The simulation results can be used to identify an ideal combination of parameters. When the rigidity of the package must be ensured throughout the line, the less open configuration is preferable (Fig.10). The stiffness of the material has a visible, though less significant, effect than the opening configuration.

These results are useful as we move to recyclable, less rigid materials since they can be used to study the effect on the process in advance. It is possible to select certain ad hoc opening configurations to compensate for dissimilar behaviors when different package formats or materials are used.

The sloshing results led to an opposing conclusion. When the machine speed is high and must be maximized, a greater aperture of the pouch should be selected to reduce the height of the waves in the fluid in the pouch. While these results show opposing directions for improvement, by relaxing some constraints (such as selecting a constant opening configuration), insightful simulations can be performed to identify the best compromise combination for each specific operation.

The results obtained for the first operation (opening and lateral motion of the empty pouch) and the final operation (lateral movement of the full pouch) show opposing positive correlations with the span of aperture. This hints at possible improvements, such as varying the span of aperture across the stages of the machine.

For more information:

Davide Marini – EnginSoft  
[d.marini@enginsoft.com](mailto:d.marini@enginsoft.com)

This work is being presented in the **Manufacturing session** of the International CAE Conference and Exhibition 2021.

# Reshaping the DEMO Tokamak's TF Coil with high fidelity Multiphysics CAE and advanced mesh morphing

by Andrea Chiappa<sup>1</sup>, Christian Bachmann<sup>2</sup>, Francesco Maviglia<sup>2</sup>, Valerio Tomarchio<sup>3</sup>, Corrado Groth<sup>1</sup>, and Marco Evangelos Biancolini<sup>1</sup>

1. University of Rome Tor Vergata - 2. EUROfusion Consortium - 3. JT-60SA European Home Team

*The next phase in the EU's ambitious nuclear fusion power generation project is the construction of a DEMOnstration powerplant. This represents the first step towards the creation of a commercial power plant and is drawing on the combined efforts of large teams of scientists and engineers across various research units. This article describes the Multiphysics optimization procedure undertaken to ensure the best compromise between electromagnetic and structural compliance for the Toroidal Field coils of the Advanced Divertor Configurations of the toroidal chamber, that holds the plasma in which the fusion reaction takes place. The TF coils are subjected to enormous Lorentz forces that are transferred to robust steel casings that hold the TF coils in place. It has been learnt that these casings should perform the dual function of shaping the super-conducting loops appropriately, and bearing the loads within a reasonable margin of safety. However, preliminary stress analyses revealed that their initial shape had structural deficiencies. FEM analyses and mesh morphing were used to optimize the shapes to the best compromise between the two functions.*

The DEMO Tokamak unquestionably represents a great challenge from a technical and technological point of view. This is due not only to the Multiphysics nature of the processes that must coexist, often leading to a trade-off of opposing requirements, but also to the unprecedented range of operation experienced by each sub-system of the assembly. This paper shows the optimization strategy adopted for the Toroidal Field (TF) coils of the Advanced Divertor Configurations (ADCs), in search of the best compromise between electromagnetic and structural compliance. Ansys simulation tools were used in the steps followed towards the final goal:

- APDL for the electromagnetic and structural analysis of the basic ADC configurations for a preliminary stress assessment
- Workbench + RBF Morph + APDL to define an optimal shape (iso-stress profile) for each TF coil

configuration from a structural point of view, and for the optimization procedure which progressively mixed the initial and the iso-stress shape of each ADC coil to find the best compromise between the two.

The DEMOnstration power plant, DEMO, will be the successor to ITER. Unlike ITER, DEMO will be more than a large-scale scientific experiment; it will be the first step toward a commercial power plant, with the goal of producing actual electricity. For this reason, DEMO will be significantly larger than ITER, testing higher loads and posing a greater challenge than its predecessor. Thousands of scientists and engineers, split across various research units, are making extraordinary efforts to achieve the conceptual design of such a machine.

With reference to Fig. 1: the fusion reaction takes place inside the plasma, producing a large amount of energy at the expense of a small portion of mass. The plasma, at extremely high temperatures, is held in a toroidal chamber by a strong magnetic field, avoiding contact with any part of the assembly. An important component of the magnetic field is generated by the Toroidal Field coils: large D-shaped devices wound with superconducting materials that form electrical circuits in the radial planes containing the machine axis. Superconductivity occurs in some materials below an extremely low critical temperature ( $< 20$  K for most cases). The

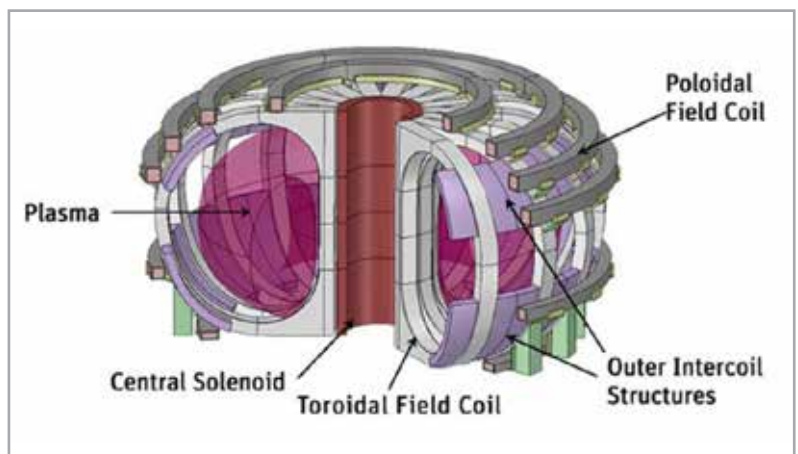


Fig. 1 - The DEMO architecture.

superconductors are arranged in a compact array called a Winding Pack (WP); supercritical helium is used for cooling, enabling very stable superconductor behavior.

The setup of the magnetic field is quite complex: a large amount of equipment (Toroidal Field coils, Poloidal Field coils, Central Solenoid) is devoted to creating a field with the desired characteristics to which the circular motion of the plasma also contributes. As a result, the conducting TF coils undergo enormous Lorentz forces that are transferred to the structural supports. The superconductors are contained in robust steel casings that hold them in place and bear these electromagnetic loads. It has become clear that these casings should perform a dual function: on the one hand, shaping the super-conducting loops appropriately, and on the other hand, bearing the loads within a reasonable margin of safety. However, the initial shape of the ADCs was designed mainly to accomplish the first function with consequent deficiencies from the structural point of view, as evidenced by the preliminary stress analyses.

**Preliminary EM and structural analyses of the DEMO ADCs**

The basic configurations of all the ADCs – Single-Null (SN), Double-Null (DN), Snow-Flake (SF) and Super-X (SX) – were subjected to preliminary electromagnetic (EM) and structural analyses. Both types of studies used Ansys APDL as the simulation environment. The EM analyses considered electricity flowing only in the TF coils, as hypothesized for the magnetization stage, and were aimed at obtaining the Lorentz forces acting on the superconductors. Stress evaluation followed the EM analyses: loads were transferred simply from one model to another by maintaining the same mesh (with nodal loads attached) for the superconductor bodies.

The structural model of each ADC involves a single coil and two half-coils on either side (for a total of two coils), as seen in Fig. 2.

Resultant component	SN	DN	SF	SX
RX (radial) [MN]	-860.211	-910.373	-917.155	-943.783
MY [MN•m]	341.530	0.182	9.053	1146.301

Table 1: Resultant Force on a single coil of ADC, magnetization stage (in-plane loads only, Ry, Rz, Mx, Mz = 0)



Fig. 2 - Example of the structural model.

	Number of nodes	Number of elements
SN	686935	818172
DN	761815	880176
SF	788911	908384
SX	896672	974600

Table 2: Number of elements and nodes in the ADC structural models

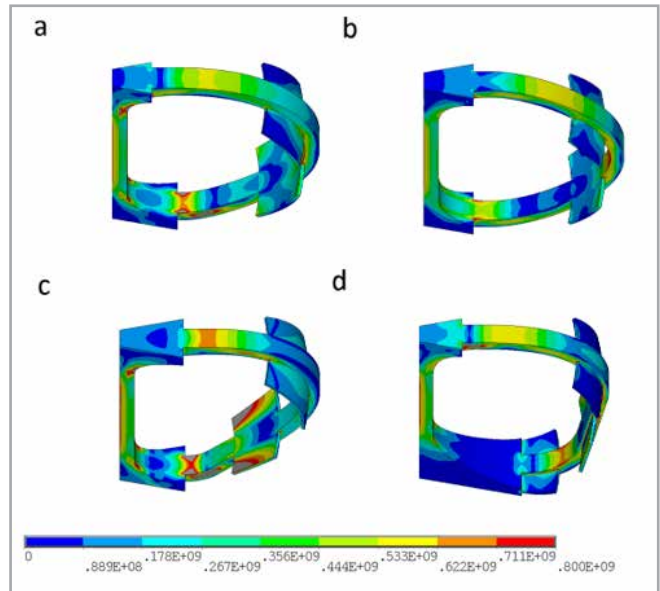


Fig. 3 - Top views of the Von Mises stress contours resulting from magnetization for SN (a), DN (b), SF (c) and SX (d).

Each coil consists of the external casing with the superconductors inside. A frictional contact condition is established between the superconductors and the casings, and between the different casings. The outer intercoil structures firmly connect one coil to the others. Table 1 lists the resultant radial force (RX) and resultant angular moments around the toroidal direction (MY) acting on a single coil for each ADC. Table 2 shows the number of elements and nodes for the structural models. Fig. 3 shows the Von Mises (VM) stress distribution over the ADC casings, revealing that large areas of material are above the assumed stress limit (700 MPa).

**Iso-stress shape of the coil**

The optimal shape of a coil, from a structural point of view, is one that undergoes only membrane stresses during the action of loads. This particular condition is achieved with a radius of curvature proportional to the radial coordinate at each point on the coil track. For each baseline coil shape, the corresponding iso-stress profile was constructed according to the additional rule of

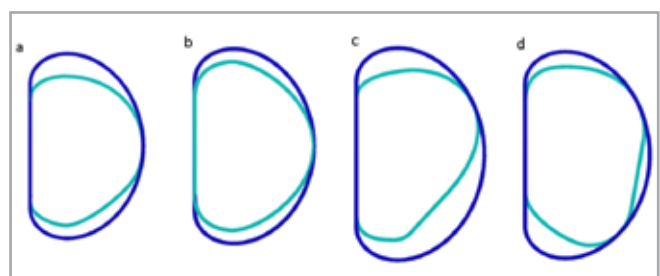


Fig. 4 - Iso-stress contours (dark blue) obtained from the ADC baselines (light blue): SN (a), DN (b), SF (c), SX (d).

always being external, or at least tangential, to the former shape. Fig. 4 shows the overlaid initial and optimal coil shapes for each of the ADCs.

**Optimization workflow**

For each shape of the ADC, the optimization workflow identified a compromise shape between each pair of associated baseline and iso-stress profiles, modifying the initial shape the absolute minimum to achieve structural integrity.

The optimization workflow was assembled according to the block diagram in Fig. 5 in the multidisciplinary Workbench platform, taking full advantage of its modular architecture.

Auxiliary geometries were imported from an external CAD to identify the shape of the coil before (baseline) and after (iso-stress) the transformation. Meshing these geometries (within a Structural module) was just a matter of convenience to make the surfaces parametric. A simplified TF coil model was introduced, representing only half of a single coil with symmetry constraints at the boundaries. RBF Morph was used to define and apply a continuous transformation to the coil shape by acting directly on the numerical model, without any attached geometry, accelerating the entire process, as shown in Fig. 6.

A series of intermediate coil configurations was obtained by starting from the auxiliary geometries and linearly scaling the

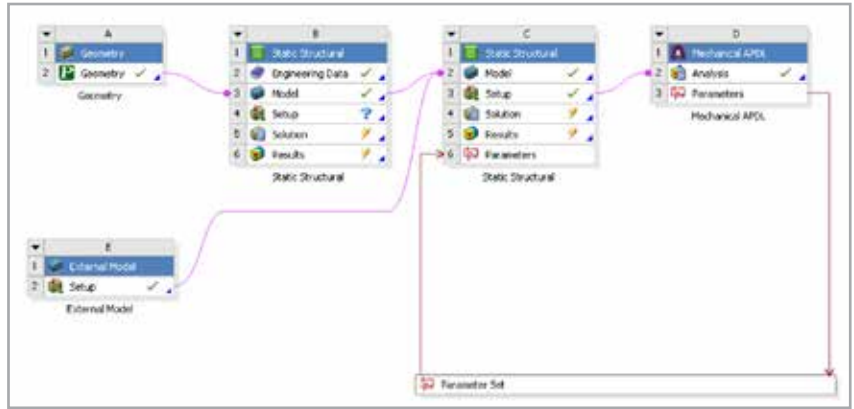


Fig. 5 - Block diagram of the optimization workflow.

transformation that converts the baseline shape into its iso-stress counterpart with a blending parameter between 0 and 1. The models obtained by the described procedure were fed to an APDL module for EM and structural analyses.

Observation of the results in terms of Von Mises (VM) stresses allowed the lowest blending parameter whose associated coil casing had less than 1% of the external volume (i.e. the volume of the curved segment of the casing) above 450 MPa of VM stress to be identified for each ADC. Four candidate shapes for the ADCs were selected such that a satisfying margin of safety was ensured while minimizing the shape change from the baseline configuration. Fig. 7 summarizes the output of the optimization

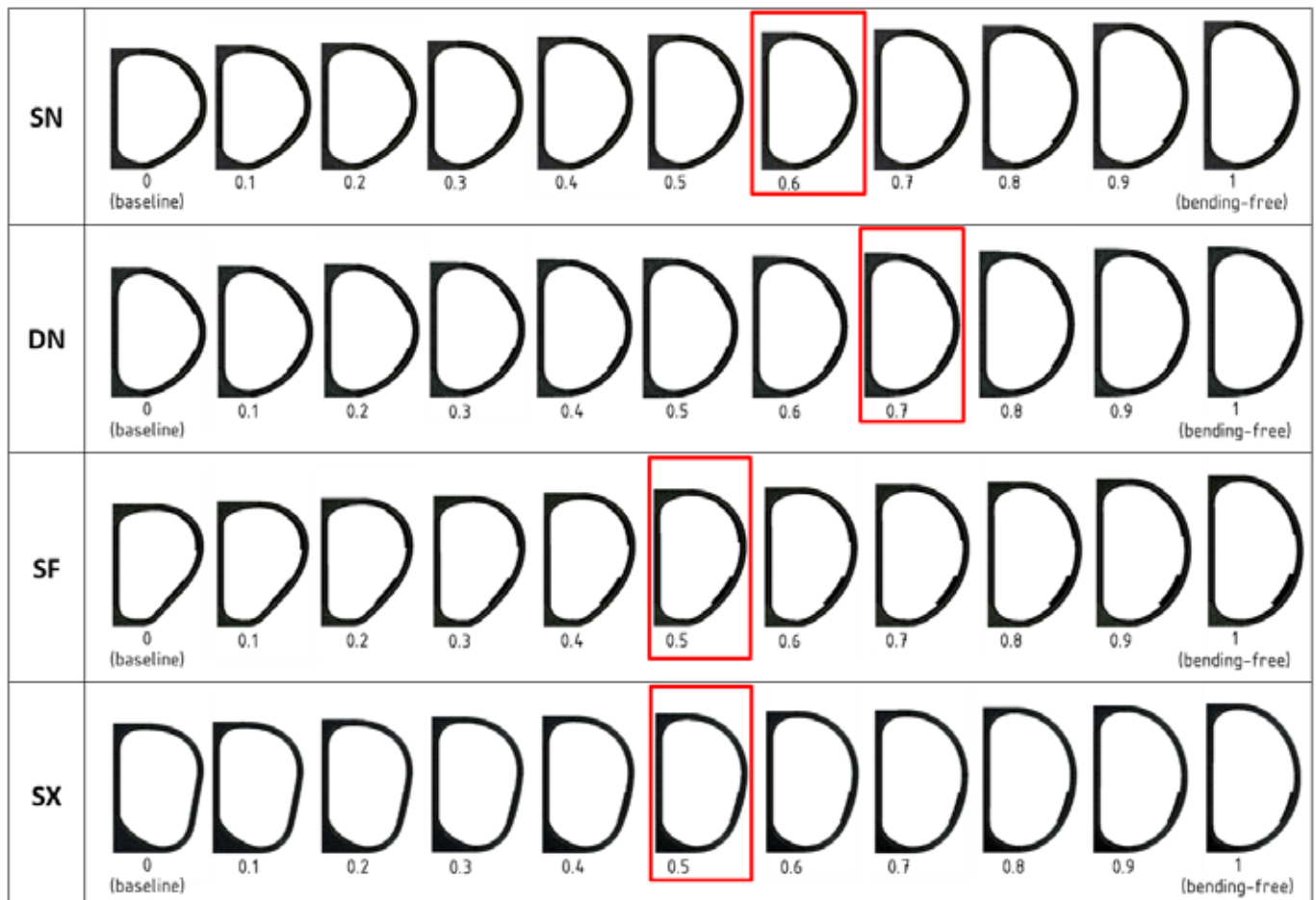


Fig. 7 - ADCs shape progressions from the initial baseline to the ideal iso-stress configurations. The profiles selected are framed in red.

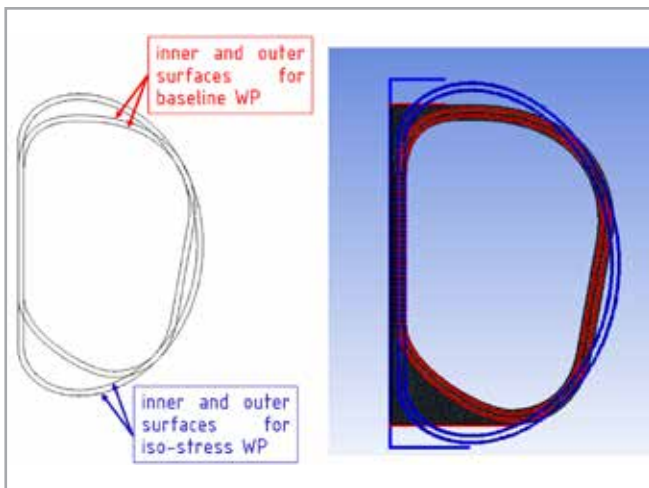


Fig. 6 Left - Schematic of the transformation moving the baseline WP onto the iso-stress WP. Right - Definition of the transformation field moving the WP and casing in their initial configuration (red) onto the deformed one (blue).

process, showing the evolution of the ADCs by increasing the blending parameter from 0 to 1 at intervals of 0.1, with the candidate shapes framed in red.

Fig. 8 shows the VM stress distribution on the ADC casings for the baseline and candidate configurations. The external casing volume percentages  $\geq 450$  MPa of VM stress were 12%, 18%, 8% and 12% for the original SN, DN, SF and SX shapes, respectively; after optimization, these had been reduced to  $< 1\%$ . A FEM model of the candidate SN shape based on the new geometry and removing all the simplifications introduced to accelerate the workflow was built from scratch as an optimization output. The results obtained after the EM and structural analyses of this brand new model were compared with the first one selected after the optimization (and including only one half of the structure); the comparison confirmed the satisfactory level of approximation of the model used for the optimization procedure, despite the simplifications introduced.

## Conclusions

The TF coils of the DEMO ADCs were originally designed to generate a magnetic field with specific characteristics. Their original shapes were not well-suited to withstanding the enormous Lorentz forces from EM interactions. In this paper, we presented an optimization procedure based on FEM analyses and mesh morphing that can find compromise shapes for the TF coils between their original configurations and a structurally optimal, iso-stress profile. The proposed workflow was able to successfully find the minimum shape modification for each ADC in order to reduce the stress level to below a specified threshold.

## Acknowledgment

This work has been carried out within the framework of the EUROfusion Consortium and has received funding from the Euratom research and training programme 2014-2018 and 2019-2020 under grant agreement No 633053. The views and opinions expressed herein do not necessarily reflect those of the European Commission.

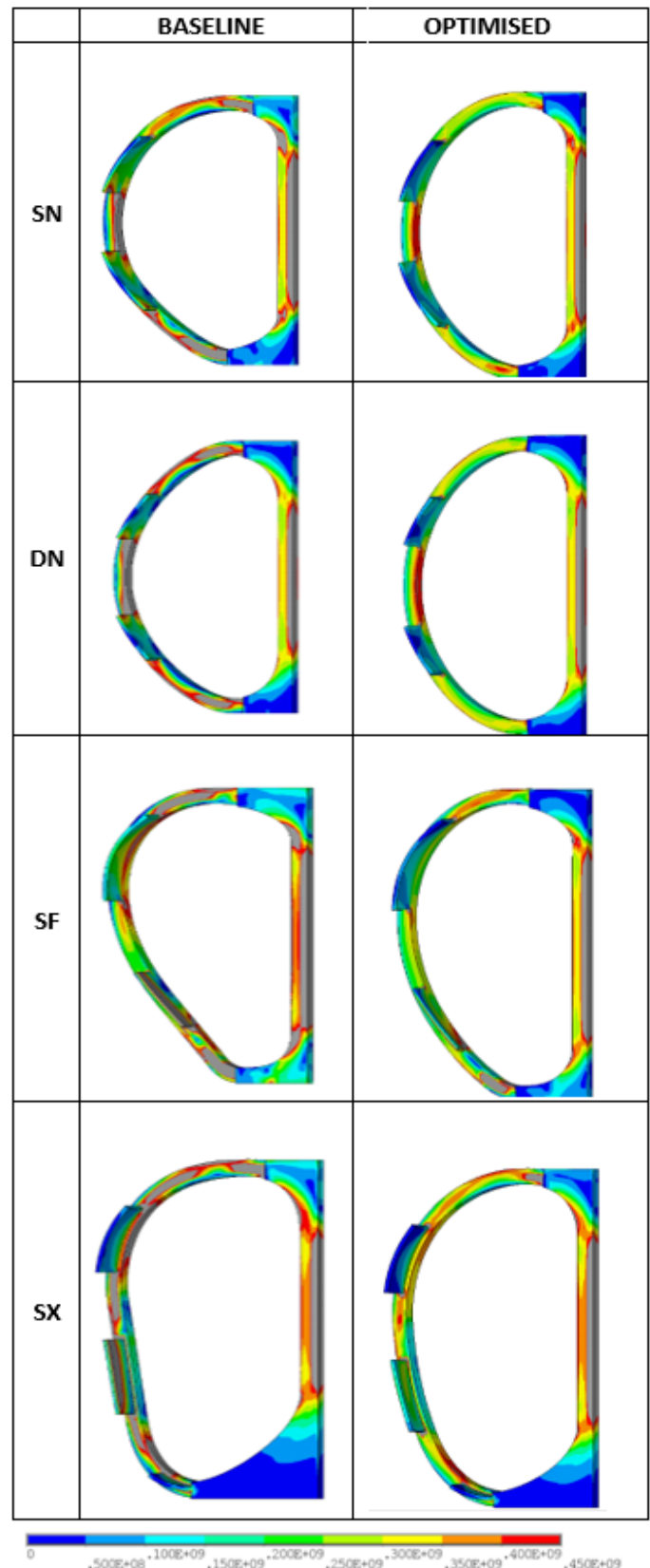


Fig. 8 - VM stress maps of the DEMO ADCs for the baseline and candidate casing shapes.

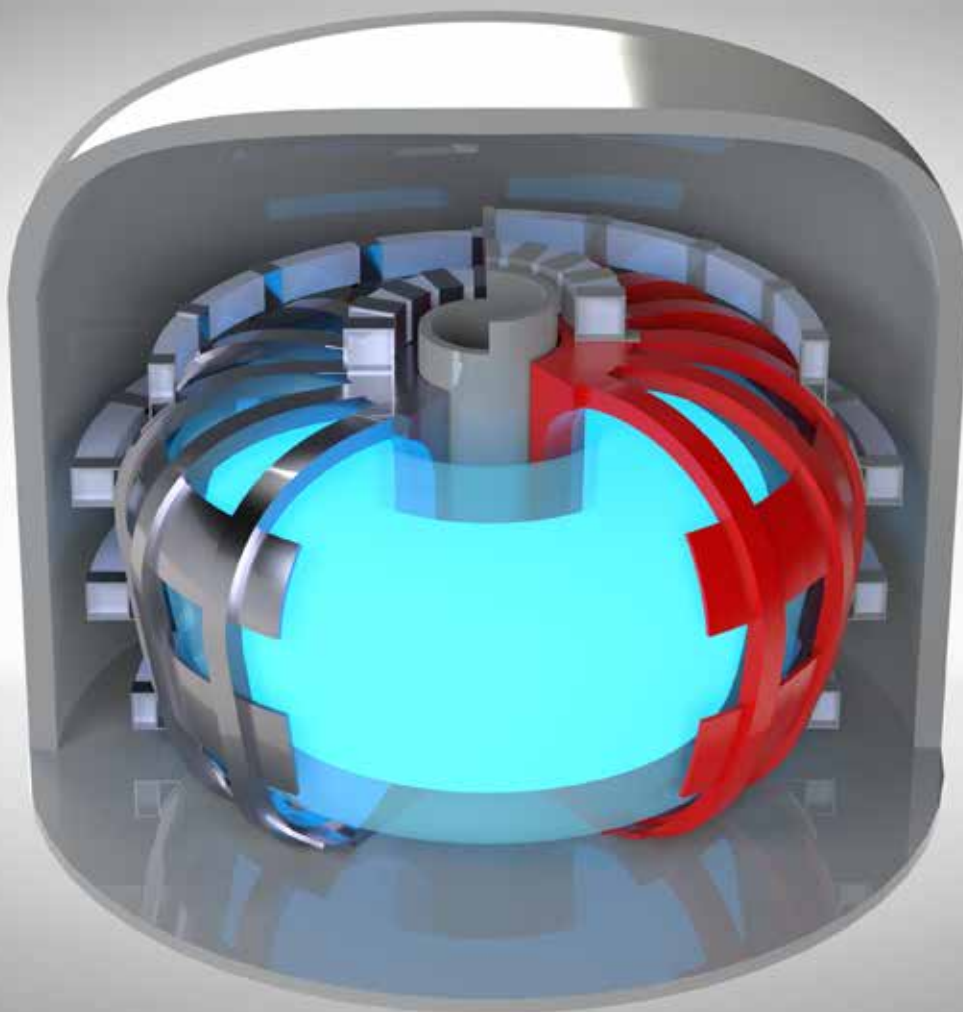
This work is being presented in the **Energy session** of the International CAE Conference and Exhibition 2021.

For more information:

Andrea Chiappa - University of Rome Tor Vergata  
andrea.chiappa@uniroma2.it

# I have heard that with fusion we can have our own stars

Come and have a look at the 3D printed prototype showing the effect of shape optimization



Visit the **RBF Morph** booth at the International CAE Conference and Exhibition 2021.

# Announcing LeaPS, a water Leak Prediction System



EnginSoft UK and MWH Treatment collaboration, with funding from Innovate UK

As leading specialists in Simulation Based Engineering Sciences, EnginSoft UK is excited to announce its collaboration with MWH Treatment to help its customers reduce water leakage, after securing funding from Innovate UK.

*"With 200 years in the water industry, MWH Treatment is the ideal partner to work with us as we continue supporting water companies to meet their challenges through the optimization of AI technology and the use of advanced predictive analytics to proactively pin-point leakage and reduce water wastage,"* states Bipin Patel, Managing Director at EnginSoft UK. He continues, *"We are excited to launch LeaPS: an innovative and efficient Leak Prediction System that leverages both EnginSoft UK's AI technology and MWH Treatment's direct engineering expertise in a project that once again places EnginSoft UK's know-how in Artificial Intelligence in the spotlight."*

## Water loss in the UK

More than three billion liters of water is lost through leaky pipes in the UK every single day, while globally the figure is estimated to be about 45 billion liters. Burst pipes are reported as being the most common cause of a loss of water supply, demonstrating the huge need for preventative measures when it comes to pipe leakage. The latest predictions estimate that if further action is not taken, between 2025 and 2050 the UK alone will need more than 3.4 billion additional liters of water per day to meet future demand for public water supply.

## The industry problem

Water companies across the UK are struggling with the financial burden posed by the costs of water leakage. To date, no technology has been available to address this problem and recent demands by the UK water services regulation authority, Ofwat, to minimize water leakage has made this challenge even more compelling. Water companies have, therefore, committed to achieving a 50% reduction in leakage by 2050 compared to 2017-18 levels.

To achieve this, water companies must:

- Mitigate the natural rate of increases in leakage
- Invest the money they receive effectively
- Reduce the frequency of unexpected burst pipes

## The traditional solution

Common solutions revolve around leak detection, using methods that include:

- Checking for subtle changes in flow rate and pressure that may indicate leaks
- Using acoustic and pressure loggers

- Identifying changes in ground conditions with drones and satellites
- Reports from the public

While improving leak detection can reduce repair times, drastically reducing leakage and bursts to meet leakage targets and the future demand for supply requires prediction and prevention instead of just detection. Typical methods of prediction involve simulation models constructed with static pipe characteristics such as material, age, diameter, and ground conditions to understand the degradation profile for each type of asset. These deterioration models often do not reflect the influence of non-static factors such as climate and environmental considerations. Using historic pipe performance data alongside the archived records of climate conditions can ensure that the tool provides insight into both short-term abnormal weather/climate occurrences (such as the 2018 'freeze thaw' event), and long-term performance trends.

## Introducing LeaPS

This water Leak Prediction System, LeaPS, utilizes advanced AI methodologies to create a predictive system modelled on biological processes that are capable of understanding the relationships between vast amounts of data. The nature of this system allows for flexible predictive methods that can adapt to the datasets available. Bipin explains, *"The aim is simple: to create a predictive system capable of augmenting the leak 'identification' process in the water industry by revolutionizing how we utilize data through the application of AI. The LeaPS project strives to be at the forefront of this approach."*

LeaPS will allow water companies to:

- Instantly predict where leakage is most likely to occur
- Understand the impact that current conditions and the characteristics of district metered areas (DMA) may have on leakage
- Acquire the knowledge to guide investments in network upgrades
- Understand how changes in DMAs over time may affect leakage

*"We estimate that up to £60m per AMP (5-year asset management plan) in operational costs can be saved by reducing unplanned burst maintenance through using LeaPS,"* states Bipin.

LeaPS is participating in the **Research Agorà initiative** at the International CAE Conference and Exhibition 2021.

For more information:  
Bipin Patel - EnginSoft  
b.patel@enginsoft.com

# Bridge the gap between testing and simulation

EikoSim creates a pathway between testing and simulation in structural mechanics using novel optical measurement techniques

by Florent Mathieu  
CEO of EikoSim

To develop mechanical products faster and reduce development costs, industries increasingly rely on simulations, following the model-based systems engineering (MBSE) strategy. But bolstering confidence in the more refined simulation models necessitates supporting these models with greater amounts of real-world data to avoid wide design margins. When a simulation model fails to match the experimental results, last-minute contingency efforts to recalibrate it to more accurately describe what happened to the prototype in the lab become unavoidable. Identifying sources of error often relies on trial-and-error manipulations of the simulation model parameters to more closely match the test results, which can be extremely time-consuming and yield uncertain outcomes.

To ensure simulation credibility, therefore, engineers compare simulation data to a set of reference test data. Strain gauges and linear variable differential transformers (LVDT) are among the most used sensors in mechanical engineering. The post-processing of such sensors for model validation can be tedious where the structural tests require large numbers of them. And despite providing many measurement points, these techniques are further limited both by the

time spent instrumenting the structure and the fact that they yield only local measurement information.

As a result, optical measurement techniques, such as digital image correlation (DIC), are gaining traction in test labs because of their ability to increase the amount of test data, and are being viewed as a means to enrich higher-level models. However, these techniques create a massive amount of test data, which presents a new kind of problem since current tools and methods cannot efficiently process these very large datasets.

The problem for simulation engineers is that current finite element (FE) simulation validation processes involve a significant amount of pointwise simulation-to-test comparisons using Excel sheets or Python/MATLAB scripts, due to the lack of more efficient solutions. In the case of DIC, this forces engineers to process virtual gauges instead of comparing displacements and strain fields to leverage all experimental data.



Fig. 1 – Modern structural testing often cannot rely on traditional sensors and requires more advanced techniques to provide a better understanding of deformation mechanisms (courtesy of IRT Saint-Exupéry).

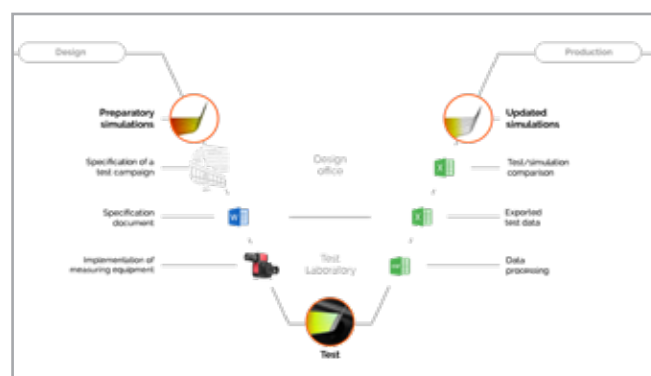


Fig. 2 – The back-and-forth between testing and simulation is often tedious and uses many unsuitable tools.

Using optical methods in conjunction with traditional sensors is seen as a way to dramatically increase confidence in simulations, but cannot alone bridge the gap between simulation and testing. The larger challenge is connecting all test data to simulation and simulation data management (SDM) tools in order to provide full access to all data in

one place for rapid decision making. To solve this challenge and improve the connection to FE models, EikoSim proposes three ingredients. The first (and central) element of the EikoTwin philosophy is that in order to bring the right kind of data to simulation engineers, the testing tools must connect to the simulation models within the test lab.

This can be achieved by considering the FE model at the test preparation stage. Whether for DIC or traditional sensors, EikoTwin collects and aggregates the test data directly on the 3D model of the specimen. The main benefit of involving finite elements from the beginning is the direct comparison of measurements to simulation results. Without this feature, the comparison requires successive tuning operations specific to each case, which results in the loss of measurement information (especially at the scatter plot/mesh transition). Integrating the measurement data on the FE mesh is to speak the simulation engineers' language, and gives them the measurement results directly without the need to transform them. This can be of significant value for large-scale structural tests where it is usually impossible to gather all the measurement data into a single usable result file.

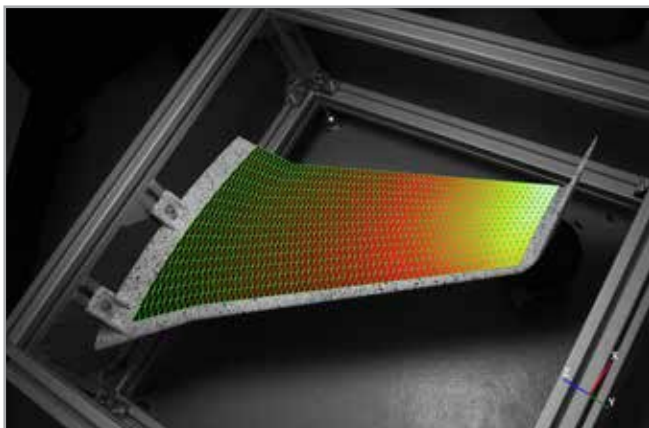


Fig. 3 – Bringing the mesh into the physical world is necessary in order to exploit the amount of data contained in images.

But the test specification also needs more consideration to make data collection seamless and to facilitate further analysis. When preparing for complex and expensive structural tests, especially when using methods such as DIC, it is even more important to evaluate feasibility and expected measurement errors to set the expectations on the simulation

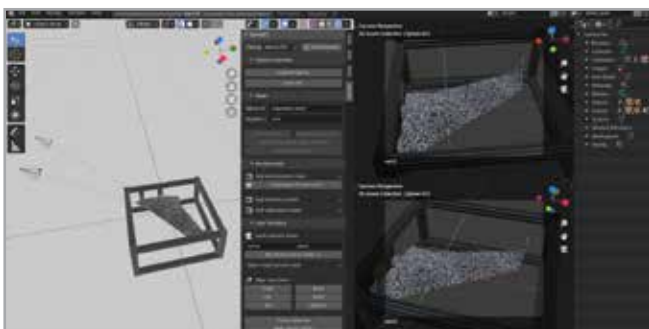


Fig. 4 – Virtual test scenes allow for smooth preparation and accurate error estimates.

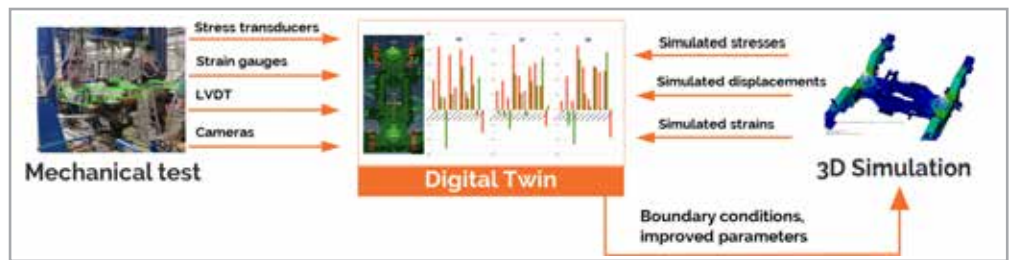


Fig. 5 – Merging simulation and measurement data in a Digital Twin allows rapid calibration of a simulation and helps predict the future outcome of a test.

side. Again, the test and simulation teams need to work together more closely around the FE model to decide which sensors to use, where. In this regard, EikoTwin makes it possible to plan the entire test in the same platform for all sensors, based on the simulation data. This saves physical preparation time and ensures that the test setup will produce measurements with the required accuracy.

The final element of an integrated model validation is the feedback loop to the simulation model. With rich measurement data now available directly on the mesh, how do engineers manage this quantity of information? Digital Twins are the modern-day answer.

EikoTwin helps close this loop by applying the digital twin concept to 3D structural calculations in mechanical engineering. It can modify the boundary conditions of the simulation to avoid overly strong hypotheses and use experimental data instead. Sensitivity analyses can also be performed to determine which parameter (material parameters, interfaces, etc.) to change first to reduce the gap between the simulation and the experiment.

Modern model validation requires the full involvement of test services to feed simulations with real-world data. The integration of the 3D model into testing practices is part of a necessary transition for organizations who require the simulation model to speak the same language as the physical prototype. Test teams have a key role to play in this transformation, not only to inform their counterparts of the realities of testing, but also to ensure that structural test data is used fully and effectively.

## About EikoSim

EikoSim is a software company that enables users to leverage validated simulation models to support design decisions. The company helps the managers of engineers responsible for structural simulations. It assists its customers in explaining the discrepancies between tests and models so that they can respond to program requests more quickly and reduce delivery times to the final customer. The EikoTwin software solution applies image analysis and simulation model management to improve both simulations and development cycles.

EikoSim is a **sponsor** of the International CAE Conference and Exhibition 2021.

For more information:  
Florent Mathieu - EikoSim  
[florent.mathieu@eikosim.com](mailto:florent.mathieu@eikosim.com)

# Component-based development for CAE with Tech Soft 3D's toolkits



by Andres Rodriguez-Villa  
Tech Soft 3D

As markets mature and players consolidate into larger entities, the way that products are built transitions from a more integrated approach – “let’s do it all” – to something more targeted – “let’s focus on our core added value”. This is particularly visible in large manufacturing industries such as automotive or aeronautics, where the component manufacturers who feed the supply chain produce virtually all the components of cars and aircraft.

Within the software and hardware businesses, the examples of Intel processors and Microsoft operating systems that power most of today’s computers demonstrates how important it is for manufacturers such as Dell, Lenovo, and HP to be able to rely on solid strategic partnerships that free resources to focus on adding their specific know-how to their products.

The smaller world of engineering software is no exception: the days when vendors developed everything from visualization to linear solvers in addition to the technologies that truly add value to their products are long gone. Creating applications using components has become the norm. Examining the standard simulation workflow more closely, there are a variety of technologies that can be handled through highly specialized and efficient development kits.

For the purposes of simulation setup, third-party components are best for importing CAD from various native formats, handling the tedious task of repairing tessellations, and reliably generating suitable 2D and 3D meshes.



Fig. 2 - Technologies that can benefit from using software components

At the core of a simulation package, solvers can also leverage efficient frameworks to implement physical modelling and, more importantly, to assemble and solve the resulting linear algebra problems. Finally, when the results are available, providing post-processing and reporting tools to end users requires specialized skills that are often best addressed by a focused component developer.

Throughout this workflow, even supporting technologies such as visualization, interoperability and automation are often too far from the core know-how mastered by CAE development teams and are, therefore, more efficiently covered by third-party contributions.

Choosing to keep any of these technologies in-house or rely on external software development kits (SDKs) is a matter of balancing the pros and cons; in other words, to evaluate the return on investment of this “buy or build” decision. The following criteria seem relevant when considering these options:

- Time-to-market: integrating external IP into a product is the fastest way to add value, compared to creating a technology from scratch or refactoring outdated code.
- Cost of features: large engineering development kits are the result of development teams working for years on market-driven innovation and hardening. Acquiring proven, off-the-shelf feature sets is cost-effective, both in terms of development and maintenance – all the more so considering the high complexity of the supporting technologies involved in the CAE workflow.
- Cost of integration: despite its higher cost, in-house development has important advantages, such as avoiding the burden of learning and integrating alien code, independence from providers’ release schedules, and producing fully customized functionality.

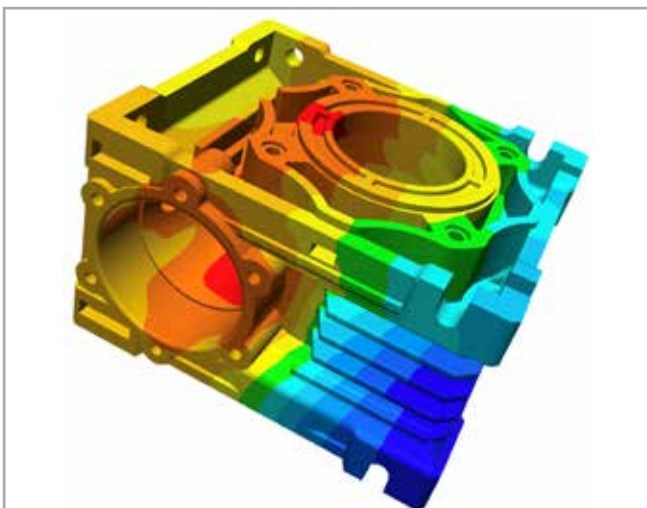


Fig. 1 - Specialized software components enhance engineering applications

With a CAE marketplace that has consolidated over the past 15 to 20 years, CAE software components have unsurprisingly become increasingly popular and critical for established independent software vendors (ISVs), budding start-ups, and enterprise development teams. Over time, Tech Soft 3D, known for its HOOPS SDK suite focused on 3D data access, visualization and reporting, has been more successful than many other providers.

Tech Soft 3D’s strategic vision to play a larger role as a Tier 1 component provider was reinforced last year by its acquisitions of Visual Kinematics and Ceetron AS, both developers of specialized CAE components. The result for the CAE market is the creation of a unique partner offering a comprehensive portfolio of SDKs covering all standard simulation workflow technologies and a promise of extended functionality as these toolkits begin to work together.

The entry point for all CAD geometries is HOOPS Exchange, the fastest and most accurate CAD data translation toolkit on the market. It provides access to over 30 native CAD formats and offers multiple capabilities to produce quality tessellations.

When input geometries are only available in tessellated format (STL files), the Polygonica SDK technology repairs these discrete surfaces to produce compliant connectivity for FEM purposes: watertight, fold-free and manifold. In addition, Polygonica offers defeaturing to eliminate details irrelevant to solving and a wide range of mesh modelling features, including Boolean operations.

Once you have bridged the gap from CAD to a clean mesh, Tech Soft 3D’s Visual Kinematics mesh SDK provides fail-free mesh generation and adaptation to produce surface or volume meshes suitable for FEM solving. Covering the most popular element types and offering a wide range of control options, the toolkit integrates smoothly and robustly into any CAE pre-processing application.

At the core of the workflow, Tech Soft 3D offers a Visual Kinematics framework for building FEM models that simplifies the work of implementing the physical modeling of a simulation. In addition, it also assembles and solves the resulting linear algebra problems, using state-of-the-art high-performance algorithms for shared memory architectures.

SDKs. Available for both desktop and browser-based web applications, these SDKs feature market-driven functionality created by experienced specialists and offer high performance and ease of use to developers

## About Tech Soft 3D

Tech Soft 3D is a leading global provider of development tools that help software teams deliver successful 3D engineering applications. Founded in 1996 and headquartered in Bend, Oregon, Tech Soft 3D also has offices in California, France, England, Japan, and Norway. The company’s toolkit products power more than 500 unique applications running on hundreds of millions of computers worldwide.

For more details, visit: [techsoft3d.com/markets/cae/](https://techsoft3d.com/markets/cae/)

through their intuitive programming interfaces (API). A set of Python modules also allows you to automate result processing to improve engineering workflows.

Finally, CAE applications often need to remain open to the global simulation environment, both when importing data from other applications and when exporting results to other file formats. This is the added value brought by Tech Soft 3D’s Visual Kinematics interoperability SDK, a unique vendor-independent toolkit that provides up-to-date access to input decks and results from over 30 industry-standard CAE applications, while allowing files to be written in more than 10 different formats.

It is difficult to predict where the CAE market will go. Emerging technologies such as process or geometry optimization using machine learning or artificial intelligence-based solving seem to be good candidates, but experience shows that market adoption is ultimately based on performance and requirements: while artificial reality (AR)/virtual reality (VR)/extended reality (XR) are already available, their widespread use is still in the making; the adoption of remote CAE is slowly increasing years after first becoming available – and the pandemic has also played a part here; previously, parallel computing also faced market inertia for years.

Whatever the future holds, creating specialized, high added-value CAE applications will not happen without component suppliers like Tech Soft 3D working behind the scenes to fuel innovation.

For more information:

Andres Rodriguez-Villa - Tech Soft 3D  
[andres@techsoft3d.com](mailto:andres@techsoft3d.com)

Tech Soft 3D is **sponsor** in the International CAE Conference and Exhibition 2021.



Fig. 3 - Reading simulation geometry from CAD files simplifies the CAE workflow



Fig. 4 - Robust 2D and 3D meshing is key to a successful CAE simulation application

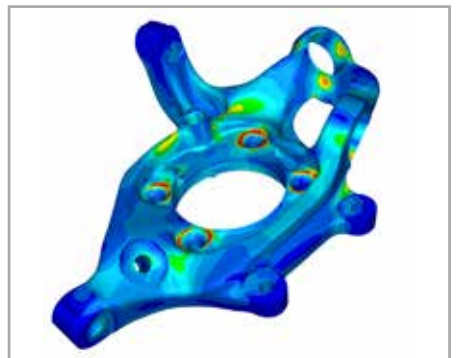


Fig. 5 - Advanced post-processing tools are required to fully exploit CAE simulations

# The Revolution in Simulation Initiative continues to expand as EnginSoft joins a growing alliance of sponsors



The global simulation industry collaboration and technology alliance Revolution in Simulation (“Rev-Sim” at [www.rev-sim.org](http://www.rev-sim.org)), created to accelerate innovation through the democratization of engineering simulation, has announced that EnginSoft ([www.enginsoft.com](http://www.enginsoft.com)) has become its newest participating sponsor and collaborator.

*“Our greatest passion is our clients and helping them to achieve unprecedented results and returns on their engineering simulation investments. We invest in building long-term relationships, whether partnering with clients’ in-house teams or providing outsourced engineering simulation. We pride ourselves on crafting customized solutions for each production context, based on the client’s business needs and objectives, that effectively leverage the skills, methods, knowledge and experience in their organization,”* - stated Stefano Odorizzi, EnginSoft President.

EnginSoft adds its name to a steadily increasing list of participating sponsors that now includes Aras, ASSESS, BETA CAE, Dassault

SolidWorks, EASA, ESRD, Front End Analytics, Future Facilities, Hexagon/MSC, Kinetic Vision, Modelon, NAFEMS, nTopology, Ohio Supercomputer Center, OnScale, PASS Suite, Phoenix Integration, Pointwise, Siemens, UberCloud and VCollab.

Each of these simulation leaders is providing expert leadership in the movement to make engineering simulation software more accessible, efficient, reliable, and impactful, not just for CAE experts but also for others across the enterprise – what is commonly referred to as the “Democratization of Simulation”. The demand for automated simulation is exploding, resulting in next-generation usage of traditional, expert-driven simulation tools and platforms.

Rev-Sim Director of Partnerships, Mike Nieburg said, *“Each of our sponsors is working to advance and expand the use and value of engineering simulation software by innovating within its market spaces. We are excited to have EnginSoft join us, demonstrating their revolutionary thought-leadership and technology in a collaborative alliance that benefits all industrial users of engineering simulation.”*

For more information:

Antonio Parona - EnginSoft

[a.parona@enginsoft.com](mailto:a.parona@enginsoft.com)

## About EnginSoft

EnginSoft is a leading technology transfer company in the field of Simulation Based Engineering Science (SBES) having been a progressive technological innovator since its foundation in 1984. Unique in our field, with both specific and advanced skills in all the disciplines and sectors in which simulation technologies are used, we assist our customers to navigate, manage and exploit their vast, complex data and their projects safely and successfully and realize the benefits of digitalization. Our knowledge and experience enables us to guide and assist customers with the process of digital transformation by identifying and resolving all the problems concerning the integration of simulation with other digital technologies, from the conception of a product, to its design and production – including plant planning and commissioning – right down to operations, across every industrial sector and business dimension, and fully consistent with the relevant development projects and investment plans. [enginsoft.com](http://enginsoft.com)

## About Rev-Sim LLC

Revolution in Simulation is a web-based resource and community-building platform that educates, advocates, collaborates and innovates for the advancement and democratization of engineering simulation. The Rev-Sim.Org website offers the largest curated collection of engineering simulation news, articles, presentations, white papers, videos, recorded webinars, case studies, and directories of software and consulting service providers to help organizations maximize the impact and ROI from simulation investments.

Existing and new industry users of simulation technologies are invited to explore our resources and submit questions about democratization to our panel of subject-matter experts and topic moderators at [www.rev-sim.org](http://www.rev-sim.org). Solution providers are invited to join the revolution by contacting: **Mike Nieburg** [mike.nieburg@rev-sim.org](mailto:mike.nieburg@rev-sim.org).



The Simulation Based Engineering & Sciences Magazine

# Newsletter

Special  
Issue

NOW  
Available

Special Issue on  
**modeFRONTIER**



RSM

RD

SPDM

PI



Choose the **best way**  
to gain **knowledge** today



---

**37<sup>th</sup>**

INTERNATIONAL CAE  
CONFERENCE  
AND EXHIBITION

---

ORCHESTRATING  
**DIGITAL**  
TRANSFORMATION  
THROUGH  
SIMULATION

---

**Channelling Technology, Processes and People**  
for Sustainable Competitive Advantage

---

**VICENZA, ITALY**  
17-19 NOVEMBER

HYBRID EVENT  
[www.caeconference.com](http://www.caeconference.com)

**2021**